



UNIVERSITY OF NAIROBI

**DETERMINATION OF HYDROCARBON SOURCE ROCK MATURITY USING
SMECTITE PERCENTAGES (S %) AND VITRINITE REFLECTANCE (R_0) OF ROCK
SAMPLES FROM LAMU BASIN, KENYA.**

BY

PURITY MWIHAKI KAMAU

Reg. No. I56/69485/2013

**A Thesis Submitted for Examination in Partial Fulfillment of the Requirements for Award
of the Degree of Master of Science in Geology (Applied Geochemistry) of the University of
Nairobi.**

NOVEMBER, 2016

DECLARATION

I declare that this thesis is my original work and has not been submitted elsewhere for examination, award of a degree or publication. Where other people's work or my own work has been used, this has properly been acknowledged and referenced in accordance with the University of Nairobi's requirements.

Signature..... Date.....

Purity Mwihaki Kamau

I56/69485/2013

Department of Geology

School of Physical Sciences

University of Nairobi

This thesis is submitted for examination with our approval as research supervisors:

Dr. Daniel Ichang'i

.....

.....

Department of Geology

Signature

Date

University of Nairobi

P.O Box 30197-00100

Nairobi Kenya

dwichangi@yahoo.com

Prof. Daniel Olago

.....

.....

Department of Geology

Signature

Date

University of Nairobi

P.O Box 30197-00100

Nairobi Kenya

dolago@uonbi.ac.ke

ABSTRACT

Lamu Basin in south eastern Kenya rests on a passively developed margin of the African plate. The Basin hosts thick sediments that are dominantly shale, sands and limestones, that overlie the Neoproterozoic metamorphic rocks of the Mozambique Belt. This research aims at determining the suitability of using smectite percentages in illite/smectite mixed layer clay minerals to identify the depth below the earth surface of hydrocarbons generation from the source rocks. The clay minerals present in Lamu Basin's rock formation were also identified with the depth and rock formation of their occurrence identified. Since 1960, sixteen petroleum exploratory wells have been drilled, though no commercial hydrocarbon deposits have been documented. Moreso, the older wells in Basin such as Walu, Kipini and Hagarso were not subjected to thorough evaluation of their hydrocarbon potential at the period of drilling. The maturity of Lamu Basin source rocks has previously been done using vitrinite reflectance, a technique that requires a rock to have vitrinite maceral component. The maceral component is a hydrocarbon compound whose light reflectance increases with maturity, that is, increase in temperature. Smectite to illite transformation has been used in tracing increase in temperature with increase in depth in sedimentary basins. For this research, forty eight (48) drilled core samples from Kipini-1, Simba-1, Walu-1, Walu-2 and Maridadi-1B wells which were drilled in the years between 1963-1987 in Lamu Basin were obtained on 15th and 16th October, 2015 from National Oil Corporation of Kenya (NOCK). The forty eight samples were analysed using X-ray diffraction clay mineral analysis three weeks later at KENGEN company laboratories at Naivasha, Kenya. In Simba-1 the illite/smectite mineral occurs at 1585-1590m with 85% smectite and at 1840-1845m with 29% smectite both from *Kipini* formation and at burial temperatures of 65-70°C. In Walu-2 well the illite/smectite mineral occurs at 1410-1411m with 55% smectite from *Barren Bed* Formation and at burial temperatures of 65-80 ° C. According to vitrinite reflectance analysis, Simba-1 hydrocarbon maturity zone is at 3050m to total depth of 3569m with vitrinite reflectance of 0.6-0.85%. Occurrence of illite/smectite mixed layer coincides with hydrocarbon source rock immature depths as indicated by vitrinite reflectance data. However, more detailed sampling should be done in the four wells and other wells in the Basin for a comparative analysis.

DEDICATION

To my son Felix Lewis Kamau, my parents, Mr. Elias Kamau Maina and Mrs. Nancy Wanjiku Mbogo, my husband Gibson Ngari Kariuki and all my siblings.

ACKNOWLEDGEMENTS

I greatly thank the Almighty God for good health, strength and provision during my study and entire life. Secondly, I highly appreciate my parents, Mr. Elias Kamau and Mrs. Nancy Wanjiku, my husband Gibson Ngari Kariuki and my siblings for their financial and moral support.

I am greatly indebted to my supervisor Dr. Daniel Ichang'i who gave me great guidance and tireless assistance in data acquisition and writing of this thesis. Great thanks also to Prof. Daniel Olago for his supervision and kind assistance in ensuring this thesis is of good quality.

My appreciation also goes to the University of Nairobi, and particularly Department of Geology, for sponsoring my M.Sc. Degree Programme, and is the reason this thesis has been completed.

I am also grateful to the National Oil Corporation of Kenya (NOCK) fraternity, and in particular the Chief Executive Officer Ms. Sumayya Hassan Athmani, the Upstream Manager Mr. Kivuti Nyaga, Ms. Elizabeth Kimburi, Ms. Florence Gaturu among others, that assisted and guided me in collecting core samples and various important pieces of information. Thank you all.

Lastly, I wish to very sincerely thank the Kengen Geothermal Director, Mr. Abel Rotich and the Senior Geologist Ms. Joyce Oloo for the very kind and rare support they gave me in X-ray diffraction analysis of clays as well as crucial guidance in clay data interpretation. May God bless you abundantly.

TABLE OF CONTENTS

DECLARATION	i
ABSTRACT	iii
DEDICATION	iv
ACKNOWLEDGEMENTS	v
TABLE OF CONTENTS	vi
LIST OF TABLES	x
LIST OF FIGURES	xi
LIST OF ABBREVIATIONS/ACRONYMS AND SYMBOLS	xii
CHAPTER ONE	1
1 INTRODUCTION	1
1.1 Statement of the problem	2
1.2 Objectives	3
1.2.1 General objective	3
1.2.2 Specific objectives	3
1.3 Justification and significance of the study	3
1.4 Scope of the research	4
1.5 Overview of the methodological approach	4
CHAPTER TWO	5
2 LITERATURE REVIEW	5
2.1 Organic Matter Richness and Maturity of Lamu Basin Source Rock	5
2.2 Illitization Process and the Relationship between Illitization, Vitrinite Reflectance and Oil Generation from a Source Rock	5
CHAPTER THREE	9
3 MATERIALS AND METHODS	9
3.1 Study Area	9
3.1.1 Location and Description	9
3.1.2 Climate	11
3.1.3 Vegetation	11
3.1.4 Land use and Land Resources	11
3.1.5 Physiography and Drainage	12

3.1.6	Geology and Structural Setting.....	12
3.1.6.1	Structural Setting of Lamu Basin.....	12
3.1.6.2	Regional Geology.....	14
3.1.6.2.1	Megasequence I (Karoo Group).....	14
3.1.6.2.2	Megasequence II (Sabaki Group).....	14
3.1.6.2.3	Megasequence III (Tana Group).....	14
3.1.6.2.4	Megasequence IV (Coastal Group).....	16
3.2	Stratigraphy of the Considered Wells.....	16
3.2.1	Maridadi 1B well.....	16
3.2.2	Simba-1 well.....	17
3.2.3	Walu-2 well.....	18
3.2.4	Kipini-1 well.....	19
3.3	X-ray Diffraction Analysis.....	20
3.3.1	Method Rationale.....	20
3.3.2	Method applied.....	22
3.3.2.1	Sample Preparation.....	22
3.3.2.1.1	Disaggregating the rock.....	22
3.3.2.1.2	Separating clay minerals from clastic, sulfates, oxides and carbonates rocks 22	
3.3.2.1.3	Preparing the Oriented Clay Mineral Aggregate.....	23
3.3.2.2	Air drying.....	23
3.3.2.3	Ethylene Glycol Solvation.....	23
3.3.2.4	Heating.....	23
3.3.2.5	Running the Samples through the X-ray Diffraction Equipment and Data Output 23	
3.3.2.5.1	Condition of Analysis.....	24
3.3.2.6	Clay Minerals Identification.....	24
3.3.3	Quality Control Measures.....	25
3.3.3.1	Precision and Accuracy Assurance.....	25
3.3.3.1.1	Use of Standard and Calibration of the Equipment.....	25
3.4	Smectite:Illite Ratio Determination.....	26

3.4.1	Method Rationale.....	26
3.4.1.1	Method (i).....	26
3.4.1.2	Method (ii).....	29
3.4.1.3	Method (iii)	30
3.4.2	Method Applied	31
3.5	Vitrinite Reflectance (R_o).....	33
3.5.1	Method Rationale.....	33
3.5.2	Method Applied	33
3.5.2.1	Sample Preparation	33
3.5.2.1.1	Making Polished Blocks	33
3.5.2.1.2	Kerogen Isolation and Slide Preparation	34
3.5.2.2	Vitrinite Reflectance Measurement.....	34
3.5.2.3	Quality Control Measures	35
CHAPTER FOUR.....		36
4	RESULTS AND DISCUSSION.....	36
4.1	RESULTS.....	36
4.1.1	Lamu Basin Source Rock Maturity Depths Based on Smectite Percentages	36
4.1.1.1	Simba-1 Well.....	36
4.1.1.1.1	Clay Minerals Present in Simba-1 well	36
4.1.1.1.2	Quantitative Analysis of Smectite Percentages in Illite/Smectite Mixed Layer in Simba-1 well	37
4.1.1.2	Walu-1 well.....	39
4.1.1.2.1	Clay Minerals Present in Walu-1 Well.....	39
4.1.1.2.2	Quantitative Analysis of Smectite Percentages in Illite/Smectite Mixed Layer in Walu-1 well.....	40
4.1.1.3	Maridadi-1B well	40
4.1.1.3.1	Clay Minerals Present in Maridadi-1B well	40
4.1.1.4	Kipini-1 well	42
4.1.1.4.1	Clay Minerals Present in Kipini-1 well	42
4.1.1.5	Walu-2 well.....	43
4.1.1.5.1	Clay Minerals Present in Walu-2 Well.....	43

4.1.2	Comparison of Smectite Percentages to Vitrinite Reflectance Hydrocarbon Maturity Depths in Lamu Basin	44
4.1.2.1	Simba-1 well	44
4.1.2.2	Walu-1 and 2 wells.....	45
4.2	DISCUSSION	47
4.2.1	Simba-1	47
4.2.2	Walu-1.....	47
4.2.3	Walu-2.....	48
4.2.4	Maridadi-1B.....	48
4.2.5	Kipini-1	48
4.2.6	Simba-1 and Walu-2 wells Burial Curves	48
4.2.6.1	Simba-1 well	49
4.2.6.2	Walu-1 & 2 Well.....	50
	CHAPTER FIVE	51
5	CONCLUSIONS AND RECOMMENDATIONS	51
5.1	Conclusions	51
5.2	Recommendations	51
	REFERENCES	53
	APPENDIX I: KIPINI 1 X-RAY DIFFRACTION DATA	i
	APPENDIX II: MARIDADI 1B X-RAY DIFFRACTION DATA.....	viii
	APPENDIX III: SIMBA X-RAY DIFFRACTION DATA.....	xii
	APPENDIX IV: WALU 1 X-RAY DIFFRACTION DATA	xx
	APPENDIX V: WALU-2 X-RAY DIFFRACTION DATA	xxii
	APPENDIX VI.....	xxviii

LIST OF TABLES

Table 4-1: Clay minerals identified in Simba-1 well using X-ray diffraction peaks in air dried, ethylene-glycol and heated treatments	36
Table 4-2: The 2θ angles of the X-ray diffraction peaks for ethylene glycol treated rock sample obtained at the depth of 1585-1590m of Simba-1 well	37
Table 4-3: The 2θ angles of the X-ray diffraction peaks for ethylene glycol treated rock sample obtained at the depth of 1840-1845m of Simba-1 well	38
Table 4-4: Clay minerals identified in Walu-1 well using x-ray diffraction peaks in air dried, ethylene-glycol and heated treatments	39
Table 4-5: The 2θ angles of the x-ray diffraction peaks for ethylene glycol treated rock sample obtained at the depth of 1410-1411m of Walu-1 well.....	40
Table 4-6: Clay minerals identified in Maridadi-1B well using X-ray diffraction peaks in air dried, ethylene-glycol and heated treatments	40
Table 4-7: Clay minerals identified in Kipini-1 well using X-ray diffraction peaks in air dried, ethylene-glycol and heated treatments	42
Table 4-8: Clay minerals identified in Walu-2 well from X-ray diffraction peaks in air dried, ethylene-glycol and heated treatments	43

LIST OF FIGURES

Figure 2-1: Generalized relationships between temperatures, hydrocarbon generation and changes in illite/smectite mixed layer (Tissot and Welte, 1984)	6
Figure 3-1: Location of Lamu Basin and Drilled Wells	10
Figure 3-2: October 2014 rainfall performance of the Republic of Kenya (Kongoti, 2014)	11
Figure 3-3: Regional gravity map of Lamu Basin, the major features are labeled in white. The scale indicates the free air gravity anomalies in mGal adopted from Osicki <i>et al.</i> (2015)	13
Figure 3-4: Lamu Basin Stratigraphy (Adapted from National Oil Corporation of Kenya, 1995)	15
Figure 3-5: Maridadi-1B well stratigraphy drilled in 1981 modified after (National Oil Corporation of Kenya, 1995)	16
Figure 3-6: Simba-1 well stratigraphy drilled in 1978 modified after (National Oil Corporation of Kenya, 1995)	17
Figure 3-7: Walu-2 well stratigraphy drilled in 1963 modified after (National Oil Corporation of Kenya, 1995)	18
Figure 3-8: Kipini-1 well stratigraphy drilled in 1971 modified after (National Oil Corporation of Kenya, 1995)	19
Figure 3-9: The plot for measuring the smectite: illite ratio based on angular distance Δd_2 between reflections 42° and $48^\circ 2\theta$ region, and reflection between 42° and $45^\circ 2\theta$ adapted from Srodon (1980).	27
Figure 3-10: The plot for estimating degree of ordering from initial S% and Δd_1 adapted from Srodon (1980)	28
Figure 3-11: Plot for measuring Illite: Smectite ratio based on 42° and $48^\circ 2\theta$ (y-axis) and the strong reflections that migrates from about 26° to $27^\circ 2\theta$ (x-axis) under glycol solvated condition, that are almost unaffected by domain thickness. Random and ordered cases are drawn separately, 1-8 layers/ domain distribution are represented, the open circle are for 1-14 domain distribution and a 16.9\AA ethylene glycol complex thickness adopted from Srodon (1980).	30
Figure 3-12: The plot for measuring smectite: illite ratio based on reflections which migrates from about 15.4° to $17.7^\circ 2\theta$ and from 15.4° to $17.7^\circ 2\theta$ for ethylene smectite-glycol layer thickness of 16.6, 16.9 and 17.2\AA adopted from Srodon (1980).	32
Figure 4-1: Simba-1 well stratigraphy, clay minerals occurrence and maturity zones identified from vitrinite reflectance analysis modified after NOCK (1995).	44
Figure 4-2: Walu-2 well stratigraphy, clay minerals occurrence and maturity zones identified from vitrinite reflectance analysis modified after NOCK (1995).	45
Figure 4-3: Burial history curves of simba-1 well and illite/smectite occurrence modified after (NOCK, 1995)	49
Figure 4-4: Burial history curves of Walu-2 well and illite/smectite occurrence modified after (NOCK, 1995)	50

LIST OF ABBREVIATIONS/ACRONYMS AND SYMBOLS

Å	Elemental bond distance
2θ	Range of diffraction angle of clays minerals.
R	Reichweite or ordering parameter (Terminology for expressing the probability of finding the next layer to be B, given layer A)
MBIB	Maridadi 1B
I/S	illite/smectite
NOCK	National Oil Corporation of Kenya
R _o	Vitrinite Reflectance
S%	Smectite percentage
IS	Illite smectite
ISII	Illite Smectite Illite Illite

CHAPTER ONE

1 INTRODUCTION

Source rock is a fine grained rock with organic matter content of more than 0.05mg/g of rock (Tissot and Welte, 1984). Common source rocks are shales and carbonates. After the source rock is deposited in a sedimentary basin, at the temperatures and depth of about 60°C and 1.5km respectively oil and gas are generated since the rock is termed mature (Tissot and Welte, 1984). These temperatures coincide with the onset of transformation of smectite to illite (Akande *et al.* 2005). Many source rocks especially those with organic matter from higher plants have a hydrocarbon compound know as vitrinite maceral. The vitrinite has widely been used to determine the maturity of hydrocarbon source rocks. Where the amount of light reflected by vitrinite compounds determines the reflectance of a source rock and eventually its maturity. The higher the amount of light reflected from a sample the higher its reflectance and the higher its maturity. Vitrinite reflectance values of between 0.6 -1.3% indicate oil generation, values less than 0.6% shows immature kerogen and those greater than 1.3% shows the rock sample is beyond the oil generation stage (over mature) (Tissot and Welte, 1984; McCarthy *et al.* 2011).

Clay minerals in depositional basins are highly susceptible to temperature changes. The chemistry and structure of clay minerals change with increasing temperatures and depth (Ahmed, 2008). A good example is smectite which alters to illite as temperature increases. Illite/smectite interstratifications is one of the most common clay components of sedimentary, igneous and metamorphic rocks and the most sensitive clay indicator of the degree of diagenesis and low grade metamorphism (Moore and Reynolds, 1989). The interesting aspect of smectite illitization is the coincidence of temperatures of transformation (illitization) with hydrocarbons source rock maturity (Akande *et al.*2005). Illite/smectite interstratifications have extremely small grain size and can be concentrated and separated by sedimentation. Akande *et al.* (2005) found the amount of smectite percentage (S %) in illite-smectite layers at the oil and gas generation zone to be between 40% and less than 10% in Cretaceous to Tertiary rift Basins in Southern Nigeria. Tissot and Welte (1984) gave the vitrinite reflectance values at the zone of organic matter maturity where oil and gas are generated to be between 0.6 and 1.3%. Interpretation of smectite

percentage (S %) values and vitrinite reflectance, a parameter which is widely used to determine maturity of source rocks, has aided the defining of zones of maturity in the stratigraphy of the study area. Correlation of maturity zones identified by vitrinite reflectance (R_o) with maturity zones identified by smectite percentages (S%) in smectite-illite layers has enabled identification of the influence of heating in various petroleum fields globally as a result of low pH level (acidity), high heat flow and high geothermal gradients associated with nearby geothermal systems (Miki, 2000). The latter leads to high vitrinite reflectance values but lagging smectite illitization, because illitization unlike vitrinite reflectance is also dependent on the mineralogical composition of a rock and pH levels in the basin other than temperature increase (Miki, 2000 and Miki, 1991). High acidity in a basin leads to high illitization at shallow depth where vitrinite reflectance is low (Miki, 2000). Comparing oil and gas generation zones identified by (R_o) to the zones identified by Smectite percentage has aided the determination of the state of geothermal gradient and hydrocarbon source rock maturity in Lamu Basin.

1.1 Statement of the problem

From previous studies, Lamu basin has shown good potential for petroleum resources; Walu- 1 and 2 have shown oil, Dondori -1 has shown oil and gas, Kipini -1 has shown oil , Maridadi -1 has shown gas, Kofia- 1 has shown oil and gas , Hagarso -1 has shown gas (National Oil Corporation of Kenya, 1995; Nyaberi and Rop, 2014 ; Nyagah, 1992). However the economic viability of the resources is not yet known. This requires a detailed study of the organic richness and maturity of the source rock. This study seeks to compliment the maturity data of Lamu Basin obtained using vitrinite reflectance analysis with that of clay mineral transformation, particularly transformation of smectite clays to illite which has not been applied in the Basin. In addition, some source rocks such as carbonates all over the world lack vitrinite, a good example being the common limestone source rock. This means that the maturity of the rocks cannot be determined using vitrinite reflectance which is a common organic source rock maturity measurement method other than rock eval-pyrolysis. I/S geothermometry provides an alternative method for maturity measurements in rocks such as carbonates which lack vitrinite maceral and are present in Lamu Basin stratigraphy, as well as a complementary method for the organic maturity measurement methods.

1.2 Objectives

1.2.1 General objective

To determine the suitability of using smectite illitization to identify depths of hydrocarbon source rock maturity.

1.2.2 Specific objectives

1. To identify maturity zones in the stratigraphy of Maridadi-1B, Walu-1 and 2, Kipini-1, Simba-1 exploratory wells in Lamu Basin by using S% in illite-smectite layers.
2. To compare maturity zones in the five wells given by smectite percentage (S %) with those given by vitrinite reflectance (R_0) data.

1.3 Justification and significance of the study

The first petroleum exploratory work in Kenya was done in Lamu Basin. The highest number of exploratory wells drilled is also in this Basin. Sixteen (16) petroleum exploratory wells have been drilled since 1960. Unfortunately there does not exist reports indicating the presence of economically viable petroleum resources. Data from the drilled wells have indicated oil and gas shows (Riakalui 1- oil shows, Pandagua 1- gas shows, Dodori 1- gas shows, Kencan 1- gas shows, Garissa 1- oil shows, Kofia 1- gas and oil shows, Maridadi 1b- gas and oil shows (NOCK, 1995). However, no economical petroleum resources have been found.

The organic methods such as vitrinite reflectance and rock-eval pyrolysis have been the dominant method for source rock maturity assessment in Lamu Basin and no consideration have been given to inorganic method such as clay transformation where limestone rocks lacking vitrinite maceral are also present. In vitrinite reflectance analysis, source rocks lacking vitrinite macerals, bitumen content is used which may not reflect the factual temperature-maturity relationship (Eberl and Pollastro, 1993).

The Illite/Smectite ratio geothermometry is an inorganic source rock maturity assessment method valuable for samples lacking vitrinite or other indicators from which maturity level of organic matter can be estimated (Akande *et al.* 2005). The significance of this study was to determine the suitability of Illite/Smectite geothermometry in determining the maturity depths in

Lamu Basin. The study provides more information on the burial temperature variation with depth as deduced from clay minerals transformation and thus sheds more light on likely depths of oil and gas occurrence.

1.4 Scope of the research

This research aimed at investigating whether it is possible to identify petroleum generation zones in Lamu Basin by determining the temperatures during drilling at various depths of maturity of Walu-1 and 2, Simba-1, Kipini-1, and Maridadi-1B exploration wells based on Smectite percentages (S%) in illite/smectite mixed layer, determined by x-ray diffractometry and reflections migration curves described by Srodon (1980), and also determining how illite/smectite maturity zones correlates to vitrinite reflectance (R_o) maturity zones determined by National Oil Corporation of Kenya (NOCK).

1.5 Overview of the methodological approach

For this research, 18 core samples of Walu-1 and 2 from depth range of 1093 to 3673m, 13 core samples of Simba-1 from depth range of 1593 to 3569m, 14 core samples of Kipini-1 from depth range of 982 to 3651m, and 5 core samples of Maridadi-1B from depth range of 3116 to 4175m exploration wells in Lamu Basin were obtained on 15th and 16th of October, 2015 from National Oil Corporation of Kenya (NOCK). The sampled depths approximated sampled depths for vitrinite reflectance analysis done by NOCK for the purpose of comparing maturity depths given by vitrinite reflectance to those given by smectite percentages. The samples were prepared and analysed using X-ray diffraction (X-RD) at KENGEN laboratories in Naivasha in the month of November, 2015. Data analysis was done using peak migration curves developed by Srodon (1980) and presentation was done using graphs and tables generated using Microsoft Excel 2007 to identify maturity zone. Finally the smectite percentage (S%) maturity zones were compared to vitrinite reflectance (R_o) maturity zones and depth of illite/smectite occurrence correlated to burial temperatures curves of the four wells to identify the relationship between smectite to illite transformation and burial temperature increase in each well.

CHAPTER TWO

2 LITERATURE REVIEW

2.1 Organic Matter Richness and Maturity of Lamu Basin Source Rock

The percentage kerogen within Lamu Basin sediments according to findings from kerogen quality, quantity and maturation in Pate, Walu and Dodori wells is above the requirement to yield commercial resources on maturation (Mutunguti, 1988). The amounts of kerogen vary with the age and type of the lithology. The basin has two types of kerogen; the amorphous and the humic types which are oil and gas generating types (Mutunguti, 1988). From kerogen colour, Mutunguti (1988) observed that some kerogen matter within source sediments was mature. However, Mutunguti (1988) did not indicate the depths of mature, immature and over mature organic matter.

Ngecu (2012) did an assessment of source rock maturity in the Lamu basin on Kipini-1, Walu, Simba-1 and Maridadi-1B wells based on well distribution, hydrocarbon shows, total organic carbon (TOC) levels, kerogen type and vitrinite reflectance. On his data interpretation for hydrogen-oxygen indices plot he highlighted that the major kerogen type in the Basin is type III which has or will generate gas at maturity. Very little Type II kerogen was observed giving an indication of some oil being generated on maturity.

2.2 Illitization Process and the Relationship between Illitization, Vitrinite Reflectance and Oil Generation from a Source Rock.

In their paper on prediction of petroleum generation intervals in Southern Nigeria Rift basins by means of clay transformations, vitrinite reflectance and fluid inclusion studies, (Akande *et al.* 2005) noted that interpretation of clay transformation and vitrinite reflectance data enables definition of petroleum generation zones. They noted the values of smectite percentages in illite/smectite (I/S) layers and vitrinite reflectance (R_o) at the oil and gas maturation zones to be 40% to less than 10% and 0.6 to 1.3% respectively. Tissot and Welte (1984) illustrates the relationship between source rock maturity and smectite transformation to illite (figure 2-1)

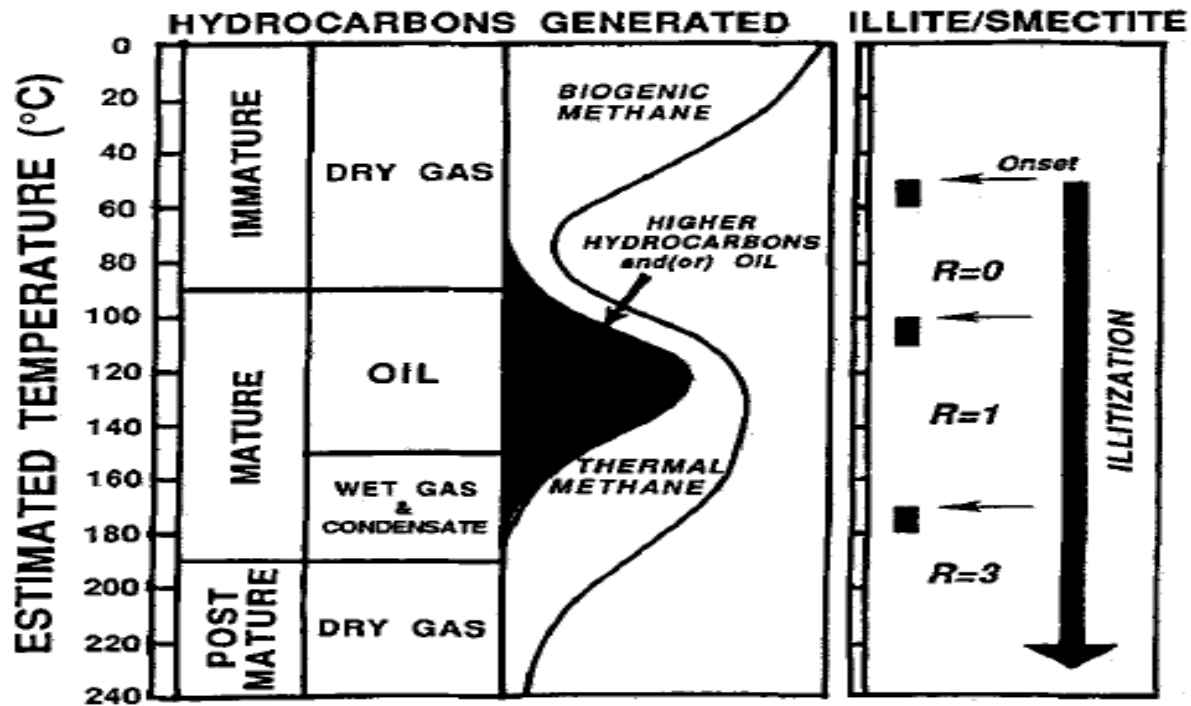


Figure 2-1: Generalized relationships between temperatures, hydrocarbon generation and changes in illite/smectite mixed layer (Tissot and Welte, 1984)

From figure (2-1) source rock maturity which is marked by the generation of oil coincides with the onset of smectite transformation to illite, according to Tissot and Welte (1984) both processes start at about 65°C.

Clay minerals vary greatly in chemical and physical properties, but most have in common platy morphology and perfect (001) cleavage, as a result of their layered atomic structures (Moore and Reynolds, 1989). Smectite is a name given to a group of minerals which include: Saponite, hectorite, montmorillonite, beidellite and nontronite (Sakharov, 1999; Stixrude and Peacor, 2002; Velde, 1986). According to Moore and Reynolds (1989) all these smectite species expands their structure when water or some organic compounds such as ethylene glycol enters the interlayer space, and contracts when the interlayer spaces lose the solvents while maintaining their crystallography.

I/S mixed layer minerals occur in sedimentary and diagenetic-hydrothermal environments (Eberl *et al.* 1984; Alt. *et al.* 1991; Bell, 1986; Kazerouni *et al.* 2012; Bloch *et al.* 2002). Sedimentary

environments are depressions on the earth surface that forms depositional basins, where rate of reactions depends on rate of deposition and subsidence, while diagenetic-hydrothermal environments are zones which have been in contact with hot waters (Eberl *et al.* 1984). In these environments, Illite/smectite mixed layers minerals are formed by dissolution of smectite mineral majorly as a result of temperature increase (Eberl & Pollastro, 1993; Neil *et al.* 1987). Smectite clays (the origin of authigenic I/S mixed layer minerals) contain more soluble elements and are therefore formed in dry climate and poorly drained soils where these elements accumulate. Eberl and Pollastro (1993) noted that the distribution of smectite minerals in marine sedimentary environments is not as regular as that of other minerals, suggesting formation of smectite through neoformation in this environment, meaning that the clays are precipitated from solution or forms from reaction of amorphous material.

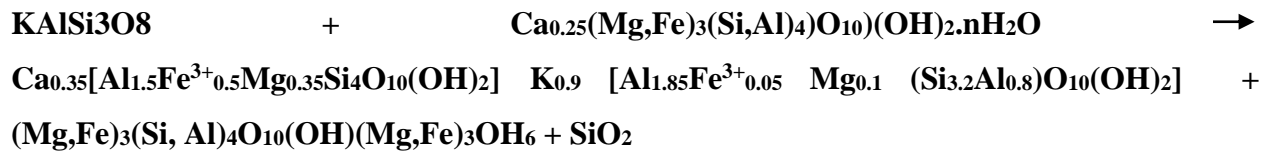
Mixed layer illite-smectite minerals are hydrous aluminium silicates just like other clay minerals. Clay minerals are classified as either phyllosilicates or layer silicates (Moore and Reynolds, 1989; Inoue, 1987; Ji *et al.* 1997; Jiang, 2012). The illite-smectite mixed layer belongs to the latter class. The term mixed-layer is synonymous to interlayer or interstratifications, it is used to refer to clay minerals formed of two or more kinds of layers. The layers are stacked along a layer perpendicular to (001). Constituent layers are stacked in random, partially ordered, or ordered sequence (Sakharov, 1999). R=1 is a type of ordering in I/S mixed layer representing 50/50 constitution of illite and smectite layers, while, R=3 ordering is represented by ISII sequence i.e., three illite layers surrounding a smectite layer (Sakharov, 1999).

The layers are developed from either corner-linked tetrahedral sheet or edge-linked octahedral sheet (Moore and Reynolds, 1989). In tetrahedral sheet the dominant cation is Si^{4+} but it is substituted by Al^{3+} frequently and occasionally by Fe^{3+} (Moore and Reynolds, 1989). The cation-oxygen ratio for tetrahedral layer silicate is 2:5. Octahedral sheet cations are usually Al^{3+} , Mg^{2+} , Fe^{2+} , Fe^{3+} but also other transition elements have been identified except Sc (Moore and Reynolds, 1989). The layer of illite mineral in mixed layer I/S is stacked on a layer of smectite mineral with similar or different sheet structure (Sakharov, 1999).

When shale containing smectite is deposited in a sedimentary environment such as a subsiding basin, it is then buried, heated and eventually undergoes diagenesis. Smectite is converted to

mixed layer illite-smectite as a result of increased burial depth and temperature. Perry and Hower (1970) noted that this reaction starts at about 60°C in U.S Gulf coast sediments. Initially, the distribution of illite and smectite layers in I/S is random, but it becomes ordered when about 65% of the layers are illite. The transformation is represented by equation (1), the overall general reaction (after Eberl and Pollastro, 1993).

K-feldspar + Smectite → I/S + Chlorite + Quartz (1)



The above reaction is considered to proceed by transformation, where the arrangement of tightly bound octahedral, tetrahedral or fixed interlayer cation is modified (Eberl and Pollastro, 1993). In U.S Gulf Coast sediments Perry and Hower (1970) noted from chemical data that Al³⁺ substitutes for Si⁴⁺ in the clays' tetrahedral sheets, thereby increasing the negative charge on the smectite interlayer. Interlayer potassium dehydrates when a critical layer charge is reached, thereby transforming expanded smectite interlayers into non-expanding illite interlayers.

While using I/S ratio in geothermometry Eberl and Pollastro (1993) highlight some of the recommended factors to consider. If possible it is important to establish the original composition of smectite/illite (I/S) in the rock units under study, because many rocks contain a heterogeneous assemblage of I/S. To add to that, presence of detrital I/S may result in a high proportion of illite layer, because previous burial may have caused extensive illitization. Eberl and Pollastro (1993) continues to argue that usually, the I/S ratio and type of ordering are heterogeneous in any one sample due to mixture of detrital and authigenic clays. Eberl and Pollastro (1993) therefore indicate that, it is necessary to analyse several samples in horizontal and vertical profiles on either local or regional scale to establish other factors other than temperature. They further suggest that use of thin section scanning electron microscopic study can aid in determining detrital and authigenic clays. Other information that they recommend to be considered about the study area includes; burial history, geothermal gradient, present day well temperatures or the possibility of local thermal events that may have quickened, slagged or inhibited diagenesis of smectite.

CHAPTER THREE

3 MATERIALS AND METHODS

The materials used in this research involved drilled core samples, X-ray diffractometer, *Brucker* and *Geographical Information System* (GIS) computer softwares and reagents used in X-ray diffraction analysis for clay minerals, Illite/Smectite mixed layer identification and quantification of illite/smectite ratio in the forty eight (48) core samples obtained from Lamu Basin, and reviewed data of vitrinite reflectance (R_o) analysis done by NOCK.

3.1 Study Area

3.1.1 Location and Description

The Lamu basin is bound by the Equator and 4°30'S latitude and by longitudes 39°00'E and 44°00'E and covers a large area of southeastern coastal Kenya with an area extent of 132,720 square kilometers (Fig. 3-1). The basin has sediment thickness ranging from 3 km onshore to 13 km offshore (Nyaberi and Rop, 2014). According to Nyagah (1995), Lamu Basin formed as a result of failed arm of a tri-radial rift system that developed passively in the Mesozoic after the subsequent drift of Madagascar from the East Africa coast. The separation of Madagascar along a strike slip transverse fault (Davie fracture zone) in late Mesozoic times created an initial transform margin structure (Reeves *et al.* 1987). Passive margin development accompanied sediment deposition on a continental margin that underwent periodic rifting and subsidence until recent times (Karanja, 1982; National Oil Corporation of Kenya, 1995). It is the largest sedimentary basin in Kenya.

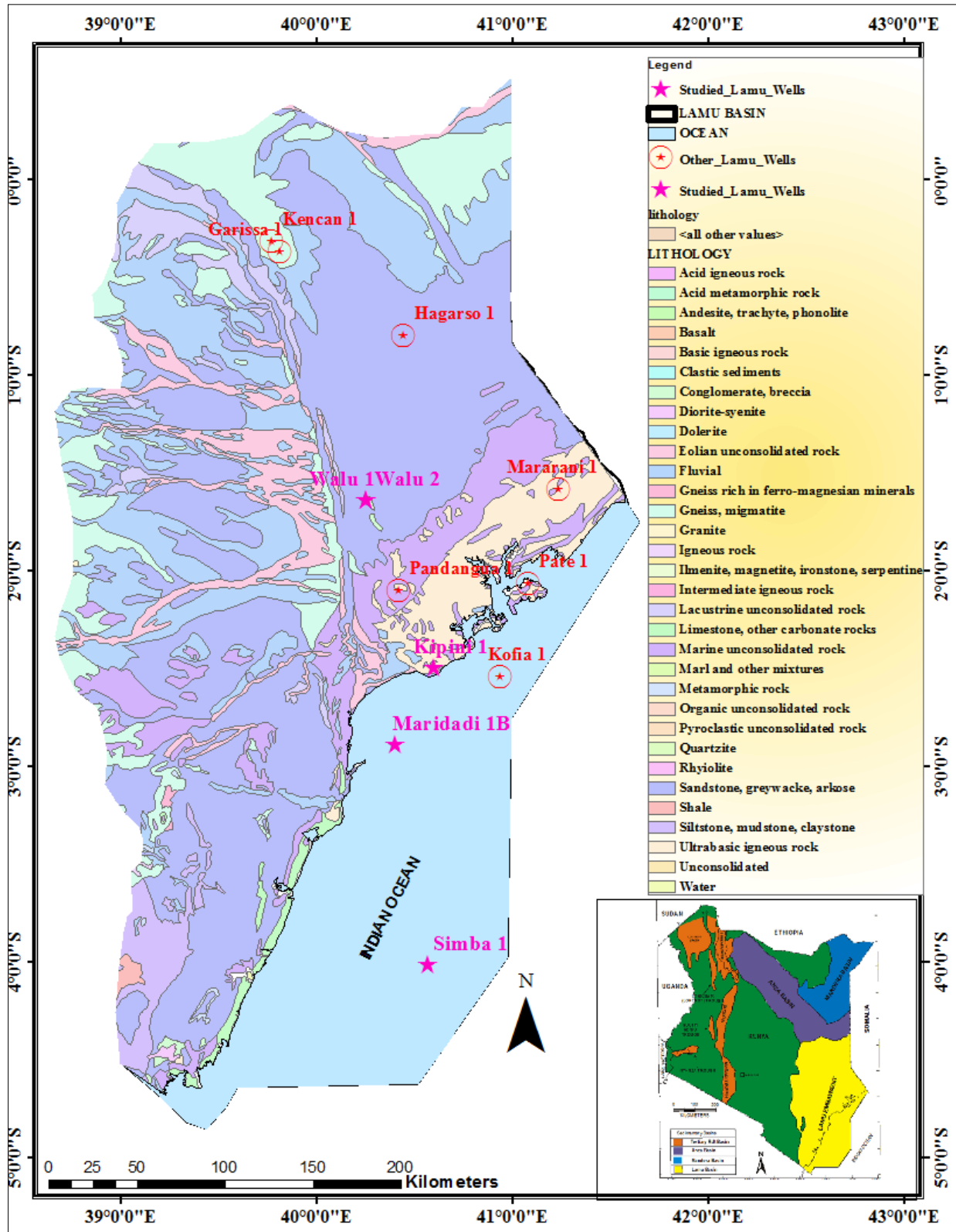


Figure 3-1: Location of Lamu Basin and Drilled Wells

3.1.2 Climate

The rainfall pattern in Lamu Basin is bimodal with the long rains falling throughout the county from mid-April to the end of June with light showers in July. Temperatures throughout the county are usually high ranging from 23°C to 30°C. (Kongoti, 2014).

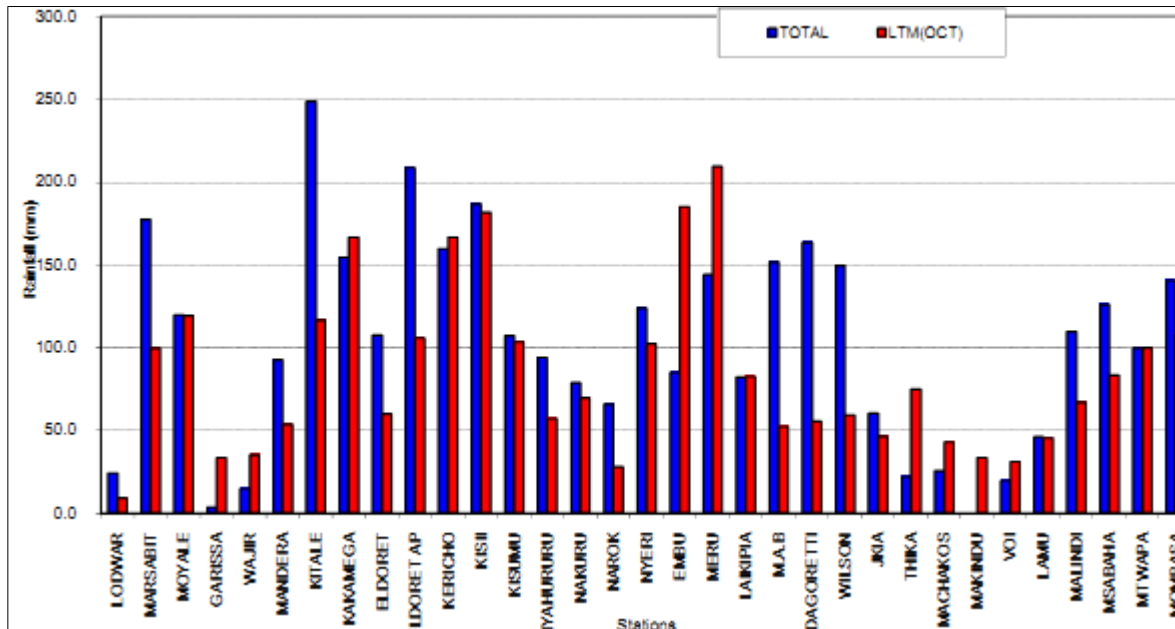


Figure 3-2: October 2014 rainfall performance of the Republic of Kenya (Kongoti, 2014)

3.1.3 Vegetation

Lamu Basin vegetation is dominantly comprised of closed to open low shrubs, closed to open woody vegetation and broad leaved evergreen multilayered trees (Ministry of Environment and Natural Resources of Kenya, 1985).

3.1.4 Land use and Land Resources

Since Lamu Basin is located on the coast line of the Indian Ocean, it benefits from beaches and islands such as Pate, Manda and Lamu among others. These provide tourism sceneries as well as fish breeding sites in the islands (Ministry of Environment and Natural Resources of Kenya, 1985).

3.1.5 *Physiography and Drainage*

The Lamu Basin is characterized by a low, almost level plain with the exception of the coastal sand dunes and the Mundane Sand Hills. The sand dunes and the sand hills hardly exceed 50 m above sea-level. Few of their slopes exceed 5. Due to the low level of the land, a large part of the Basin is susceptible to flooding. Although most of the land is a low plain, it can be divided into six terrain types as follows: the Tana Delta, the coastal plains, the Podori river plain, the sand dune system, offshore islands and the Indian ocean water (Ministry of Environment and Natural Resources of Kenya, 1985 and Nyandat & Oswaggo, 2013).

3.1.6 *Geology and Structural Setting*

3.1.6.1 *Structural Setting of Lamu Basin*

Situated in the northern part of the Basin is a NW-SE trending structural basement high (the Garissa High), while in the southern part is a N-S trending basement uplift (the Walu and Tana synclines), this is believed to be an onshore continuation of the Davie Fracture Zone and the Cap Saint Andre Axis (NOCK, 1995). On the western boundary of the basin is an N-S trending fault that separates the Karroo rocks from the outcropping Precambrian basement, which shows a distinct tectonic direction, exhibited by structural elements in the basin. An example of a structural element is the Hargaso anticline (section of 181 km running NW–SE), which includes Hargaso well in Dodori area in the basin (NOCK, 1995). There are few unconformities in the stratigraphy of Lamu sedimentary Basin. For instance, the unconformity on the lap of Paleocene and late Eocene on the Cretaceous period is very clear (Nyagah, 1995). The major structural elements in the Lamu basin include; the ENE-WSW structural high trending from Garissa to Walmerer High, with N-S strike and NE-SW structural low (Simiyu, 1989 and Nyagah, 1992). In the Triassic, common traps are mainly block faulted anticlinal structures (Nyaberi and Rop, 2014). In the Cretaceous, structural-stratigraphic traps associated with the Ewaso sand and Kofia sands are present within the sequence (NOCK, 1995). Various large intra-basinal anomalies have been mapped, using seismic, gravity and by aeromagnetics, along the near shore areas of the coast (Osicki *et al.* 2015). The largest of these structures covers 400 sq. km.

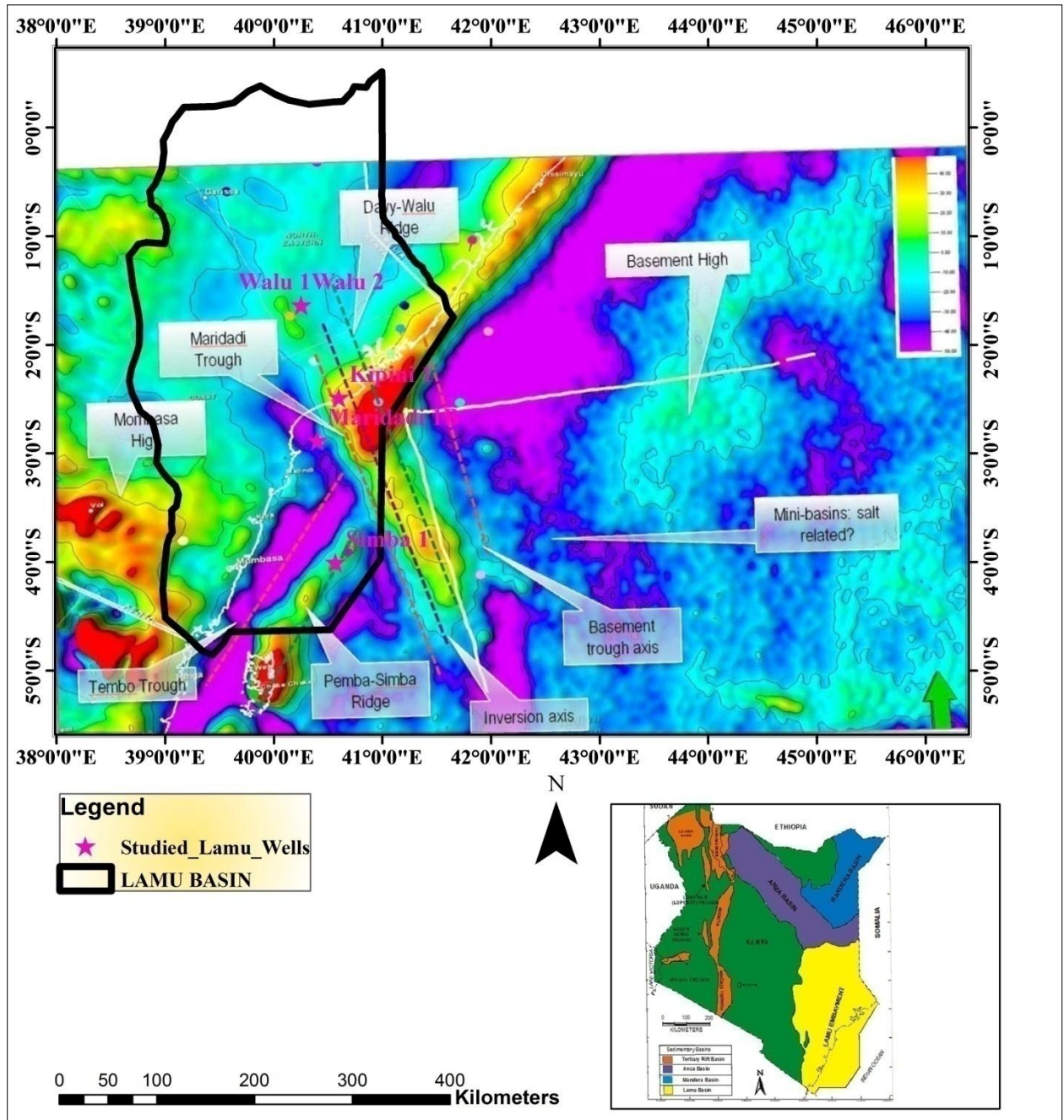


Figure 3-3: Regional gravity map of Lamu Basin, the major features are labeled in white. The scale indicates the free air gravity anomalies in mGal adapted from Osicki *et al.* (2015)

3.1.6.2 Regional Geology

Regional geology of Lamu Basin comprises Neoproterozoic high-grade Metamorphic rocks of the Mozambique Belt, overlain by thick sedimentary sequences (about 3-12 km thick) (Tissot and Welte, 1984). The high grade metamorphic rocks of the Mozambique belt include: granite, granitoids gneisses, quartzites, migmatites, biotite and hornblende gneisses and amphibolites (Caswell, 1953). The sedimentary sequences are grouped into four major stratigraphic sequences which are of Jurassic through to Tertiary age. They are; *Megasequence I (Karoo Group)*, *Megasequence II (Sabaki Group)*, *Megasequence III (Tana Group)* and *Megasequence IV (Coastal Group)*, from the oldest to the youngest (Nyagah, 1995).

3.1.6.2.1 Megasequence I (Karoo Group)

Comprise of sandstones and represents the oldest sedimentary units of Lamu Basin. The sandstones include; Upper Mazeras sandstones, Mazeras sandstones, Mariakani sandstones, Maji ya Chumvi limestones, and Taru grits. They are of Permian through to Triassic age (Nyagah, 1995). Karoo rocks in Lamu Basin are typically sequences of terrigenous clastic sediments associated with long periods of continental intracratonic sedimentation (National Oil Corporation of Kenya, 1995).

3.1.6.2.2 Megasequence II (Sabaki Group)

It is formed by lithostratigraphic assemblages ranging in age from Early Cretaceous to Early Paleocene. The assemblages formed from two marine regressions and one transgression. They include: the Ewaso Sands, the Walu Shale, the Hagarso Limestone, the Frere Limestone and the Kofia Sands (Nyagah, 1995).

3.1.6.2.3 Megasequence III (Tana Group)

Consist of rocks of Eocene to Oligocene that were deposited in three phases of sea level rise and a single regressive phase of deposition. The rocks units of the Tana Group are: *Kipini Formation*, comprising of Pate Limestone, Linderia Limestone and Dadori Limestone Members and the *Barren Beds Formation* (National Oil Corporation of Kenya, 1995).

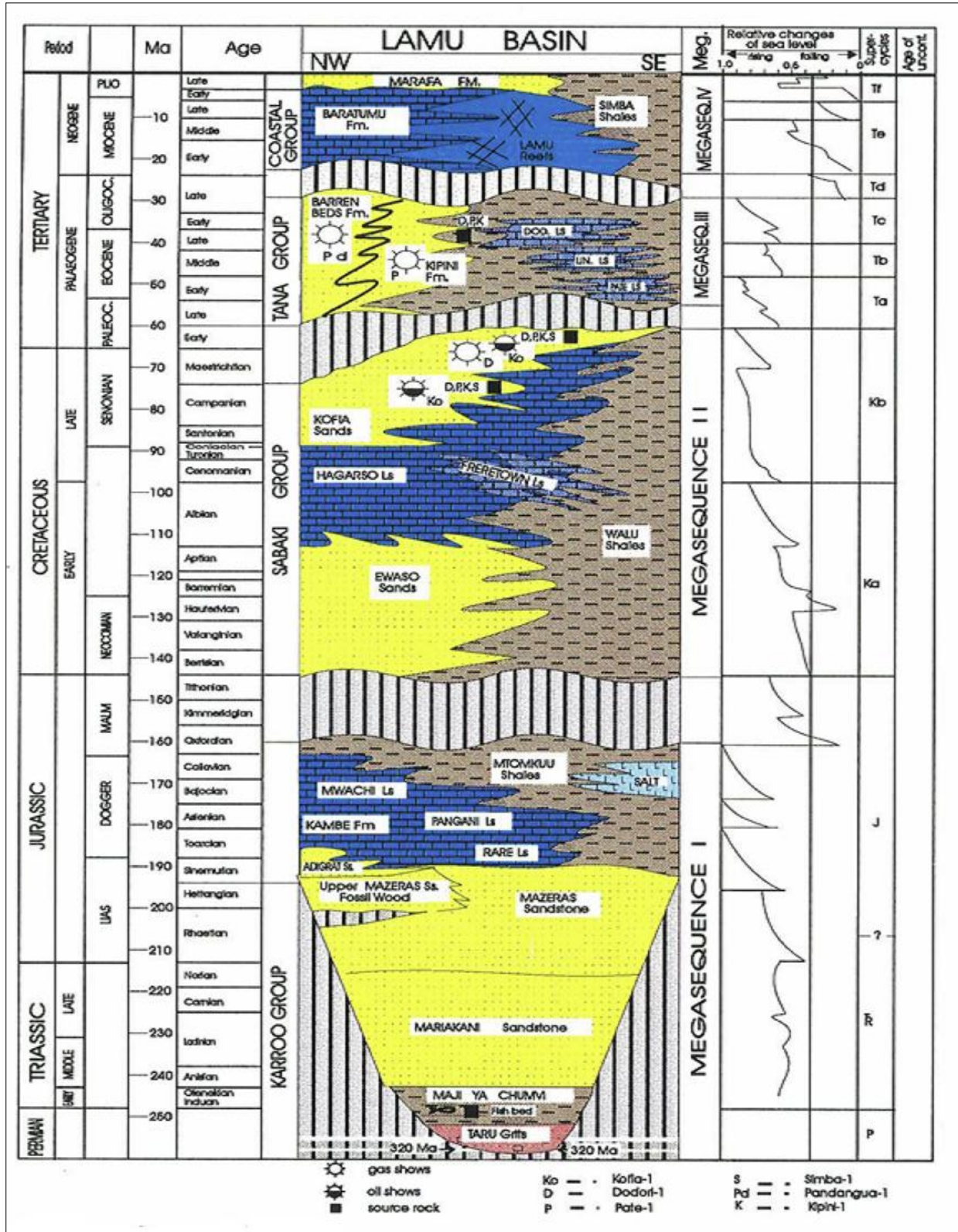


Figure 3-4: Lamu Basin Stratigraphy (Adapted from National Oil Corporation of Kenya, 1995)

3.1.6.2.4 Megasequence IV (Coastal Group)

It is made of carbonate sequences associated with marine shales and an overlying siliciclastic sequences. The lithostratigraphic units of the Coastal Group were deposited during three major cycles of sea level change and they include: the Baratumu Formation, the Lamu Reefs, the Simba Shales, and the Marafa Formation (National Oil Corporation of Kenya, 1995).

3.2 Stratigraphy of the Considered Wells

The wells were selected based on availability of core samples and vitrinite reflectance data at National Oil Corporation of Kenya facilities.

3.2.1 Maridadi 1B well

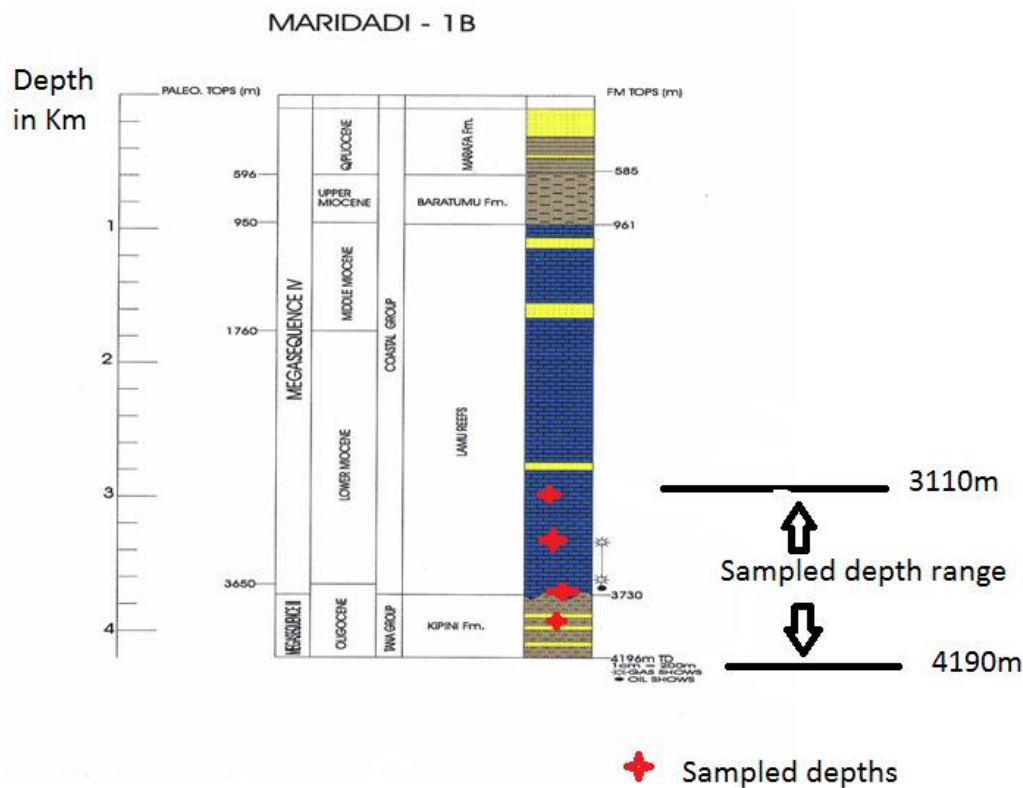


Figure 3-5: Maridadi-1B well stratigraphy drilled in 1981 modified after (National Oil Corporation of Kenya, 1995)

A total of ten samples were obtained from Maridadi-1B offshore well; two samples from limestone of the *Lamu Reefs* and eight samples from limestones and shales of the *Kipini* formation.

3.2.2 Simba-1 well

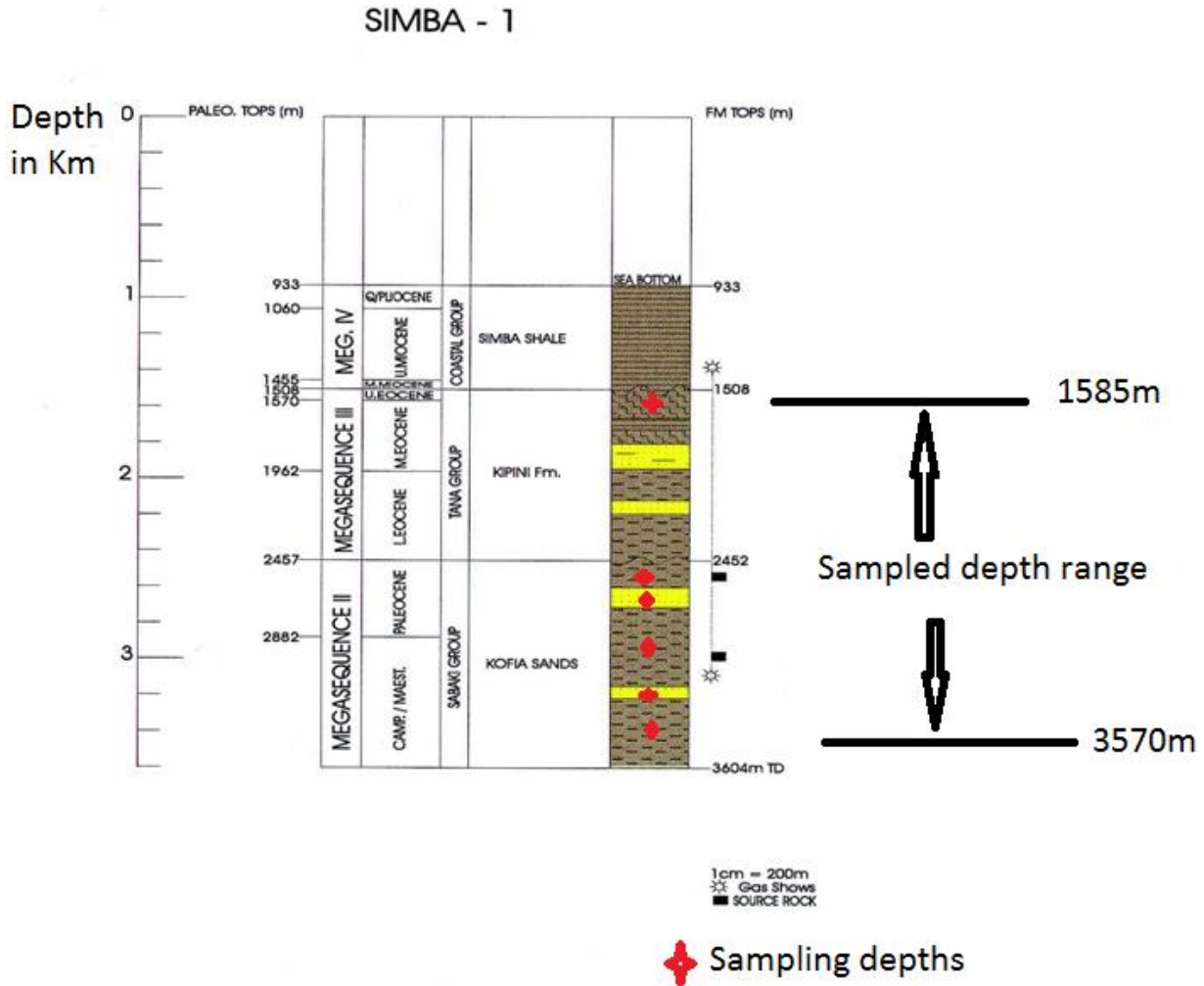


Figure 3-6: Simba-1 well stratigraphy drilled in 1978 modified after (National Oil Corporation of Kenya, 1995)

A total of fourteen samples were obtained from Simba-1 offshore well; two from shales of the *Kipini* formation, eight from shales and four from sandstones both of the *Kofia sands* formation.

3.2.3 Walu-2 well

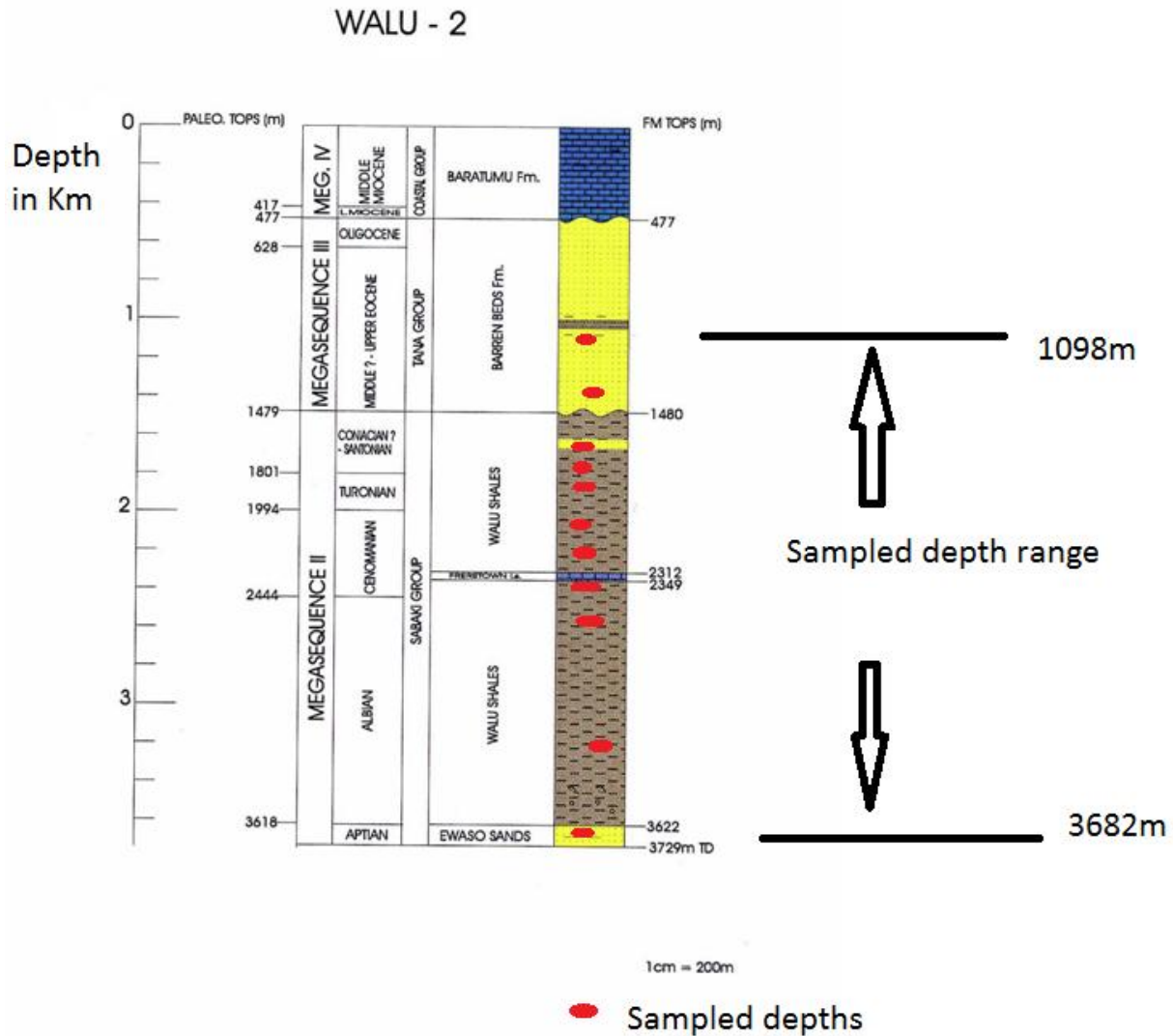


Figure 3-7: Walu-2 well stratigraphy drilled in 1963 modified after (National Oil Corporation of Kenya, 1995)

A total of fifteen samples were obtained in Walu-2 onshore well; two from sandstones of the *Barren bed* formation, one from sandstones of the *Walu shales*, ten from shales of the *Walu shales* and two from sandstones of the *Ewaso sands*.

3.2.4 Kipini-1 well

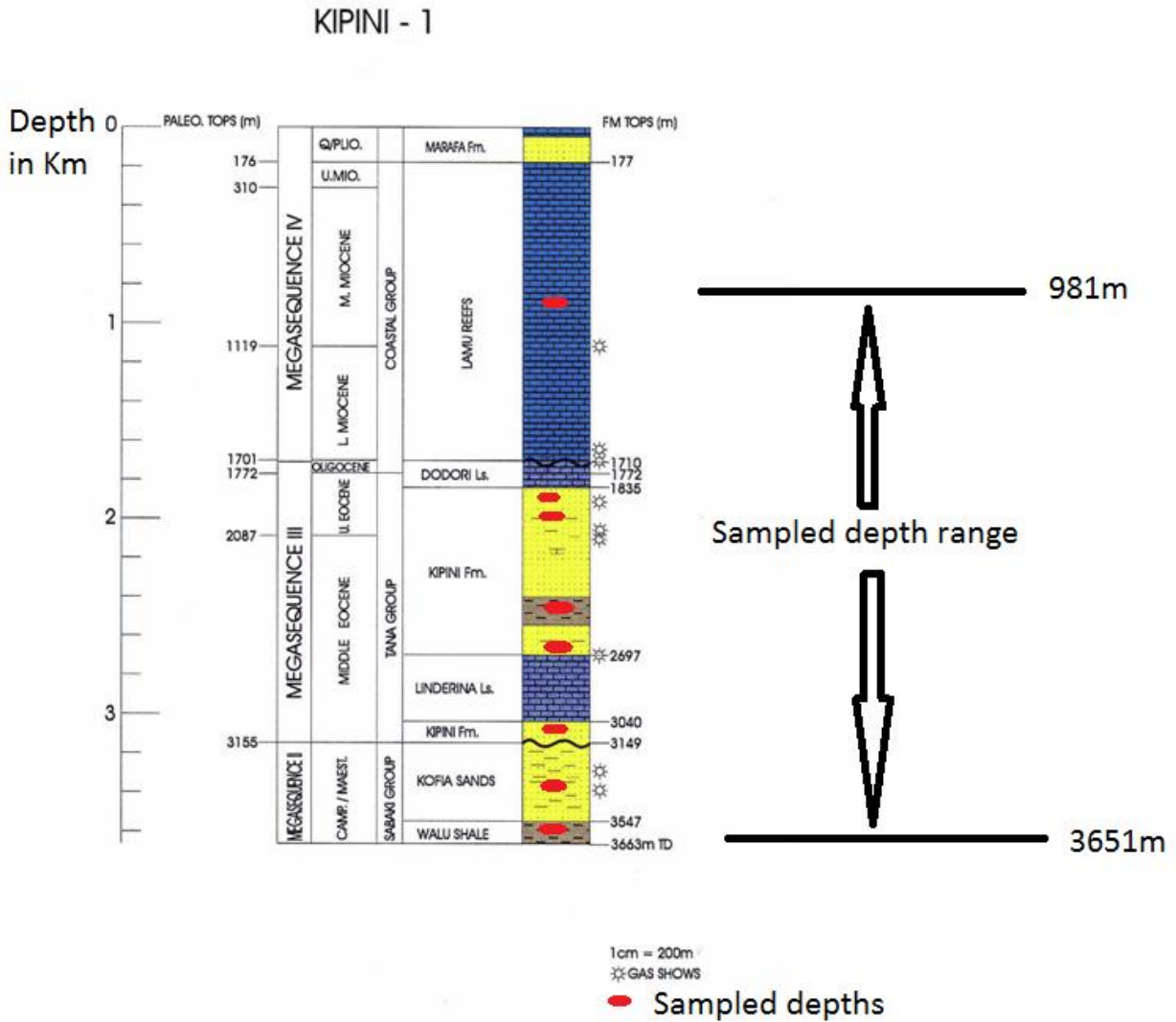


Figure 3-8: Kipini-1 well stratigraphy drilled in 1971 modified after (National Oil Corporation of Kenya, 1995)

A total of twelve samples were obtained in Kipini-1 onshore well; one sample each from limestones of the *Lamu reefs* and the *Dodori limestones*, three samples each from sandstones and limestones both of the *Kipini Formation*, one from limestones of the *Linderina limestones*, two from sandstones of the *Kofia sands* and one from limestones of the *Walu shales*.

3.3 X-ray Diffraction Analysis

3.3.1 Method Rationale

Clay minerals are identified using X-ray diffraction patterns (diffractograms) of oriented aggregates that enhance basal reflections (along z-direction); this is because structures of most clay minerals are very similar in x-y direction. The atomic pattern along z direction is what is different from one clay mineral to another (Moore and Reynolds, 1989; Reynolds, 1992). Description of mixed layered/ interstratified clay minerals requires identification of types of layers involved (e.g. illite and smectite), the proportion of each, the type of order and the thickness of ethylene the glycol interlayer (Srodon, 1980).

X-rays used in X-ray diffractometer are generated when electrons moving at high velocity collide with matter. An incident electron may hit and displace a tightly held electron near the nucleus of the atom (K-shell) creating a vacancy (Klug and Alexander, 1954). This makes the atom unstable and the vacancy may be filled by an electron from one of the outer shells. If an electron from the second energy level (L-shell electron) fills the vacancy the emitted energy is designated K_{α} radiation and if the vacancy is filled by an electron from the third energy level (M-shell electron) the emitted energy is designated K_{β} radiation (Klug and Alexander, 1954). This change of energy level by electron leads to emission of monochromatic X-ray radiation with a wavelength that is characteristic of the atom involved. The X-ray diffractometer uses K_{α} radiations (Klug and Alexander, 1954).

When describing the sample preparation procedure for clay X-ray diffraction analysis (Moore and Reynolds, 1989) suggested that treatments to eliminate organic matter and iron oxides are likely to alter the mixed-layered clay minerals. Yet if they are not removed, the diffraction patterns may be so poor that one will not be able to have acceptable interpretations. They recommend that the poor diffraction patterns can be improved by using step-scanning procedures with long count-time intervals or by recording the pattern at slow goniometry and strip chart speeds in conjunction with long time constants.

Organic matter can also produce broad X-ray diffraction peaks, increase the background and inhibit dispersal of other minerals if found in significant amounts (Moore and Reynolds, 1989). Iron oxide also cements particles together and therefore inhibits dispersion of clay mineral

particles. They proposed use of sodium hypochlorite (NaOCl) to chemically remove organic matter, because it is quicker, cheaper and safer than the frequently recommended hydrogen peroxide. However, Moore and Reynolds (1989) warn that use of sodium hypochlorite can oxidize ferrous iron in the octahedral site, causing a change in the silicate layer charge and altered clay mineral diffraction characteristics.

In precise identification of illite/smectite interstratifications by X-ray powder diffraction there is a possible variation in peak position mainly due to variable thickness of the smectite-ethylene glycol complex (Srodon, 1980). Reynolds and Hower (1970) gave the thickness of the smectite-ethylene glycol complex to be between 16.90 Å and 17 Å. (Srodon, 1980) noted that the difference between 17Å and 16.9Å is large enough to account for 15-20% error in estimation of the component ratio of illite/smectite if a wrong value of the smectite-ethylene complex thickness is chosen.

Use of peak migration-curves to estimate interstratifications in illite/smectite mixed layer minerals, can only be used for two-component illite/smectite with Random or Maximum ordering of R=1, 2 or 3 but not for illite/smectite with segregated illite or smectite layers or with intermediate degree of ordering (Srodon, 1980). Moreover, the peak migration-curves are used for ethylene glycol treated illite/smectite and usually are based on the assumptions that all smectite interlayers contain two glycol layers and that their swelling properties do not depend on exchangeable cations, and that, the smectite layers are K-bearing (Sakharov, 1999).

Moore and Reynolds (1989) and Sakharov (1999) recommend the use of a technique that is based on comparison between experimental X-ray diffraction curves and curves calculated for structural models to determine smectite percentage in illite/smectite clay minerals. They termed the technique as the most effective for determination of the structural parameters for mixed layer minerals. However the simulation of X-ray diffraction patterns requires many structural and instrumental parameters that are known only approximately and require extensive work to determine (Sakharov, 1999).

X-ray diffraction basal spacing d ((001) of pure illite and smectite are 10Å and 15Å respectively under air dried condition (Sakharov, 1999; Moore and Reynolds, 1989, Eberl and Pollastro, 1993). Under ethylene glycol-solvated condition the diffraction pattern of smectite changes

significantly to 19Å (Moore and Reynolds, 1989). Srodon (1980) stated that mixed-layer illite/smectite under solvated condition produces diffraction patterns at the region near 16 to 17° 2θ. The interstratifications are ordered and probably reach in smectite if ethylene glycol solvation produces a peak at 5.2 and 8.7°2θ (Srodon, 1980).

3.3.2 Method applied

X-ray diffraction analysis was done on forty eight (48) core samples from Walu-1 and 2, Kipini-1, Simba-1 and Maridadi-1B wells of Lamu Basin, at KENGEN laboratories in Naivasha using **SHIMADZU XRD 700**x-ray diffractometer. **Brucker** software was used in identifying the X-ray diffraction reflection peaks. The forty eight samples were first prepared appropriately prior to running them through the X-ray diffractometer.

3.3.2.1 Sample Preparation

The forty eight (48) core samples from Walu-1, Simba-1, Maridadi-1B and Kipini-1 in Lamu Basin, were prepared following KENGEN procedures for clay minerals analysis as described below.

3.3.2.1.1 Disaggregating the rock

About 25g of each sample was crushed with an iron mortar and pestle, until the grains were about less than two millimeters (2mm) in diameter, to increase the specific surface area of the grains and make the subsequent procedures effective.

3.3.2.1.2 Separating clay minerals from clastic, sulfates, oxides and carbonates rocks

10g of the crushed sample was weighed and mixed with 0.15g of sodium hydroxide (dispensing agent) in a 500ml bottle, 100ml of distilled water was added into the bottle and the mixture was well shaken. The mixture was sieved through a 63µm sieve and then poured into a litre-measuring cylinder, into which distilled water was added upto the 1000ml mark. The mixture was left to settle overnight with various rock sizes settling out of the mixture according to Stoke's law. Which states that clay minerals grains occupy the suspension from the surface of the mixture to about 20.9cm mark, while the carbonates, sulphates, oxides and clastic rocks occupy the rest of the mixture, from the 20.9cm mark to the bottom.

A graduated tube was immersed into the mixture in the measuring cylinder until the 20.9cm mark touched the clay and the water mixture level. The clay sample was then drawn into the tube using a peristaltic pump after which it was dried in an oven at 105°C to get rid of water and the dispersing agent.

3.3.2.1.3 Preparing the Oriented Clay Mineral Aggregate

80mg of the dry sample was weighed and mixed with 1ml of distilled water in a test tube. The test tube with the sample and the water mixture was placed in an ultrasonic bath and agitated for 1hour for further clay dispersion. A slurry was produced which was drawn from the test tube and mounted on a glass slide where it was flattened by gently pressing using a flat firm object.

3.3.2.2 Air drying

The clay samples on the glass slide were left to dry overnight, after which they were ready for air dried X-ray diffraction analysis.

3.3.2.3 Ethylene Glycol Solvation

After recording diffraction patterns for the air dried condition, the same samples were mixed with 2-3 drops of ethylene glycol and left for some time for the ethylene glycol to be well absorbed in clays' lattice. After which the samples were ready for glycol-solvated X-ray diffraction analysis.

3.3.2.4 Heating

After recording the diffraction pattern in glycolated condition, the samples were heated in a furnace for 2hrs at 220°C, and then left to cool slowly in an oven for 2hrs, after which the samples were ready for heated X-ray diffraction analysis.

3.3.2.5 Running the Samples through the X-ray Diffraction Equipment and Data Output

Ten samples were run through *SHIMADZUXRD 700* X-ray diffractometer at a go during each analysis (air dried, glycolated and heated analysis), until all the forty six samples were analysed, at five runs for every analysis. The recorded diffraction patterns were relayed to a computer, where a *Brucker* software helps in displaying the diffraction graphs and identifying the strongest peak reflections.

3.3.2.5.1 Condition of Analysis

The X-ray diffraction analysis was done under the following condition:

X-ray generation was done using copper (Cu) target, voltage of 30.0kV, and current of 30.0mA. Measurements done were axis measurement in Theta-2-Theta (θ 2 θ). Scan range was at $10.0000 < \theta < 80.0000$ degrees, step size was 0.0200 degrees, count time was 0.60 seconds, at the speed of 2.0000 (degrees/minute) in continuous scan mode. Slits used were; Divergence of 1.00000 (degrees), Scatter of 1.00000 (degrees), and Receiving of 0.30000 mm.

3.3.2.6 Clay Minerals Identification

Identification of clay minerals was done by comparing peak position and intensities to published values in the literature. Other than illite/smectite mixed layer, chlorite, illite, and smectite were identified since they are common in sedimentary rocks. According to Moore and Reynolds, (1989) chlorite and kaolinite have basal diffraction peaks based on first order reflection of 14.2 Å and 7.1Å respectively. Sodium saturated vermiculite gives a strong peak in the $7^{\circ}2\theta$ region (Moore and Reynolds, 1989) while magnesium rich vermiculite gives a strong peak in the $14.5^{\circ}2\theta$ region that is not affected by glycol solvation.

Smectite is identified by comparing the diffraction patterns of air-dried and ethylene glycol-solvated preparations (Srodon, 1980: Moore and Reynolds, 1989). In glycol treated preparation smectite gives very strong 001 reflection at about $5.2^{\circ}2\theta$ (16.9Å), which in the air-dried condition shifts to about $6^{\circ}2\theta$ (15Å). Illite has a strong 001 reflection of 10Å under air dried, ethylene glycol solvation and heated treatments (Moore and Reynolds, 1989).

The illite/smectite mixed layer was identified by studying and comparing diffraction patterns produced from both air dried and ethylene glycol-solvated sample preparations. Under ethylene glycol solvation condition the smectite X-ray reflection peak shifts from $15^{\circ}2\theta$ to between 17 and $19^{\circ}2\theta$. The significant change in diffraction pattern between an air dried and ethylene glycol-solvated clay is as a result of smectite structure swelling after absorbing water molecules from ethylene glycol (Eberl and Pollastro, 1993: Moore and Reynolds, 1989). This peak shift confirms the presence of a smectite component. Since ethylene glycol solvation has little effect

on vermiculite, and other likely layers are not affected at all by this treatment (Moore and Reynolds, 1989).

According to Moore and Reynolds (1989) the interstratification is random if the ethylene glycol solvation produces a peak near $5.2^{\circ}2\theta$. A reflection of 002/003 (the second or third ordering) at the region near 16 to $17.7^{\circ}2\theta$ from an ethylene glycol-solvated sample indicates presence of an illite/smectite phase (Moore and Reynolds, 1989).

Confirmation of the illite/smectite identification was done by heating the sample to 220°C for two hours, (the temperatures and time of heating depends with the sample thickness). The heating dehydrates the smectite structure thus reducing in size (collapses). The diffraction pattern of heated sample should be similar to that of pure illite (10\AA structure) with a relatively weak 003 reflection (Moore and Reynolds, 1989).

3.3.3 Quality Control Measures

3.3.3.1 Precision and Accuracy Assurance

Precision is the ability to get the same answer (correct or incorrect) from each of a set of multiple measurements, while accuracy is the difference between the obtained results and the correct answer (Moore and Reynolds, 1986). To uphold accuracy and precision in this analysis, the techniques of using standard and calibrating equipment were used as described below.

3.3.3.1.1 Use of Standard and Calibration of the Equipment

A silicon standard sample was used. Silicon has three strong and distinct diffraction peaks at $28.4160^{\circ} 2\theta$, $47.2709^{\circ} 2\theta$ and $56.0857^{\circ} 2\theta$. Therefore the standard sample was run at the beginning and at the end of any analysis to monitor the accuracy of the equipment. Quartz peak positions are invariant because the quartz structure tolerates no significant atomic substitutions. Thus silicon grain is used as a standard against which accuracy and precision of peak position can be estimated for other phase present.

The *SHIMADZUXRD 700X*-ray diffractometer equipment is calibrated once an year by the supplier. The equipment also calibrates automatically once switched on before any analysis is started.

3.4 Smectite:Illite Ratio Determination

3.4.1 Method Rationale

Reynolds and Hower (1970), Corbato (1982) and Corbato (1987) recommended a method for determining illite/ smectite ratio in a mixed layer mineral which involves the determination of the position of the illite/smectite reflection. They suggested using the reflection which migrates from 15.7° to $17.7^\circ 2\theta$ (peak migration curves) for Cu k_α , after having taken into account the type and degree of ordered interstratification. They argued that using these reflections avoided most of the error caused by peak shift due to small domain (volume of a structure which scatters X-rays coherently) size. Srodon (1980) redescribed Reynolds and Hower (1970) method of determining illite/smectite ratio but demonstrated the importance of determining the layer spacing of a smectite treated with ethylene glycol to obtain accurate illite to smectite ratio. To achieve this Srodon (1980) explained that additional peak position must be determined because the layer spacing of smectite glycol complex is an additional variable.

Three illite/smectite interstratifications quantification methods by peak migration curves are described in Srodon (1980); Srodon (1981); Srodon (1984); Srodon (2009); (i) use of difference in 2θ of the reflections in the region 42° to $48^\circ 2\theta$ (Cu K_α), (ii) Use of the stronger of the reflections between 42° and $48^\circ 2\theta$ and the strong reflection that migrates from about 26° to $27^\circ 2\theta$, and (iii) use of peaks which migrates from 26° to $27^\circ 2\theta$ and from 15.4° to $17.7^\circ 2\theta$. These methods are useful for samples free of individual illite (not part of illite/smectite interstratifications).

3.4.1.1 Method (i)

Srodon (1980) termed method (i) the most preferred since it avoids any significant error caused by domain size by using peak position at high diffraction angles. However, Srodon (1980) informs that the peaks are relatively weak, and may not be measurable for some samples. More so, the reflections merge at high illite content. In such an instance Srodon (1980) recommends the use of the second or third method.

Method (i) uses the difference in 2θ of the two reflections in the region $42^\circ - 48^\circ 2\theta$ (Cu K_α). Srodon (1980) terms the difference as Δd_2 and is independent of domain size and only slightly affected by ethylene glycol-smectite layer thickness. The relationship between percent smectite

layer and 2θ difference depend greatly on the nature of interlayering, but for highly expandable, randomly interstratified clays the difference also depends on the spacing/thickness of ethylene glycol-smectite complex (Srodon, 1980). Therefore, for accurate determination of illite: smectite ratio, the type and perfection of any ordered interlayering and the spacing of glycol-smectite layer must be taken into account.

Srodon (1980) provides a migration curve for the reflections between 42° and $45^\circ 2\theta$ (Figure 3-9B) generated using **NEWMOD** computer program, which can be used to select the correct thickness of the ethylene glycol complex. To determine if the interstratification is random or ordered, a complete analysis of X-ray diffraction pattern is required (Srodon, 1980). If no reflections occurs between 5.3° and $8.7^\circ 2\theta$ Cu K_α , then the interstratification is random, and if reflection occur between 5.3° and $8.7^\circ 2\theta$ Cu K_α then the interstratification is ordered.

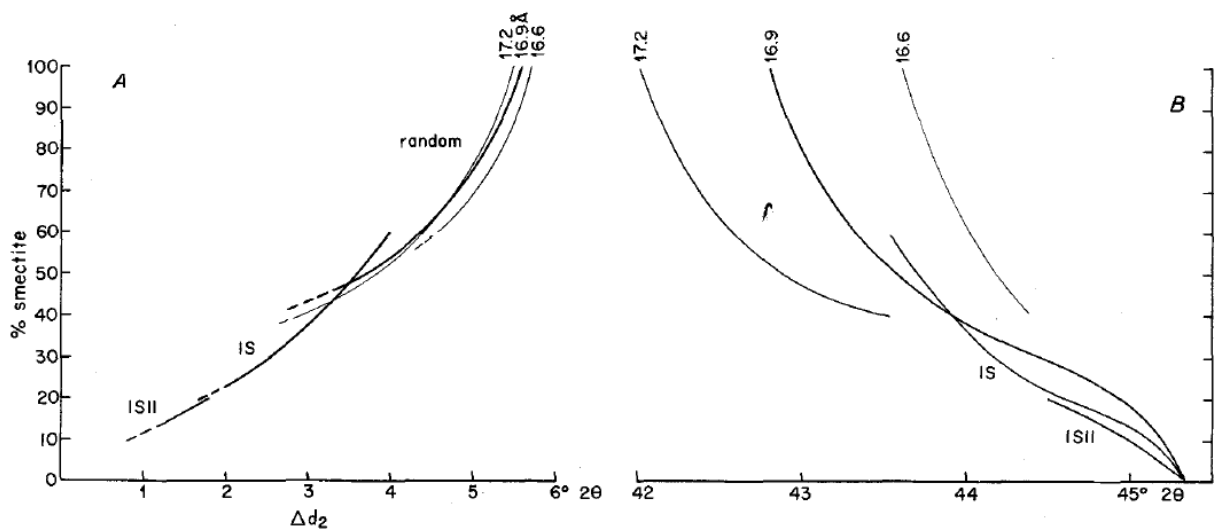


Figure 3-9: The plot for measuring the smectite: illite ratio based on angular distance Δd_2 between reflections 42° and $48^\circ 2\theta$ region, and reflection between 42° and $45^\circ 2\theta$ adapted from Srodon (1980).

The reflections between 42° and $45^\circ 2\theta$ (Fig.3-5B) are used to select the proper thickness of ethylene glycol complexes for smectite dominated compositions. Dashed parts of the curve (Fig. 3-9A) represent composition range beyond which Δd_2 cannot be measured because of merging analytical reflections (Srodon, 1980).

Using figure (3-9A), illite to smectite ratio and thickness of ethylene glycol complex can be determined for random interstratifications. A given Δd_2 value gives a range of smectite content, depending on the thickness of ethyl glycol complex. The range of smectite content along with the position of 42° and 45° 2θ migration peak, give a preliminary value for the thickness of the ethylene glycol complex from the curves in figure (3-9B) above. This value is then used to refine the smectite content from the curve of figure 3-9A (Srodon, 1980).

If a reflection occurs between 5.3° and 8.7° 2θ in the diffraction pattern of an ethylene glycol-solvated illite/smectite, the interstratifications are ordered to a certain degree (Srodon, 1980). An initial value for percent smectite is then determined from the “ordered” IS curve in figure (3-9A). The degree of perfection of ordering is estimated from the difference in 2θ between the reflections that occur from 5.2° to 8.2° 2θ ($\text{Cu K}\alpha$) and from 8.8° to 10.4° 2θ ($\text{Cu K}\alpha$). Srodon (1980) defines this difference as Δd_1 . Srodon (1980) argues that there exists a relationship between Δd_1 and S/I ratio and the perfection of ordering as illustrated in figure (3-10).

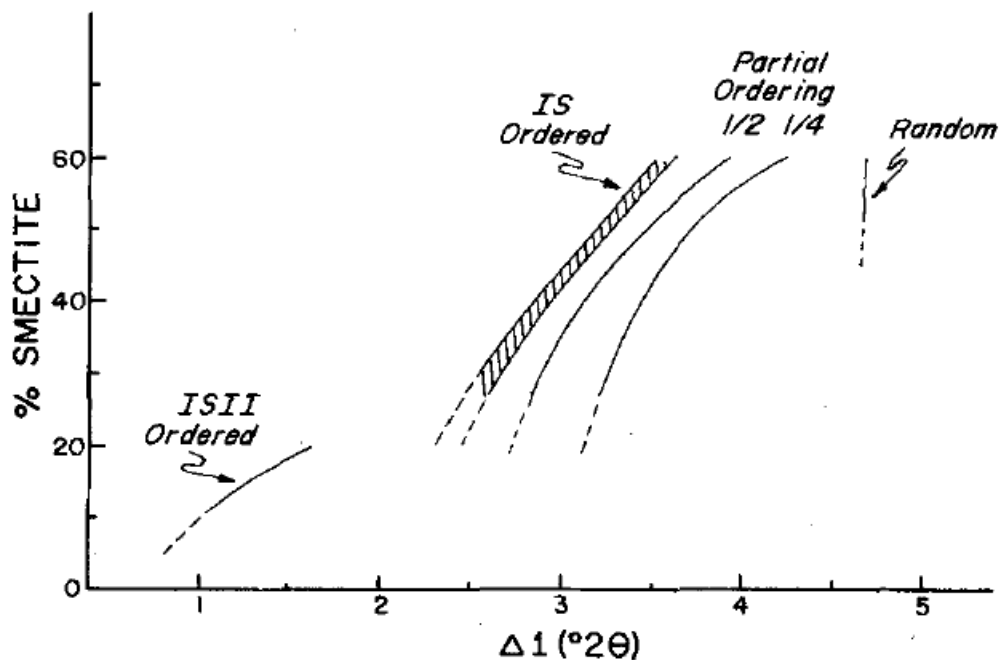


Figure 3-10: The plot for estimating degree of ordering from initial S% and Δd_1 adapted from Srodon (1980)

The initial value of percent smectite layers is then used in figure (3- 10) to estimate the degree of perfection of the ordered interlayering. The initial estimation is correct if the interstratifications are perfectly ordered (lies on either IS line or ISII). If not, the percent smectite values are picked from both the random and the ordered curves of figure (3-9A), and the final value is determined by interpolation (mean value). Srodon (1980) advises that the above described procedure is important if smectite composition is in the range of 60-30%. For more illite minerals the error in the percent smectite determination is not majorly affected by degree or type of ordering. If Δd_1 point falls to the left of IS maximum ordered curve the illite/smectite is ISII ordered (Srodon, 1980).

3.4.1.2 Method (ii)

Srodon (1980) indicates that method (ii) uses the stronger of the two reflections between 42° and $48^\circ 2\theta$ and the strong reflections that migrates from about 26° to $27^\circ 2\theta$. Domain size has minor effect on the S /I ratio determination, which is majorly affected by the type of interstratifications and ethylene glycol-smectite layer thickness (Srodon, 1980). Figure (3-11) shows the migration curves for this reflections, calculated for 1-8 layers (domain size) for random and ordered interstratifications, and ethylene glycol -smectite layer thickness of 16.6, 16.9 and 17.2 Å. The figure also includes points of the migration curve for domain size of 1-14 layers and an ethylene glycol-smectite layer thickness of 16.9 Å. Figure (3-11) includes an addition curve at low smectite contents for the 17.2 Å ethylene glycol - smectite complex, using the curves that migrate from 45° to $48^\circ 2\theta$. The challenges of using this peak are that the $42-45^\circ 2\theta$ is weak in the 17.2 Å ethylene glycol smectite complexes and cannot be resolved at low smectite content.

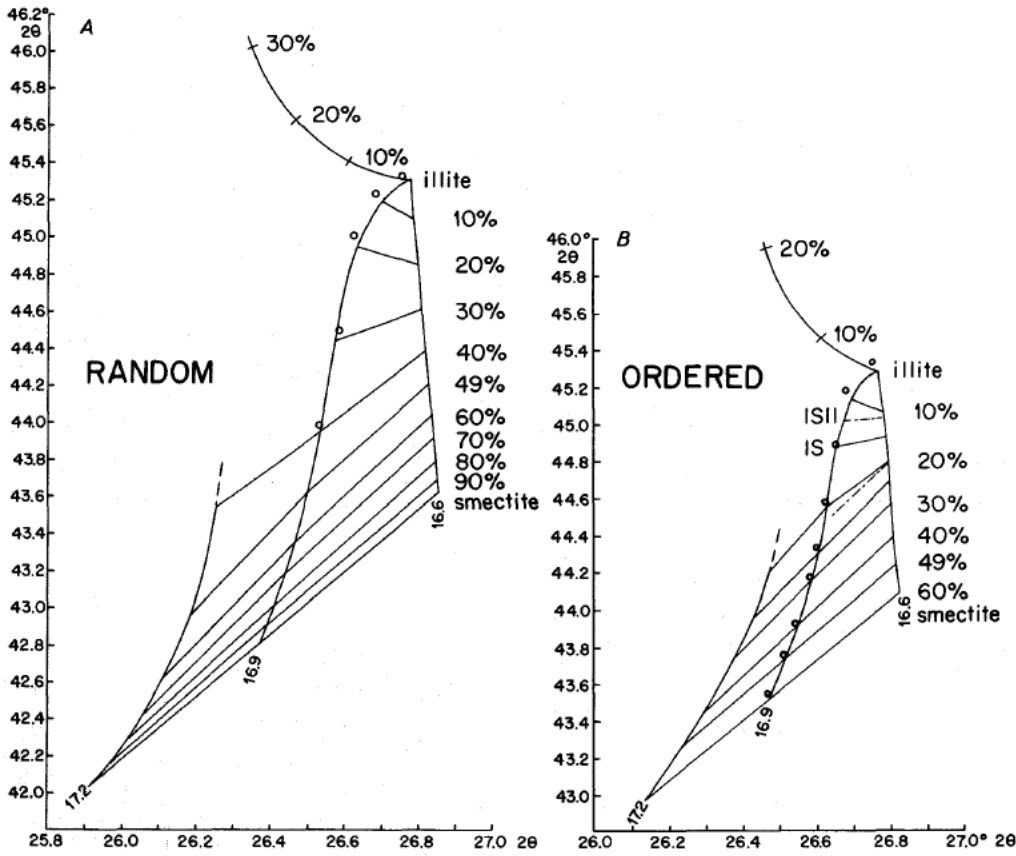


Figure 3-11: Plot for measuring Illite: Smectite ratio based on 42° and $48^\circ 2\theta$ (y-axis) and the strong reflections that migrates from about 26° to $27^\circ 2\theta$ (x-axis) under glycol solvated condition, that are almost unaffected by domain thickness. Random and ordered cases are drawn separately, 1-8 layers/ domain distribution are represented, the open circle are for 1-14 domain distribution and a 16.9\AA ethylene glycol complex thickness adopted from Srodon (1980).

3.4.1.3 Method (iii)

Srodon (1980) method (iii) uses reflection peaks which migrate from about 26° to $27^\circ 2\theta$ and from 15.4° to $17.7^\circ 2\theta$. The I/S ratio determination is strongly affected by ethylene glycol-smectite layer thickness, type of interstratifications and domain size (Srodon, 1980) see further explanation in (3.3.2 below).

3.4.2 Method Applied

Method (iii) of Srodon (1980) for determining smectite: illite ratio was used. This decision was influenced by the absence of high angle reflection peaks (42 to $48^\circ 2\theta$) in the X-ray diffraction data obtained.

The method uses peak which migrates from about 26° to $27^\circ 2\theta$ and from 15.4° to $17.7^\circ 2\theta$ for ethylene glycol solvation X-ray diffraction analysis. The peaks migrate due to difference in smectite-glycol layer thickness and type of ordering which is influenced by the amount of illite and smectite in an illite/smectite mineral (Srodon, 1980). The illite/smectite ratio determination is strongly affected by ethylene glycol-smectite layer thickness, type of interstratifications and domain size (Srodon, 1980). Figure 3-8 shows illite/smectite percentages variation with changes in reflections that migrates from 26° to $27^\circ 2\theta$ and from 15.4° to $17.7^\circ 2\theta$, calculated for 1-8 domain distribution for random and ordered interstratifications, and for ethylene smectite-glycol layer thickness of 16.6, 16.9 and 17.2 Å. The solid circles in figure 3-12 represent ISII type of ordering. Random and ordered cases are drawn separately. The curves were obtained by simulation where the experimental X-ray diffraction patterns were compared to calculated theoretical models developed using *NEWMOD* computer program.

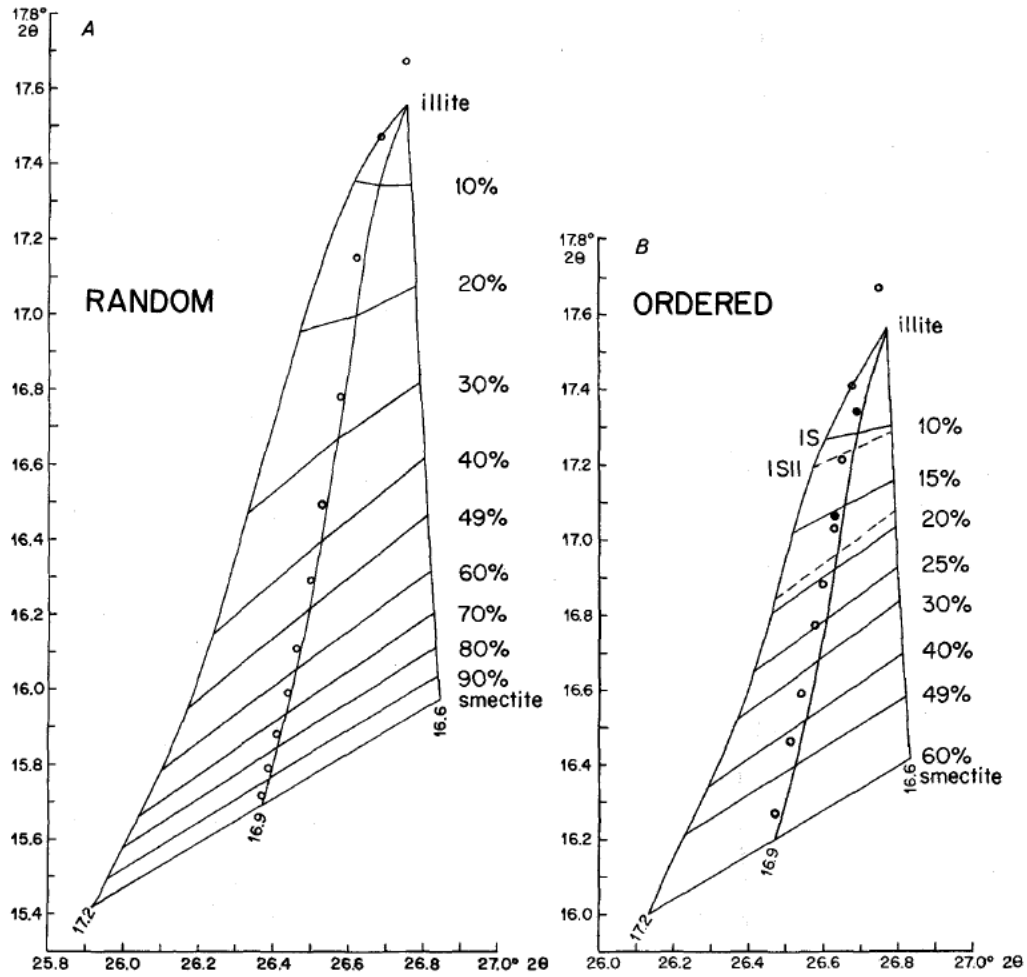


Figure 3-12: The plot for measuring smectite: illite ratio based on reflections which migrates from about 15.4° to $17.7^\circ 2\theta$ and from 15.4° to $17.7^\circ 2\theta$ for ethylene smectite-glycol layer thickness of 16.6, 16.9 and 17.2 Å adopted from Srodon (1980).

3.5 Vitritinite Reflectance (R_o)

3.5.1 Method Rationale

Vitritinite reflectance is a measure of the percentage of light reflected off the vitritinite maceral at X500 magnification in oil immersions. The intensity of light reflected from a sample is measured repeatedly from different parts of a sample and from different samples from the sampling area. Then, a statistical analysis determines the amount of vitritinite in the sample and its thermal maturity (Reyes *et al.* 2013). Vitritinite reflectance measurements are carefully calibrated against glass or mineral-reflectance standards and reflectance measurements represent the amount of light reflected in oil, designated as R_o (reflectance of oil) (Reyes *et al.* 2013).

A thin section is made from a rock sample and mounted on a glass slide, ready for observation under a microscope equipped with an oil-immersion objective lens and photometer. Vitritinite reflectance values of between 0.6 -1.3% indicate oil generation, values less than 0.6% shows immature kerogen and those greater than 1.3% shows the rock sample is beyond the oil generation stage (over mature) (Tissot and Welte, 1984; McCarthy *et al.* 2011).

3.5.2 Method Applied

For this research forty six (46) samples from the depth range of 982-4175m in Simba-1, Maridadi-1B, Walu-1, and Kipini-1 wells in Lamu Basin were subjected to vitritinite reflectance analysis at the National Oil Corporation of Kenya laboratories and the following procedures were followed.

3.5.2.1 Sample Preparation

Sample preparation for vitritinite reflectance analysis is done in two steps, making polished blocks and kerogen isolation and slide preparation.

3.5.2.1.1 Making Polished Blocks

The whole rock samples were dried, crushed with a mortar and a pestle into granular sizes and sieved through a 420 μ m diameter sieve. After crushing the samples were set in pellet protective cups with a casting epoxy resin mould and allowed to cure for one night in an oven to solidify into blocks. The epoxy resin is used to extract hydrocarbons, making them easily detectable

under microscope without any chemical reaction. The blocks were polished using isopropanol polishing medium and successively finer grades of polishing discs (120, 240, 600, 1200 grits followed by 3.0 μm , 1.0 μm and 0.1 μm) on an automatic polishing unit. This was done to make a shiny mirror like surface, free of scratches so as to increase accuracy in optical measurements. The isopropanol polishing medium lubricates the sample and prevents swelling of clay minerals which would occur if water was used.

3.5.2.1.2 Kerogen Isolation and Slide Preparation

To isolate kerogen, samples were made to powder and treated with benzene-methanol solvent to remove any soluble organic matter. The obtained samples were air-dried and about 20g used for isolation. The samples were then treated with hydrochloric acid and stirred to remove present carbonates before addition of hydrofluoric acid and left to stand overnight. The samples were then washed with water for neutralization purpose and to ensure that all carbonates were removed. Addition of Hydrofluoric acid then followed to remove silicate minerals and the same procedure for stirring and washing was done. After acids treatments, the samples were centrifuged and decanted to remove any liquid before zinc bromide was added. After which the samples were agitated, rinsed and centrifuged to ensure all the kerogen floats on the top of the sample. The floating kerogen was then removed and washed several times using hydrochloric acid. The kerogen was then subdivided into two portions: sieved one where the amorphous content has been removed and the unsieved one. A releasing agent was then sprayed on two petrographic slits prior to addition of a few drops of the sieved kerogen sample on one slit, and two drops of the unsieved kerogen sample on the other. After drying for about four hours a few drops of resin were added on each of the samples on petrographic slit, each sample was then mounted on slide and left to dry for a few hours. The slits were removed and slides polished using successively fine polishing disc; 3.0 μm , 1.0 μm , and 0.1 μm respectively using water as a lubricant.

3.5.2.2 Vitrinite Reflectance Measurement

Vitrinite reflectance measurements were done using petrographic light microscope with total magnification of x500. A drop of immersion oil was added on sieved and unsieved kerogen slides before scanning on the microscope. The immersion oil increases the identification of low

reflectance materials and increases the contrast between different macerals. Vitrinite reflectance of oil (R_o) was determined by comparing light reflected from samples with that reflected from standards of known reflectance. The reflectivity of about 20 grains of vitrinite from a sample was measured and mean reflectance value taken.

3.5.2.3 Quality Control Measures

The microscope was calibrated using 0.588% and 1.69% reflectance standards to ensure linearity of the microscope.

CHAPTER FOUR

4 RESULTS AND DISCUSSION

4.1 RESULTS

4.1.1 Lamu Basin Source Rock Maturity Depths Based on Smectite Percentages

Clay minerals in core rock samples obtained from Simba-1, Walu 1 and 2, Maridadi-1B, and Kipini-1 wells in Lamu Basin were identified by studying the X-ray basal diffraction angles and patterns in air dried, ethylene glycol and heated treatments (Appendix I - V). Percentage of smectite in illite/smectite mixed layer in the samples was determined using peak migration method (iii) by Srodron (1980) this decision was influenced by the absence of higher diffraction angles that are required in Srodron (1980) method (ii) and (i).

4.1.1.1 Simba-1 Well

4.1.1.1.1 Clay Minerals Present in Simba-1 well

Table 4-1: Clay minerals identified in Simba-1 well using X-ray diffraction peaks in air dried, ethylene-glycol and heated treatments

Well	Depth (m)	Air dried (dÅ)	Glycolated (dÅ)	Heated (dÅ)	Clay minerals present
Simba-1	1585-1590	14.17	19.19	9.98	illite/smectite mixed layer
	"	7.3	7.3	No peak	chlorite
	1840-1845	15.02	19.43	10.02	illite/smectite mixed layer
	"	7.26	7.26	No peak	chlorite
	2498	No peak	No peak	10.02	illite
	"	7.15	7.15	No peak	chlorite
	2544	No peak	No peak	10.05	illite
	"	7.18	7.18	No peak	chlorite
	2670	10.11	10.11	10.11	illite
	"	7.24	7.24	Nopeak	chlorite
	2820	No clay	No clay	No clay	No clay
	2895	No clay	No clay	No clay	No clay
	3005	10.17	10.17	10.17	illite
	"	7.11	7.11	No peak	chlorite
	3142	10.26	10.26	10.26	illite
"	7.24	7.24	No peak	chlorite	

Well	Depth (m)	Air dried (dÅ)	Glycolated (dÅ)	Heated (dÅ)	Clay minerals present
Simba-1	3206	10.1	10.1	10.1	illite
	"	7.24	7.24	No peak	chlorite
	3298	10.39	10.39	10.39	illite
	"	7.13	7.13	No peak	chlorite
	3480	10.72	10.72	10.72	illite
	"	7.14	7.14	No peak	Chlorite
	3568	10.06	10.06	10.06	illite
	"	7.12	7.12	No peak	Chlorite
	3570	10.59	10.59	10.59	Illite
	"	7.15	7.15	7.15	Chlorite

The X-ray diffraction patterns indicate presence of illite/smectite mixed layer and chlorite clay minerals in the core samples collected at the Simba-1 well between the depth of 1585-1590m and 1840-1845m. From the depth of 2498m to the total depth of 3604m chlorite and illite clay minerals were identified.

4.1.1.1.2 Quantitative Analysis of Smectite Percentages in Illite/Smectite Mixed Layer in Simba-1 well

Illite-smectite interstratifications in Simba-1 well occur at the depth of 1585-1590m and 1840-1845m, the 2θ angles of the x-ray diffraction peaks under ethyl-glycol treated condition for the samples from the said depths are as below.

Table 4-2: The 2θ angles of the X-ray diffraction peaks for ethylene glycol treated rock sample obtained at the depth of 1585-1590m of Simba-1 well

Well	Depth (m)	Glycolated °2θ
simba-1	1585-1590	4.9800
	"	8.6600
	"	12.2100
	"	15.9700
	"	17.800
	"	18.6600
	"	19.3700
	"	20.7400
	"	21.3600
	"	22.0800
	"	23.1800
	"	23.7600
	"	24.9800

Well	Depth (m)	Glycolated $\circ 2\theta$
Simba-1	"	26.5910
	"	27.6400
	"	29.3966
	"	30.8800
	"	31.8400

Using Srodon (1980) method (iii), X-ray diffraction reflections within 26 to 27° 2θ region in this sample is 26.5910° 2θ and the reflection within 15.4 to 17.7° 2θ region is 15.9700° 2θ. The sample has a reflection within 5.3 and 8.7° 2θ region, therefore the illite/smectite interstratifications is ordered and the smectite percentages are read off figure 3-8B. From the figure smectite percentage in this sample is far above 60% and by extrapolation it is approximately between 80 and 90%. According to Akande *et al.* (2005) this composition indicates temperatures below the threshold for hydrocarbon source rock maturity. The smectite percentages indicate diagenesis temperatures that are below 60 °C.

Table 4-3: The 2θ angles of the X-ray diffraction peaks for ethylene glycol treated rock sample obtained at the depth of 1840-1845m of Simba-1 well

Well	Depth (m)	Glycolated $\circ 2\theta$
simba-1	1840-1845	5.2562
	"	8.8698
	"	9.6722
	"	12.2852
	"	16.0687
	"	17.4492
	"	17.8884
	"	19.1056
	"	19.9430
	"	20.8005
	"	21.5984
	"	23.1747
	"	23.4741
	"	25.0709
	"	26.5883
	"	27.6865
	"	29.4698
	"	30.7824
	"	31.6214
	"	33.1797
"	33.9389	

The sample has no reflection within 5.3 and 8.7° 2θ region, therefore the illite/smectite interstratifications is random and the smectite percentages are read off figure 3-8A. The sample has X-ray diffraction reflection within 26 to 27° 2θ region (26.5883° 2θ) and the reflection within 15.4 to 17.7° 2θ region (16.0687 and 17.4492° 2θ giving a mean of 16.75895° 2θ). From figure 3-8A smectite percentage is about 29%. The smectite composition indicates hydrocarbon generation temperatures of above 60°C (catagenesis) because the value is below Akande *et al.* (2005) threshold of 40% smectite.

4.1.1.2 Walu-1 well

4.1.1.2.1 Clay Minerals Present in Walu-1 Well

Table 4-4: Clay minerals identified in Walu-1 well using x-ray diffraction peaks in air dried, ethylene-glycol and heated treatments

Well	Depth (m)	Air dried (dÅ)	Glycolated (dÅ) ^o	Heated (dÅ)	clay minerals present
Walu-1	1098-1100	No peak	17.66	10.14	Illite/smectite mixed layer
	"	7.19	7.19	No peak	Chlorite
	1410-1411	No peak	17.66	10.17	illite/smectite mixed layer
	"	7.16	7.16	No peak	Chlorite
	1604-1606	10.20	10.20	10.20	Illite
	"	7.18	7.18	No peak	Chlorite
	1732-1733	No peak	10.14	10.14	Illite
	"	7.21	7.21	No peak	chlorite

The X-ray diffraction patterns indicate presence of illite/smectite mixed layer and chlorite clay minerals in the core samples collected at the Walu-1 well between the depth of 1098-1100 m and 1410-1411m. From the depth of 1604m to 1733m chlorite and illite clay minerals were identified.

4.1.1.2.2 Quantitative Analysis of Smectite Percentages in Illite/Smectite Mixed Layer in Walu-1 well

Illite-smectite interstratifications in Walu-1 well occur at the depth of 1410-1411m , the 2 θ angles of the X-ray diffraction peaks for the ethyl-glycol treated sample from the said depths are as below.

Table 4-5: The 2 θ angles of the x-ray diffraction peaks for ethylene glycol treated rock sample obtained at the depth of 1410-1411m of Walu-1 well

Well	Depth (m)	Glycolated $\circ 2\theta$
Walu-1	1410-1411	5.2973
	"	9.1371
	"	12.3648
	"	15.6731
	"	16.8504
	"	19.7037
	"	20.9053
	"	21.8179
	"	23.0350
	"	23.9531
	"	24.9586
	"	26.6336
	"	27.4669
	"	28.5653
"	29.4440	

The sample has no reflection within 5.3 and 8.7 \circ 2 θ region, therefore the illite/smectite interstratifications is random and the smectite percentages are read off figure 3-8A. The sample has X-ray diffraction reflection within 26 to 27 \circ 2 θ regions as 26.6336 \circ 2 θ and the reflection within 15.4 to 17.7 \circ 2 θ region as 15.6737 \circ 2 θ and 16.8304 \circ 2 θ giving a mean of 16.26175 \circ 2 θ . By using the two reflections on figure 3-8A, smectite percentage is about 55%. This shows that the temperatures at this depths range are within immature hydrocarbon maturity range below 60 \circ C.

4.1.1.3 Maridadi-1B well

4.1.1.3.1 Clay Minerals Present in Maridadi-1B well

Table 4-6: Clay minerals identified in Maridadi-1B well using X-ray diffraction peaks in air dried, ethylene-glycol and heated treatments

Well	Depth (m)	Air dried (dÅ)	Glycolated (dÅ) ^o	Heated (dÅ)	clay minerals present
Maridadi -1B	3110	10.07	10.07	10.07	illite
	"	7.20	No peak	7.20	chlorite
	3550	7.60	7.60	No peak	chlorite
	3850	10.87	10.87	10.87	illite
	"	7.16	7.16	No peak	chlorite
	3860	10.23	10.23	10.23	illite
	"	7.19	7.19	No peak	chlorite
	3930	10.29	10.29	10.29	illite
	"	7.13	7.13	No peak	chlorite
	4110	10.17	10.17	10.17	illite
	"	7.18	7.18	No peak	chlorite
	4160-4190	10.62	10.62	10.62	illite
	"	7.08	7.08	No peak	chlorite

The X-ray diffraction patterns indicate presence of illite and chlorite clay minerals in the core samples collected at the Maridadi-1B well from the depth between 3010m and 4190m but no illite/smectite mineral.

4.1.1.4 Kipini-1 well

4.1.1.4.1 Clay Minerals Present in Kipini-1 well

Table 4-7: Clay minerals identified in Kipini-1 well using X-ray diffraction peaks in air dried, ethylene-glycol and heated treatments

Well	Depth (m)	Air dried (dÅ)	Glycolated (dÅ)	Heated (dÅ)	clay minerals present
Kipini-1	981-983	10.32	10.32	10.32	Illite
	"	7.11	7.11	No peak	Chlorite
	1867-1868	10.11	10.11	10.11	Illite
	"	7.21	7.21	No peak	Chlorite
	1911-1913	10.23	10.23	10.23	Illite
	"	7.13	7.13	No peak	Chlorite
	2004-2006	9.28	9.28	9.28	Illite
	"	7.65	7.65	No peak	Chlorite
	2147-2149	7.57	7.57	No peak	Chlorite
	2582-2583	9.21	9.21	9.21	illite
	"	7.65	7.65	No peak	Chlorite
	2766-2768	9.18	9.18	No peak	Illite
	"	7.64	7.64	No peak	Chlorite
	3031-3032	No peak	No peak	No peak	No clay
	3147-3149	No peak	No peak	No peak	No clay
	3453-3454	10.36	10.36	10.36	Illite
	"	7.19	7.19	No peak	Chlorite
	3397-3490	10.29	10.29	10.29	Illite
	"	7.16	7.16	No peak	Chlorite
	3649-3651	10.72	10.72	10.72	Illite
"	7.10	7.10	No peak	Chlorite	

The X-ray diffraction patterns indicate presence of illite and chlorite clay minerals in the core samples collected at the Kipini-1 well from the depth between 981m to 3651m but no illite/smectite mineral.

4.1.1.5 Walu-2 well

4.1.1.5.1 Clay Minerals Present in Walu-2 Well

Table 4-8: Clay minerals identified in Walu-2 well from X-ray diffraction peaks in air dried, ethylene-glycol and heated treatments

Well	Depth (m)	Air dried (dÅ)	Glycolated (dÅ)	Heated (dÅ)	clay minerals present
Walu-2	1861-1862	14.61	No peak	No peak	chlorite
	"	7.19	7.19	No peak	Chlorite
	"	No peak	10.49	10.49	illite
	2028-2030	No peak	No peak	10.11	illite
	"	7.13	7.13	No peak	chlorite
	2189	14.17	No peak	No peak	Chlorite
	"	No peak	10.01	10.01	Illite
	"	7.16	7.16	No peak	Chlorite
	2289-2291	7.19	7.19	No peak	Chlorite
	2423	14.23	14.23	14.23	chlorite
	"	10.36	10.36	10.36	Illite
	"	7.08	7.08	7.08	chlorite
	2041-2642	7.10	7.10	No peak	chlorite
	2783-2784	10.08	10.08	10.08	illite
	"	7.13	7.13	No peak	Chlorite
	2873-2874	10.23	10.23	10.23	Illite
	"	7.13	7.13	No peak	Chlorite
	3498-3499	10.59	10.59	10.59	Illite
	"	7.1	7.1	No peak	Chlorite
	3626-3627	10.07	10.07	10.07	Illite
"	7.10	7.10	No peak	Chlorite	
3681-3682	No peak	No peak	No peak	No clays	

The X-ray diffraction patterns indicate presence of illite and chlorite clay minerals in the core samples collected at the Walu-2 well from the depth between 1861m and 3682m but no illite/smectite mineral.

4.1.2 Comparison of Smectite Percentages to Vitrinite Reflectance Hydrocarbon Maturity Depths in Lamu Basin

The comparison was done for only Simba-1 offshore well and Walu-1 onshore well which indicated presence of illite/smectite clay mineral.

4.1.2.1 Simba-1 well

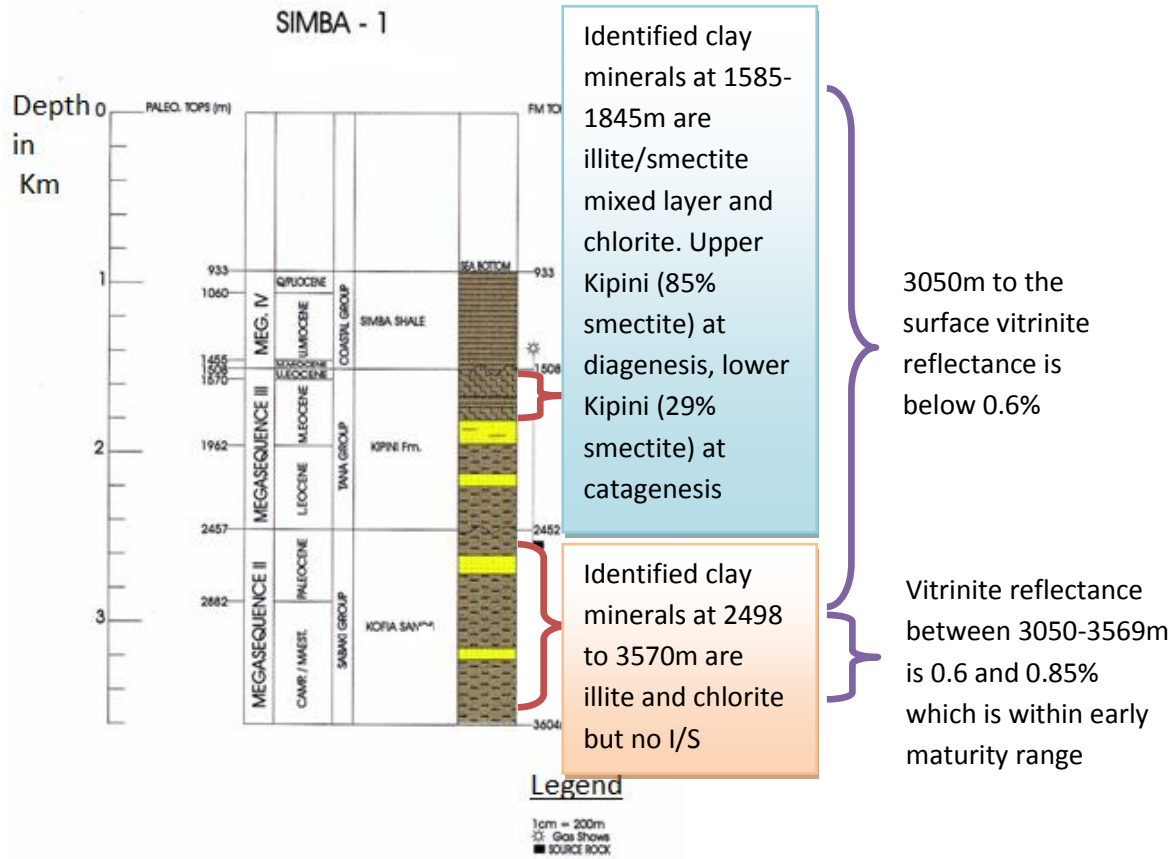


Figure 4-1: Simba-1 well stratigraphy, clay minerals occurrence and maturity zones identified from vitrinite reflectance analysis modified after NOCK (1995).

The samples analysed for vitrinite reflectance from Simba-1 well were obtained from the depth range of 1593m and 3569m (Appendix iv). The samples have vitrinite reflectance values of between 0.28 and 0.86%. Simba-1 rock samples with vitrinite reflectance values that are within hydrocarbon maturity zones were obtained at the depth of 3050m to 3569m. The samples have vitrinite reflectance values of 0.6 to 0.86% which indicates early hydrocarbon maturity zone. This zone coincides with occurrence of illite and chlorite clay minerals. Samples with vitrinite reflectance below 0.6% (immature) occur from the depth of 3050m to the surface, this zone

coincides with occurrence of illite/smectite bearing 29% smectite which indicate catagenesis temperatures.

4.1.2.2 Walu-1 and 2 wells

WALU - 2

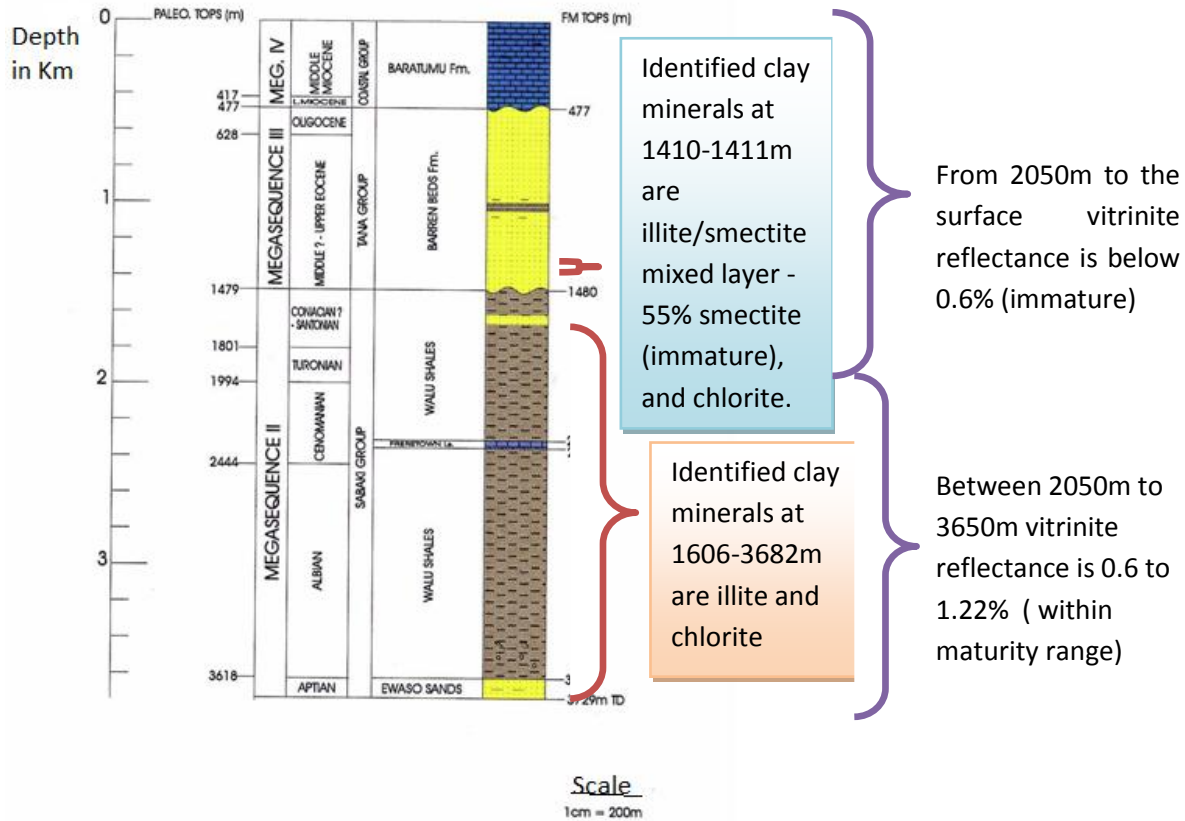


Figure 4-2: Walu-1 and 2 well stratigraphy, clay minerals occurrence and maturity zones identified from vitrinite reflectance analysis modified after NOCK (1995).

The samples analysed for vitrinite reflectance from Walu-1 and 2 well were obtained from the depth range of 1093m and 3673m. The samples have vitrinite reflectance values of between 0.21 and 1.22% (Appendix vi). Rock samples from Walu-1 and 2 well with vitrinite reflectance values that are within hydrocarbon maturity zones were obtained at the depth of 2050m to 3650m. The samples have vitrinite reflectance values of 0.6 to 1.22% which indicates early to late hydrocarbon maturity zone.

The identified clay minerals in Walu-1 and 2 well were illite/smectite mixed layer and chlorite from the core samples obtained at the depth of 1098 to 1480m. The amount of smectite in the

illite/smectite mixed layer minerals in the sample obtained from this depth is about 55%. The smectite percentage indicate that the rock is at immature stage (diagenesis), as explained by Akande *et al.* (2005).The hydrocarbon immature zone identified by smectite percentage coincides with hydrocarbon immature zone identified by vitrinite reflectance. Illite/smectite and chlorite clay minerals occur together.

From 1606m to 3682m illite and chlorite clay minerals seem to occur together in all the samples. The occurrence of high temperatures illite and chlorite clay minerals coincides with hydrocarbon generation depths, determined by vitrinite reflectance.

4.2 DISCUSSION

4.2.1 *Simba-1*

Illite/smectite, illite and chlorite are the characteristic clay minerals in Simba-1 well. Illite and chlorite minerals occur together in all rock samples irrespective of depth or rock formation. The illite/smectite mixed layer clay mineral occurs at the depth of 1585-1590m with 85% smectite, and 1840-1845m with 29% smectite both from *Kipini* Formation.

Simba-1 hydrocarbon maturity zone is at 3050m to total depth of 3569m with vitrinite reflectance of 0.6-0.85%. From 3500m to the surface of Simba-1 well the rocks are immature with vitrinite reflectance below 0.6%. Smectite percentage of 85% in illite/smectite mixed layer which indicates immature or rocks at diagenesis, occur in this region in *upper Kipini* Formation, thus the Smectite percentage maturity zone in this section of Simba-1 is in agreement with vitrinite reflectance maturity zone. Smectite percentage of 29% in illite/smectite mixed layer which indicate rocks at oil generation stage (catagenesis) also occur in this section but in *middle Kipini* Formation, just above the start of vitrinite reflectance maturity zone. This contradicting results between smectite percentages and Vitrinite reflectance could be as a result of the difference in lithology of *upper Kipini* Formation which is shales and *middle Kipini* Formation which is sandstones.

4.2.2 *Walu-1*

Illite/smectite, illite and chlorite are the characteristic clay minerals in Walu-1 well. The illite and chlorite clay minerals occur together in all rock samples irrespective of depth or rock formation. The illite/smectite mixed layer clay mineral occurs at the depth of 1410-1411m with 55% smectite from *Barren Bed* Formation. From 2050m to the surface the rocks are immature with vitrinite reflectance below 0.6%. Smectite percentage of 55% in illite/smectite mixed layer which indicate source rocks at immature stage (diagenesis) occurs in this section between (2500m to the surface). Therefore, hydrocarbon maturity zone defined by Smectite percentage in illite/smectite mixed layer in Walu-1 well, agrees with the maturity zones defined by vitrinite reflectance.

4.2.3 *Walu-2*

Illite and chlorite are the characteristic clay minerals in Walu-2 well. The clay minerals occur together in all rock samples irrespective of depth or rock formation. This well lacks illite/smectite clay mineral. Walu-2 hydrocarbon maturity zone is at 2050m to total depth of 3622m with vitrinite reflectance of 0.6 to 1.22%.

4.2.4 *Maridadi-1B*

Illite and chlorite are the characteristic clay minerals in Maridadi-1B well. The clay minerals occur together in all rock samples irrespective of depth or rock formation. This well lacks illite/smectite clay mineral probably because of its geology and acidic condition that lead to quickened illitization as explained by (Miki, 2000). Maridadi-1B hydrocarbon maturity zone is at 3500m to total depth of 4196m with vitrinite reflectance of 0.6-0.8%.

4.2.5 *Kipini-1*

Illite and chlorite are the characteristic clay minerals in Kipini-1 well. The clay minerals occur together in all rock samples irrespective of depth or rock formation. This well lacks illite/smectite clay mineral. Kipini-1 hydrocarbon maturity zone is at 2600m to total depth of 3663m where vitrinite reflectance is 0.6-0.88%.

4.2.6 *Simba-1 and Walu-2 wells Burial Curves*

Burial curves show the development of a basin with time, the increase in thickness of the deposited sediments as well as the temperature variation with depth and time. Figures 4-3 and 4-4 show the burial curves of Simba-1 and Walu-1 and 2 wells respectively and the depths of illite/smectite clay mineral occurrence.

4.2.6.1 Simba-1 well

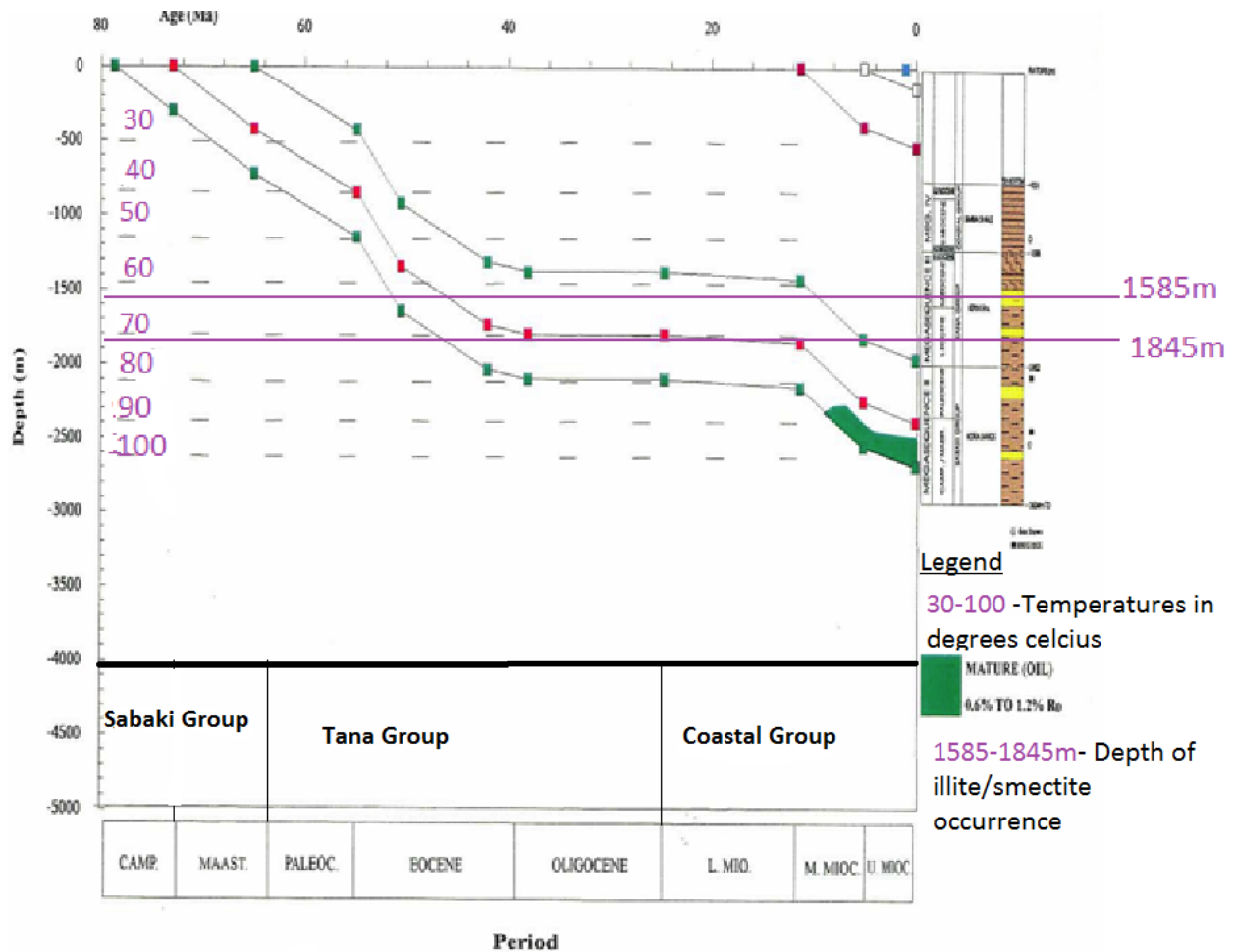


Figure 4-3: Burial history curves of simba-1 well and illite/smectite occurrence modified after (NOCK, 1995)

Smectite in illite/smectite is 85% in upper part of *Kipini* Formation at 1585-1590m and 29% in lower part of *Kipini* Formation at 1840-1845m. The occurrence of illite/smectite mixed layer clay minerals in Simba-1 well corresponds to burial temperatures of about 65-70°C. This marks the onset of hydrocarbon source rock maturation.

4.2.6.2 Walu-1 & 2 Well

As explained in section 4.1.1.2.2, the occurrence of illite/smectite mixed layer clay minerals in Walu-1 well is at 1410-1411m in *Barren bed* formation and has 55% of Smectite. The smectite composition corresponds to burial temperatures of 65-80 °C (Fig 4-4). These temperatures also coincide with the onset of hydrocarbon generation from the source rock.

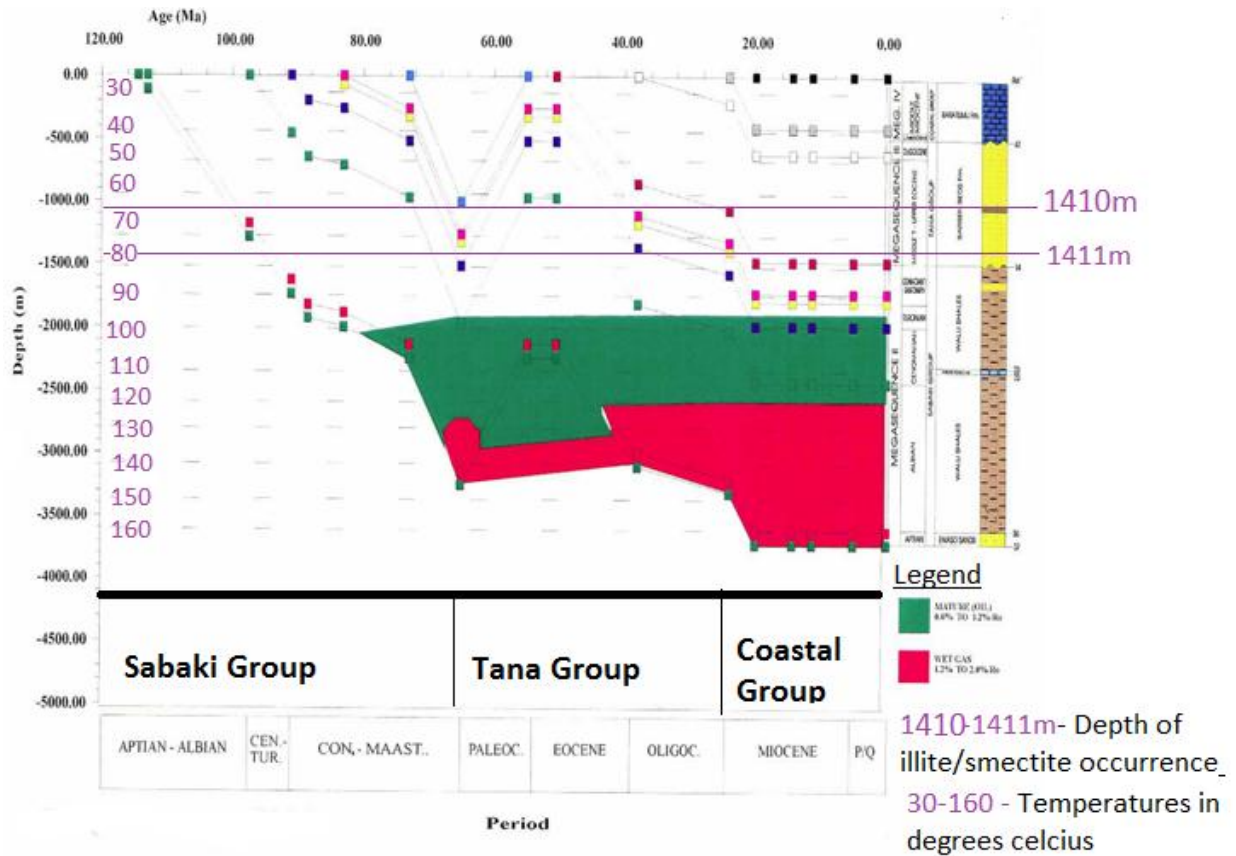


Figure 4-4: Burial history curves of Walu-2 well and illite/smectite occurrence modified after (NOCK, 1995)

CHAPTER FIVE

5 CONCLUSIONS AND RECOMMENDATIONS

5.1 Conclusions

Occurrence of smectite whether in mixed layer or as an individual mineral corresponds to vitrinite reflectance values indicating immature source rock or source rock that is about to enter into mature stage (catagenesis). Values of smectite percentage that are within 40% to less than 10% smectite which is Akande *et al.* (2005) source rock maturity zone, indicate a rock that is about to get into maturity zone. For instance the 29% smectite in Simba-1 well occurs slightly above the beginning of source rock mature zone of vitrinite reflectance. The smectite percentage source rock maturity zone established using the two samples out of the three samples bearing illite/smectite mixed layer clay mineral that is, Simba-1 (1840-1845m) and Walu-1 (1410-1411m) agree to the vitrinite reflectance maturity zones. Occurrence of illite and chlorite corresponds to vitrinite reflectance values indicating hydrocarbon generation depths.

The occurrence of the illite/smectite clay mineral in the samples studied in this research indicates burial temperatures of 60-80 °C, which marks the onset of oil generation from a source rock.

5.2 Recommendations

- The sample preparation procedures used in this research for clay minerals x-ray diffraction analysis was for identification of clay minerals than quantitative for determining amount of clay minerals, particularly in mixed layer minerals as recommended by Srodon (1980) this was contributed by the available resources. Therefore, a quantitative clay minerals analysis should be considered by improving the sample preparation procedures to match a quantitative analysis and ensure highly accurate x-ray diffraction peaks patterns are obtained.
- X-ray diffraction equipment with high sensitivity should also be innovated to ensure low and high diffraction angles are captured and this will allow use of relatively accurate methods of smectite quantification in illite/smectite mixed layer clay minerals as

described by Srodon (1980). Unidentified low and high diffraction angles as a result of improper quantitative oriented sample preparation and low sensitivity of X-ray diffraction equipment, highly affect the clay ratios in mixed layer clay minerals.

- Detailed sampling of Simba-1 especially in *Kipini* Formation and Walu-2 wells in *Barren Bed Formation* should be considered in order to trace the illitization process of smectite clay mineral so as to correlate smectite percentages and vitrinite reflectance at every depth.
- More wells within and outside Lamu Basin should be analysed for Illite/smectite clay minerals and the relationship between smectite percentages in the clay minerals to hydrocarbon maturity of rocks as defined by vitrinite reflectance should be determined and correlated to that of Simba-1 and Walu-2 wells to establish if the relationship between smectite percentages and vitrinite reflectance identified in the two wells persists.
- National Oil Corporation of Kenya should consider improving on the sampling and storage of the core samples, where samples can be collected from a specific depth and properly packaged to avoiding spilling and mixing of the samples. This would avoid getting erroneous data and conclusions.

REFERENCES

- Ahmed, W. (2008). Contrast in clay mineralogy and their effect on reservoir properties in sandstone formations. *Bulletin of the Chemical Society of Ethiopia*, 22(1), 50-55.
- Akande, S., Viczian, I., & Erdtmann, B. (2005). Prediction of petroleum generation intervals in Southern Nigeria Rift basins by means of clay transformations, vitrinite reflectance and fluid inclusion studies. *NAPE Bulletin*, 16, 38-51.
- Alt, J. & Jiang, W. (1991). Hydrothermally precipitated mixed-layer illite-smectite in recent massive sulfide deposits from the sea floor. *Geol*, 19(6), 55-70.
- Bell, T. (1986). Microstructure in mixed-layer illite/smectite and its relationship to the reaction of smectite to illite. *Clays and Clay Minerals*, 34(2), 146-154.
- Bloch, S., Lander, R., & Bonnell, L. (2002). Anomalously high porosity and permeability in deeply buried sandstone reservoirs: Origin and predictability. *Bulletin*, 86, 20-28.
- Caswell, P. (1953). *Geology of Mombasa-Kwale Area*. Nairobi: Geological Survey of Kenya, 32, 10-18.
- Corbato, C. (1982). Two examples of quantitative analysis by simulated x-ray powder diffraction patterns. *Clay Minerals*, 17(4), 393-399.
- Corbató, C. (1987). Analysis of illite-smectite interstratification. *Clay Minerals*, 22(3), 269-285.
- Eberl, D., Farmer, V., & Barrer, R. (1984). Clay mineral formation and transformation in rocks and soils. *Philosophical Transactions of the Royal Society A: Mathematical, Physical and Engineering Sciences*, 311(1517), 241-257.
- Eberl, D., & Pollastro, R. M. (1993). Consideration and application of the illite/smectite geothermometry in hydrocarbon rocks of Miocene to Mississippian age. *Clay and Clay Minerals*, 41, 119-133.
- Inoue, A. (1987). Chemical and morphological evidence for the conversion of smectite to illite. *Clays and Clay Minerals*, 35(2), 111-120.
- Ji, J., Browne, P., & Liu, Y. (1997). Occurrence of mixed-layer illite/smectite at temperature of 285° C in an active hydrothermal system and its significance. *Chinese Science Bulletin*. 30-32.
- Jiang, S. (2012). *Clay Minerals from the Perspective of Oil and Gas Exploration* (1st ed., pp.30-45). INTECH Open Access Publisher.

- Karanja, F. (1982). *Report on the Geology of the Kilifi, Gede and Sokoke Area*. Nairobi: Geological Survey of Kenya, 28, 31-39.
- Kazerouni, A., Poulsen, M., Friis, H., Svendsen, J., & Hansen, J. (2012). Illite/smectite transformation in detrital glaucony during burial diagenesis of sandstone: A study from Siri Canyon - Danish North Sea. *Sedimentology*, 60(3), 679-692.
- Klug, H. & Alexander, L. (1954). *X-ray diffraction Procedures for Polycrystalline and Amorphous Materials*. John Willey & Sons, Inc. (pp. 100-120).
- Kongoti, J. (2014). *Review for the Weather in October and Outlook for November 2014*. Republic of Kenya Ministry of Environment, Water and Natural Resources Department of Environment and Natural Resources Kenya Meteorological Service (pp. 5-6).
- Mc Carthy, K., Niemann, M., Palmowski, D., Peters, K., & Stankiewicz, A. (2011). *Basic Petroleum Geochemistry for Source Rock Evaluation* (pp. 1-7). Schlumberger.
- Miki, T. (1991). Relationships between authigenic mineral transformation and variation in vitrinite reflectance during diagenesis: An Example from the Tertiary of Northern Kyushu, Japan. *Clay Minerals*, 26(2), 179-187.
- Miki, T. (2000). Prediction of petroleum generation by means of R_o and $S\%$ in I/S diagram. *SEAPEX Press Singapore*, 3(5), 30-34.
- Ministry of Environment and Natural Resources of Kenya. (1985). *Lamu District Environmental Assessment Report* (pp. 20-23). Nairobi: Government of Kenya.
- Moore, D. & Reynolds, R. (1989). *X-ray diffraction and the identification and analysis of clay minerals* (1st ed., pp. 20-50). Oxford [England]: Oxford University Press.
- Mutunguti, F. (1988). *Kerogen Analysis of Sediments in Lamu Embayment of Kenya*. *Unpublished M.Sc. Thesis* (pp. 7-10). Nairobi: Thesis National Oil Corporation of Kenya.
- National Oil Corporation of Kenya (NOCK). (1995). *Hydrocarbon potential of the coastal onshore and offshore Lamu Basin of southeast Kenya Integrated Report* (p. 97). Nairobi: National Oil Corporation of Kenya.
- Neil S. Fishman, Christine E. Turne. (1987). Early Diagenetic Formation of Illite: Implications for Clay Geothermometry: ABSTRACT. *Bulletin*, 71, 12-15.
- Ngecu, J. M. (2012). *Assessment of Source Rock Maturity in the Lamu Basin Based on Well distribution, Hydrocarbon shows, Total Organic Carbon (TOC) Levels, Kerogen type and Vitrinite Reflectance* (M.Sc.). University of Nairobi.

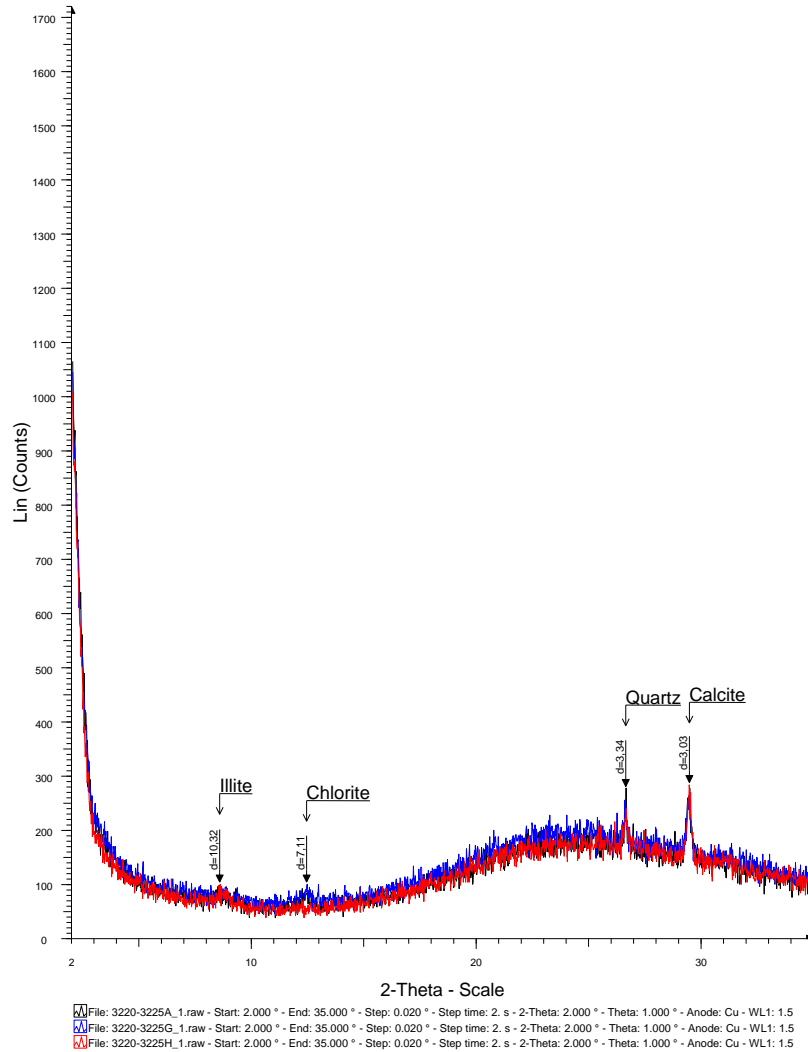
- Nyaberi, M. & Rop, B. (2014). Petroleum prospects of Lamu Basin, South-Eastern Kenya. *Journal of the Geological Society of India*, 83(4), 414-422.
- Nyagah, K. (1992). *Hydrocarbon exploration in the sedimentary basins of Kenya*. In: P.S. Plummer, Ed., *Proceedings of the Indian Ocean-First Regional Seminar on Petroleum Exploration* (pp. 53-66). United Nations Department of Technical Co-operation for Development, Seychelles.
- Nyagah, K. (1995). *Stratigraphy, depositional history and environments of deposition of Cretaceous through Tertiary strata in the Lamu Basin, southeast Kenya and implications for reservoirs for hydrocarbon exploration* (pp. 43-71). Nairobi: National Oil Corporation of Kenya.
- Nyagah, K. (1992). Stratigraphy, Deposition History and Environments of Deposition of Cretaceous through Tertiary Strata in the Lamu Basin, South-East Kenya and Implications on Hydrocarbon Exploration. *Bulletin*, 76, (50-65).
- Nyandat, N. & Oswaggo, O. (2013). *Soil Survey of Mkunguya Area, Lamu District* (p. 31). Kenya Agricultural Research Institute.
- Osicki, O., Schenk, O., & Kornpihl, d. (2015). *Prospectivity and Petroleum Systems Modelling of the offshore Lamu Basin, Kenya. Implication for an Emerging Hydrocarbon Province*. Presentation, Istanbul.
- Perry, E. & Hower, J. (1970). Burial diagenesis in Gulf coast pelitic sediments. *Clays and Clay Minerals*, 18(3), 165-177.
- Reeves, C., Karanja, F., & MacLeod, I. (1987). Geophysical evidence for a failed Jurassic rift and triple junction in Kenya. *Earth and Planetary Science Letters*, 81(2-3), 299-311.
- Reyes, J., Saad, S., & Lane, L. (2013). *Organic Petrology and Vitrinite Thermal Maturation Profiles for Eight Yukon Petroleum Exploration Wells in Eagle Plains and Liard Basins*. Geological Survey of Canada. 43, (30-42).
- Reynolds, R. (1992). X-ray Diffraction Studies of Illite/Smectite from Rocks, < 1 μm Randomly Oriented Powders, and < 1 μm Oriented Powder Aggregates: The Absence of Laboratory-Induced Artifacts. *Clays and Clay Minerals*, 40(4), 387-396.
- Reynolds, R.C. & Hower, J. (1970). The nature of interlayering in mixed layer illite-montmorillonites. *Clay and Clay Minerals*, 18, 25-26.
- Sakharov, B. (1999). Determination of illite-smectite structures using multispecimen X-ray diffraction profile fitting. *Clays and Clay Minerals*, 47(5), 555-566.

- Simiyu, S. (1989). *Geophysical studies in Lamu Embayment to determine its structures and stratigraphy* (M.Sc.). University of Nairobi, 22-30.
- Środoń, J. (1980). Precise identification of illite/smectite interstratifications by x-ray powder diffraction. *Clays and Clay Minerals*, 28(6), 401-411.
- Środoń, J. (1981). X-Ray identification of randomly interstratified illite-smectite in mixtures with discrete illite. *Clay Minerals*, 16(3), 297-304.
- Środoń, J. (1984). Mixed-layer illite-smectite in low-temperature diagenesis: data from the Miocene of the Carpathian foredeep. *Clay Minerals*, 19(2), 205-215.
- Środoń, J. (2009). Quantification of illite and smectite and their layer charges in sandstones and shales from shallow burial depth. *Clay Minerals*, 44(4), 421-434.
- Stixrude, L. & Peacor, D. (2002). First-principles study of illite–smectite and implications for clay mineral systems. *Nature*, 420(6912), 165-168.
- Tissot, B. & Welte, D. (1984). *Geochemical Prospecting, Geology Prospecting*. Springer-Verlag, 699p.
- Velde, B. (1986). Pressure-Temperature-Composition of illite/smectite mixed-layer minerals: Niger Delta mudstones and other examples. *Clays and Clay Minerals*, 34(4), 435-441.

APPENDIX I: KIPINI 1 X-RAY DIFFRACTION DATA

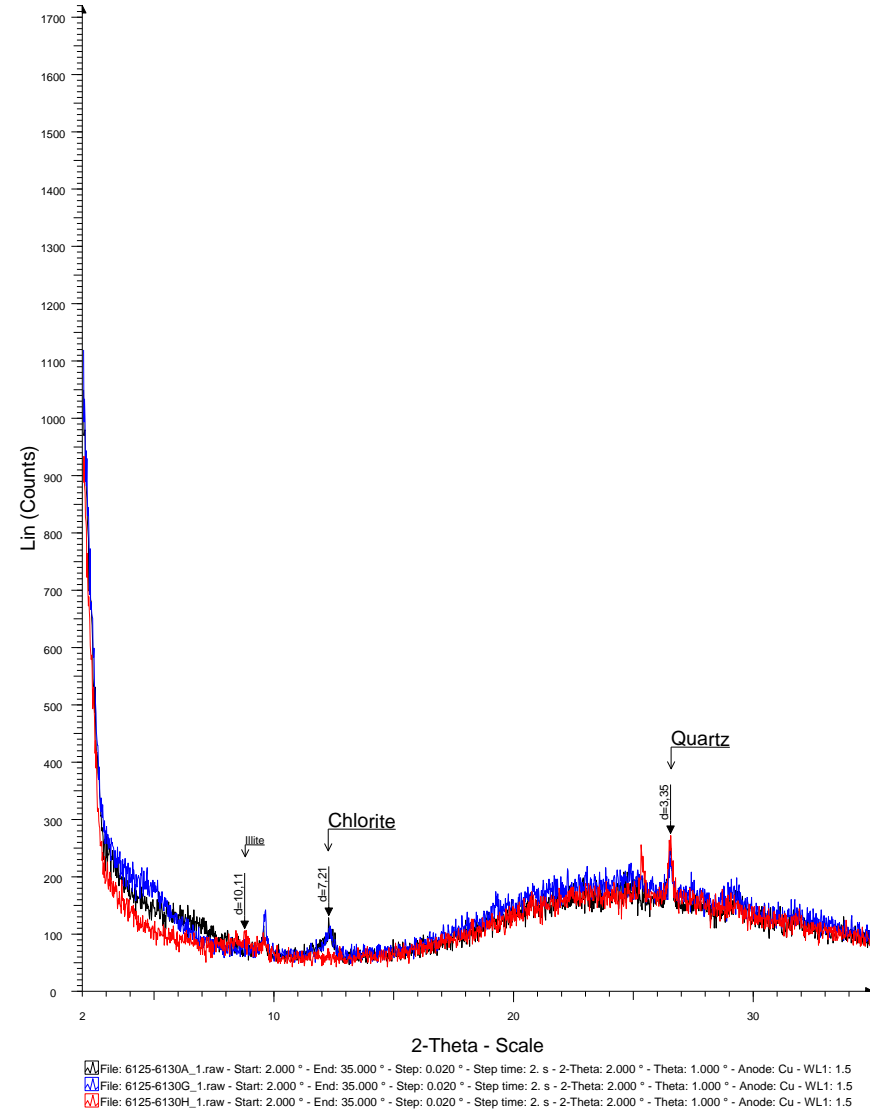
X-ray diffractograms obtained for the forty eight (48) core samples during x-ray diffraction analysis of clay minerals are as given below. The black curve is the air dried, blue is the glycol treated and the red is the heated analysis. The values marked in the curves is the diffraction angles given in Å as identified by *brucker* software. The diffraction angles are used for identifying the clay minerals and not the $\theta 2\theta$ angles on the y-axis of the curves.

KIPINI1:3220-3225



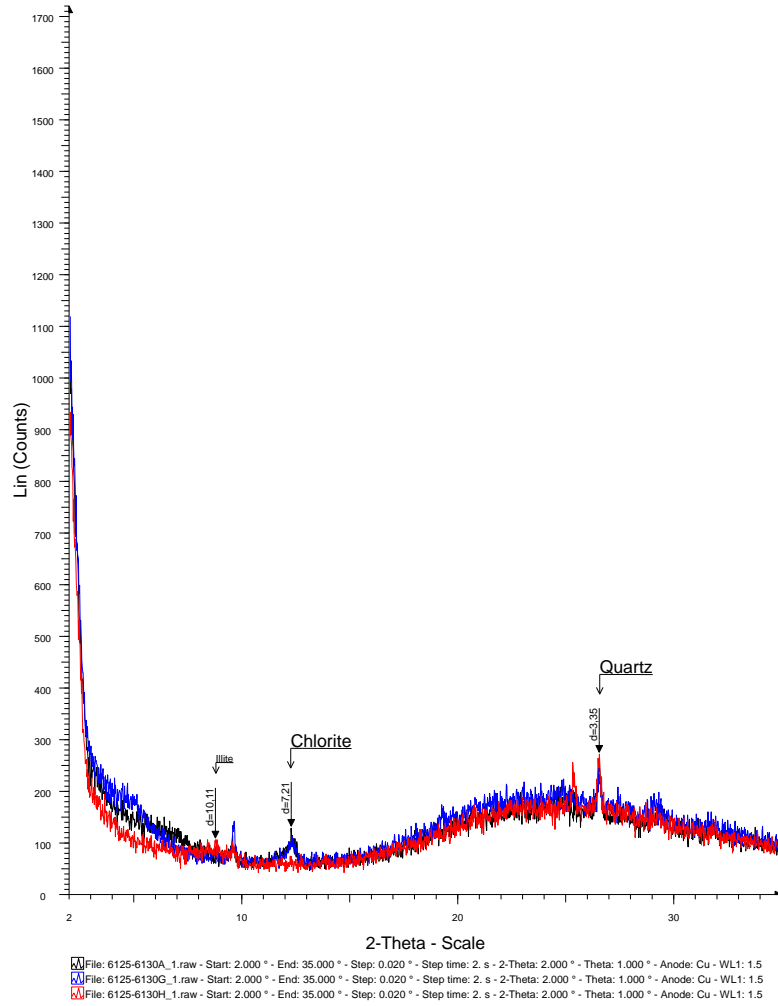
981-983m

KIPINI1:6125-6130ft



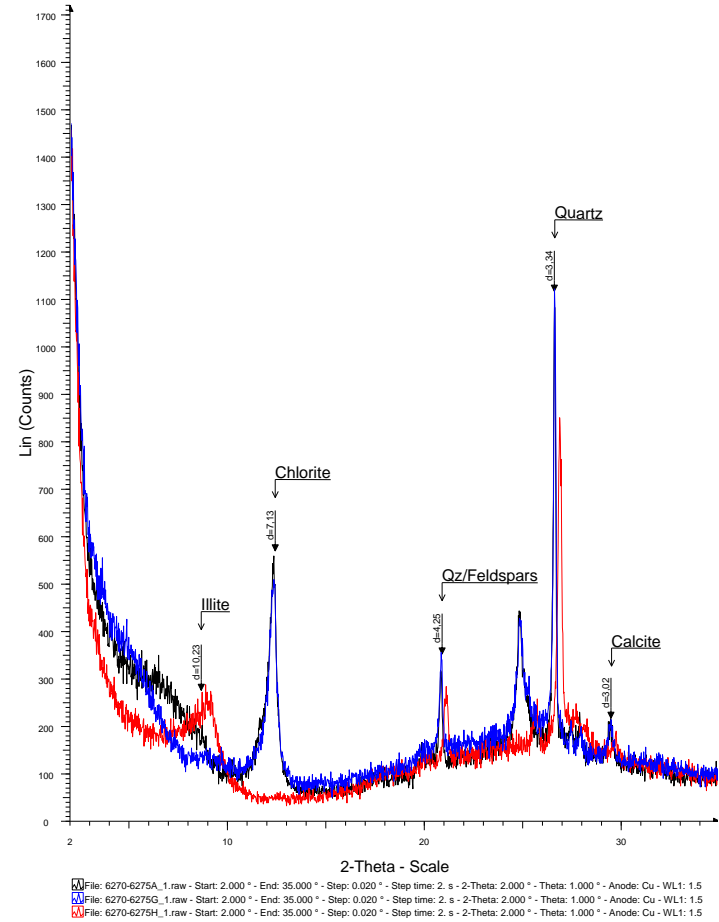
2042 – 2043m

KIPINI1:6125-6130ft



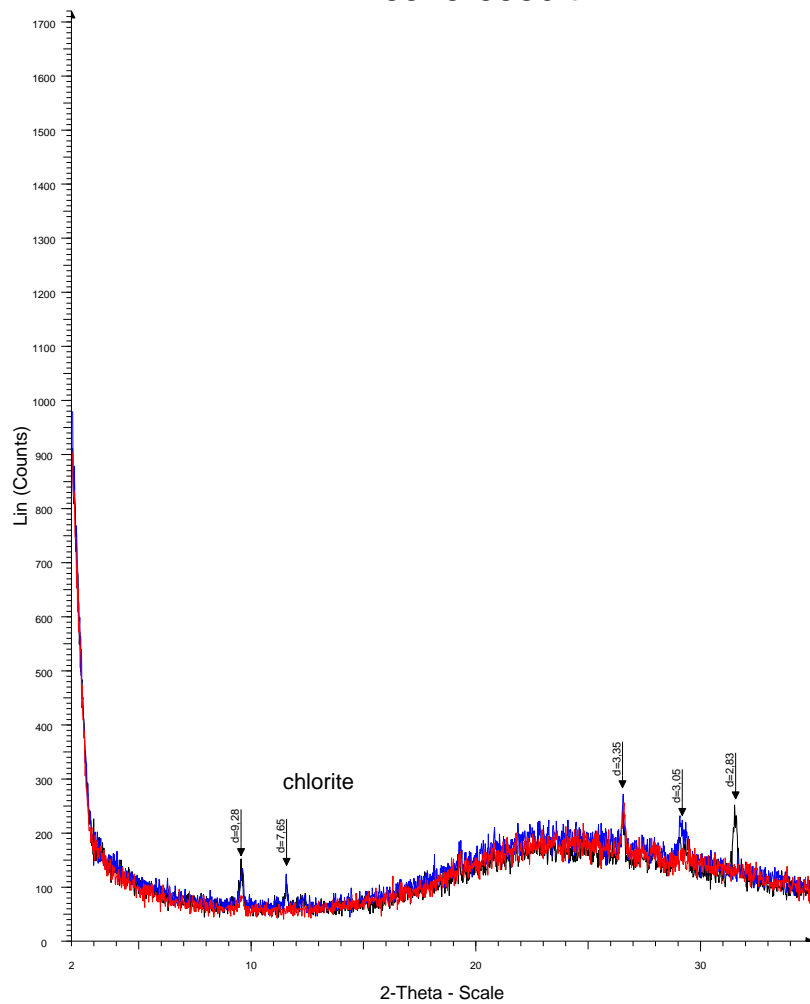
1839 – 1840m

KIPINI1:6270-6275ft



1867-1868m

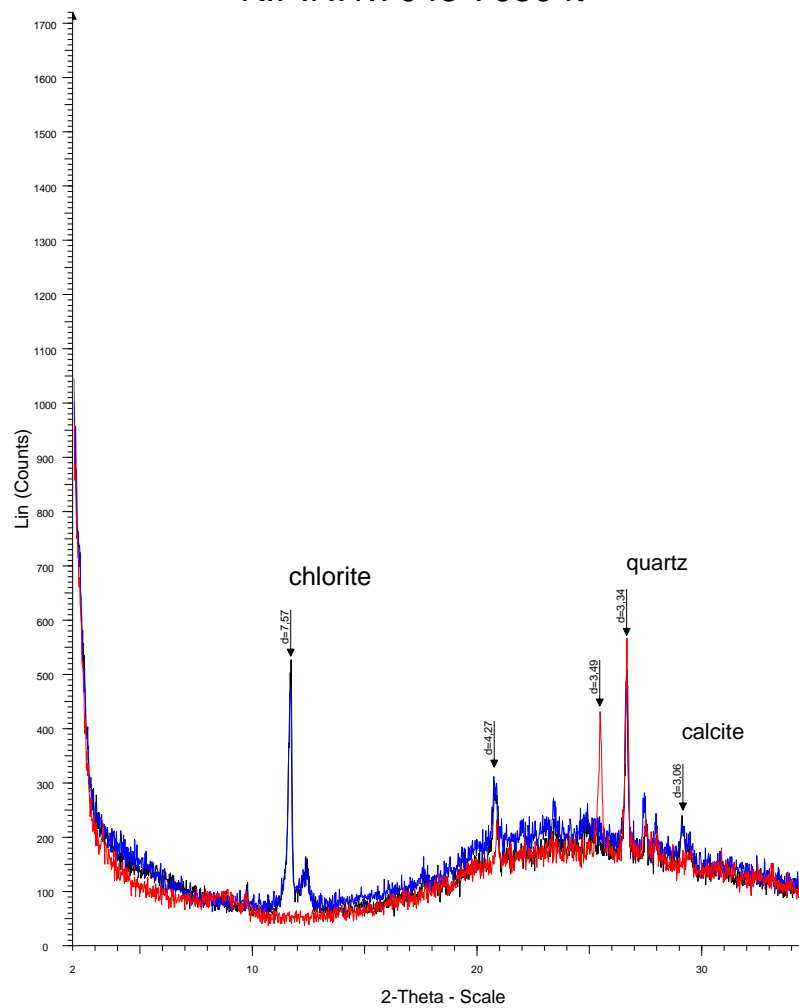
KIPINI1:6575-6580ft



File: 6575-6580A_1.raw - Start: 2.000 ° - End: 35.000 ° - Step: 0.020 ° - Step time: 2. s - 2-Theta: 2.000 ° - Theta: 1.000 ° - Anode: Cu - WL1: 1.5
File: 6575-6580G_1.raw - Start: 2.000 ° - End: 35.000 ° - Step: 0.020 ° - Step time: 2. s - 2-Theta: 2.000 ° - Theta: 1.000 ° - Anode: Cu - WL1: 1.5
File: 6575-6580H_1.raw - Start: 2.000 ° - End: 35.000 ° - Step: 0.020 ° - Step time: 2. s - 2-Theta: 2.000 ° - Theta: 1.000 ° - Anode: Cu - WL1: 1.5

2004-2006m

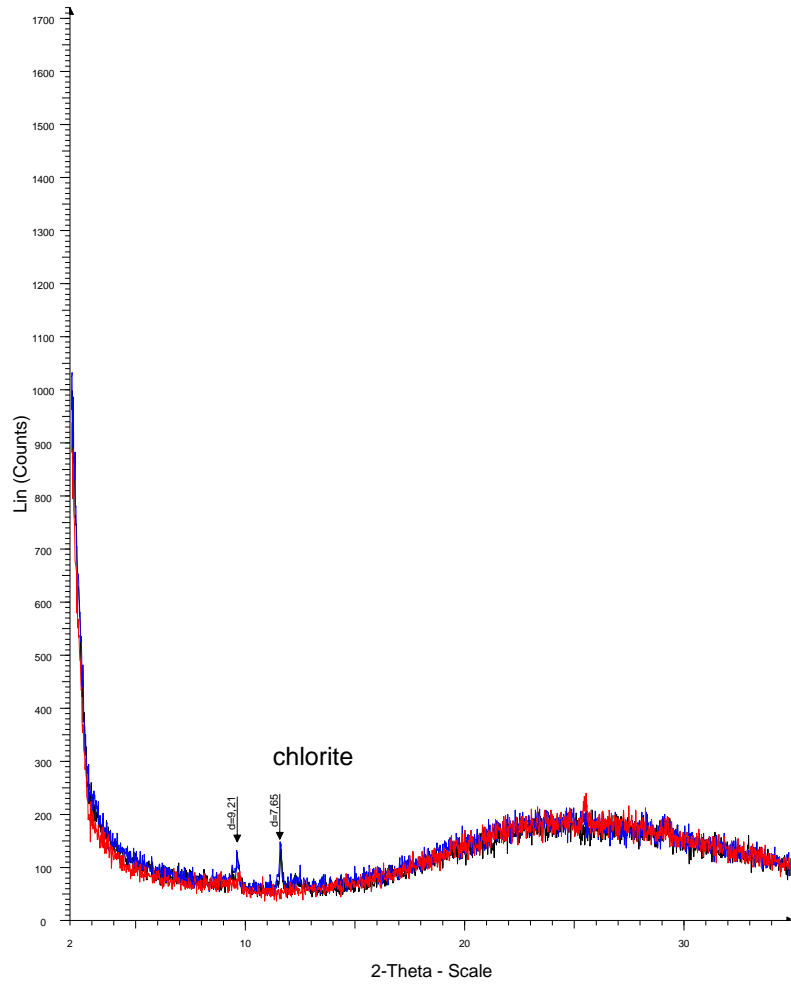
KIPINI1:7045-7050 ft



File: 7045-7050A_1.raw - Start: 2.000 ° - End: 35.000 ° - Step: 0.020 ° - Step time: 2. s - 2-Theta: 2.000 ° - Theta: 1.000 ° - Anode: Cu - WL1: 1.5
File: 7045-7050G_1.raw - Start: 2.000 ° - End: 35.000 ° - Step: 0.020 ° - Step time: 2. s - 2-Theta: 2.000 ° - Theta: 1.000 ° - Anode: Cu - WL1: 1.5
File: 7045-7050H_1.raw - Start: 2.000 ° - End: 35.000 ° - Step: 0.020 ° - Step time: 2. s - 2-Theta: 2.000 ° - Theta: 1.000 ° - Anode: Cu - WL1: 1.5

2147-2149m

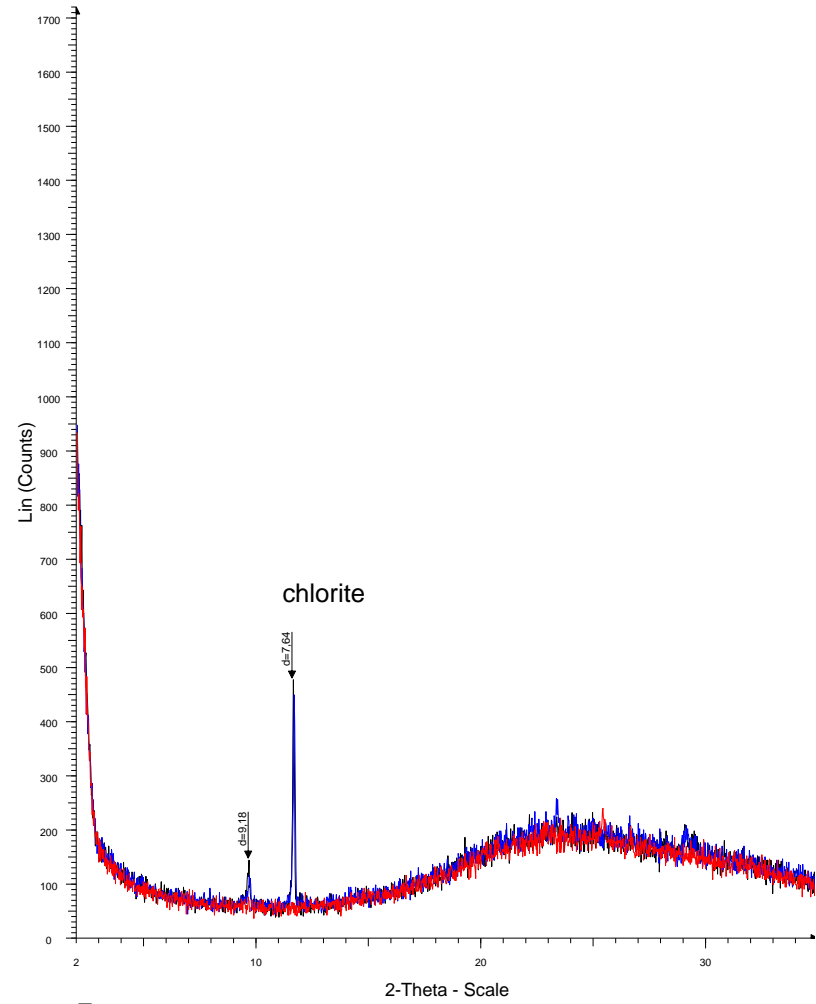
KIPINI1:8470-8475 ft



File: 8470-8475A_1.raw - Start: 2.000 ° - End: 35.000 ° - Step: 0.020 ° - Step time: 2. s - 2-Theta: 2.000 ° - Theta: 1.000 ° - Anode: Cu - WL1: 1.5
File: 8470-8475G_1.raw - Start: 2.000 ° - End: 35.000 ° - Step: 0.020 ° - Step time: 2. s - 2-Theta: 2.000 ° - Theta: 1.000 ° - Anode: Cu - WL1: 1.5
File: 8470-8475H_1.raw - Start: 2.000 ° - End: 35.000 ° - Step: 0.020 ° - Step time: 2. s - 2-Theta: 2.000 ° - Theta: 1.000 ° - Anode: Cu - WL1: 1.5

2582-2583m

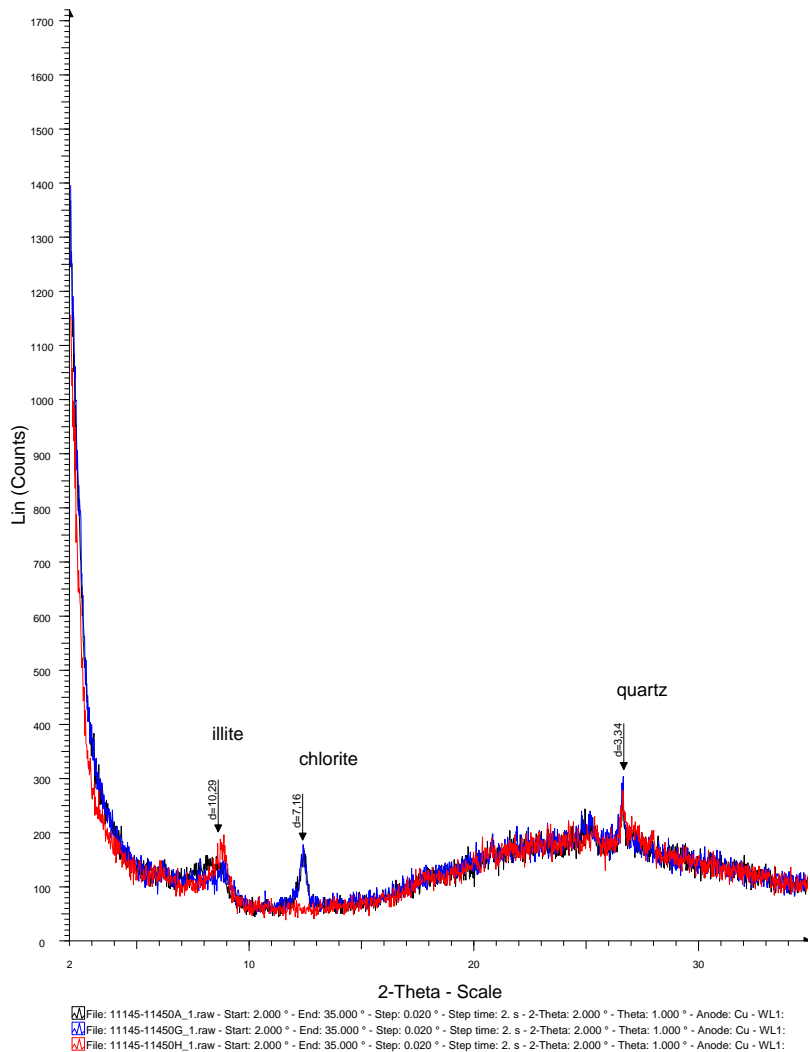
KIPINI1: 9075-9080 ft



File: 9075-9080A_1.raw - Start: 2.000 ° - End: 35.000 ° - Step: 0.020 ° - Step time: 2. s - 2-Theta: 2.000 ° - Theta: 1.000 ° - Anode: Cu - WL1: 1.5
File: 9075-9080G_1.raw - Start: 2.000 ° - End: 35.000 ° - Step: 0.020 ° - Step time: 2. s - 2-Theta: 2.000 ° - Theta: 1.000 ° - Anode: Cu - WL1: 1.5
File: 9075-9080H_1.raw - Start: 2.000 ° - End: 35.000 ° - Step: 0.020 ° - Step time: 2. s - 2-Theta: 2.000 ° - Theta: 1.000 ° - Anode: Cu - WL1: 1.5

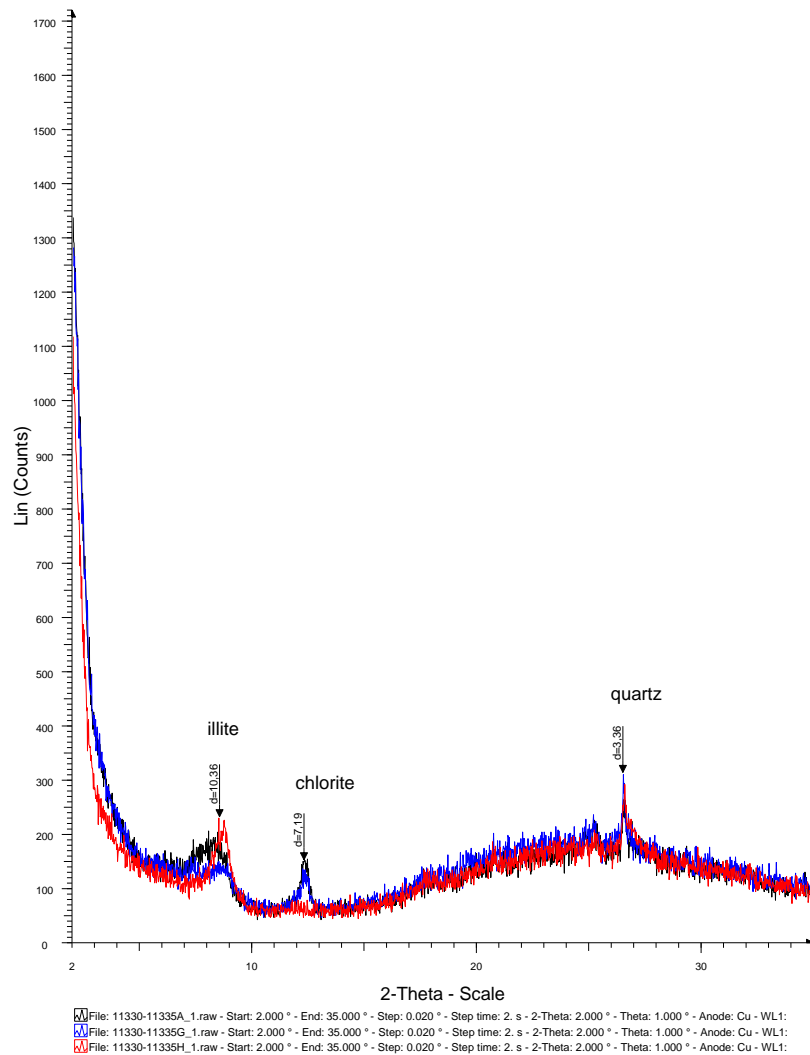
2766-2768m

KIPINI1: 11145-11450 ft



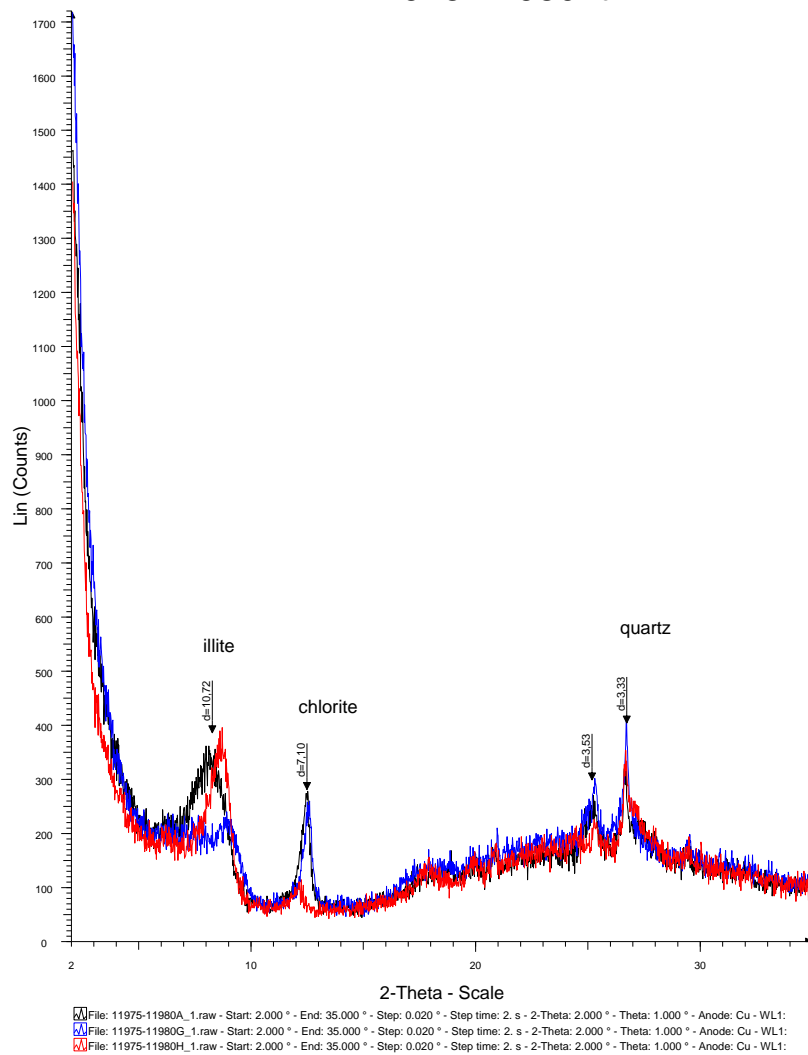
3397-3490m

KIPINI1: 11330-11335 ft



3453-3454m

KIPINI1: 11975-11980 ft

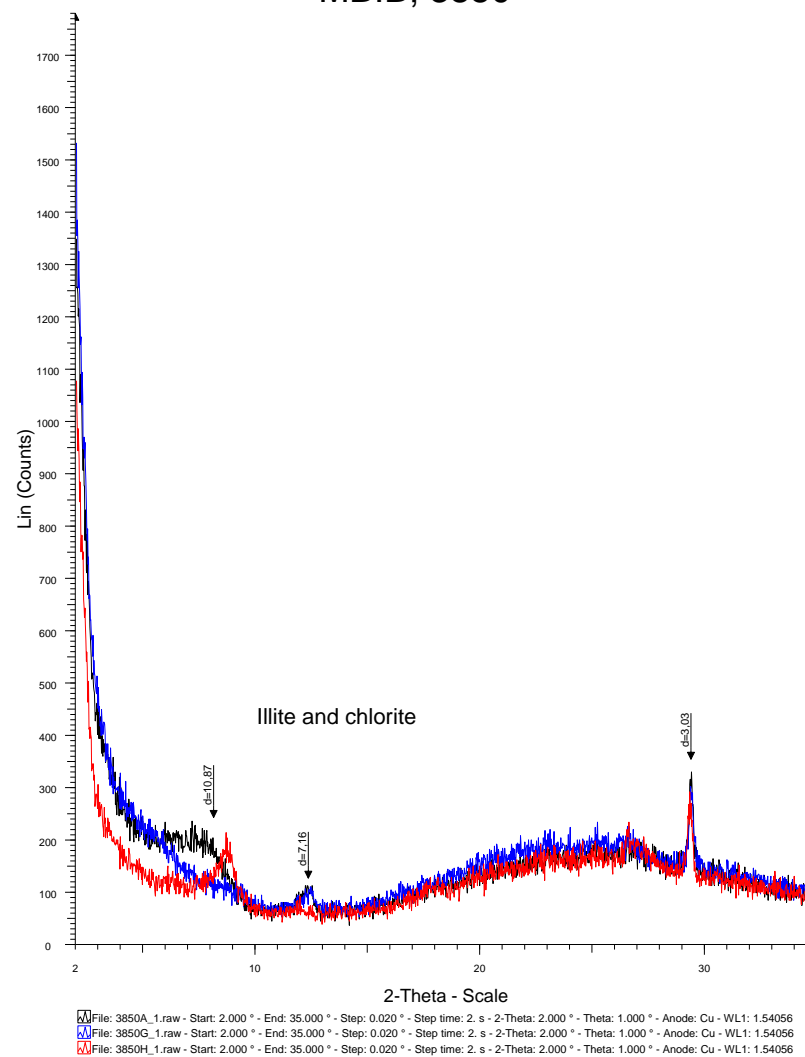
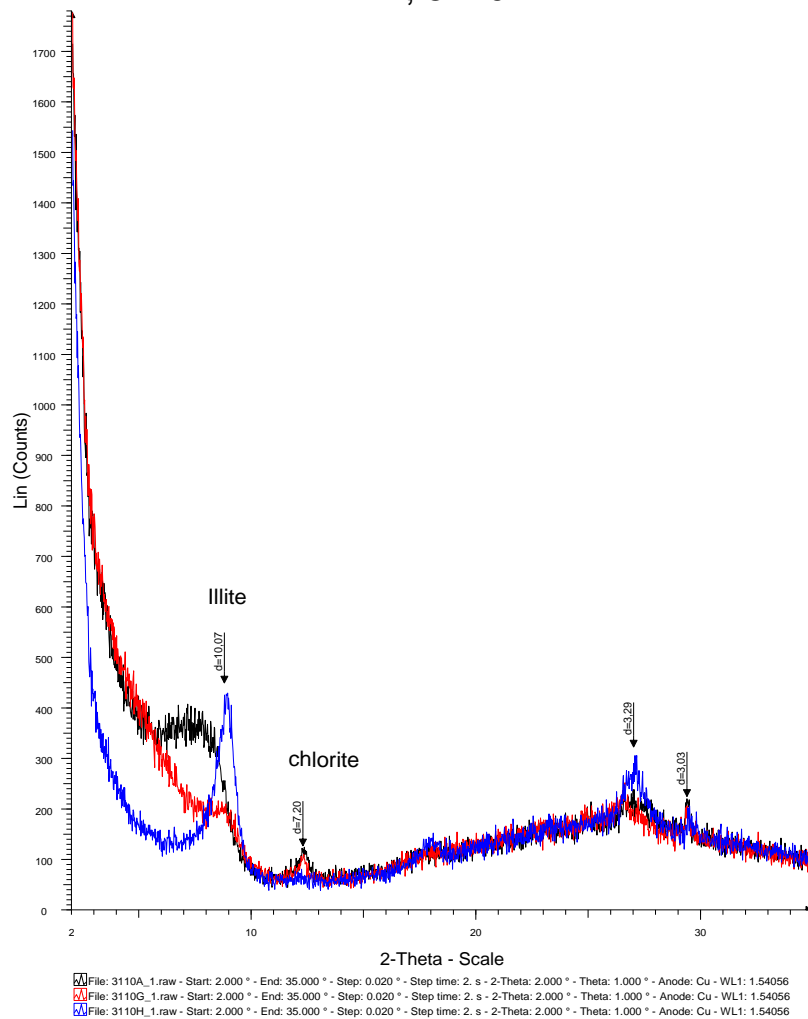


3649-3651m

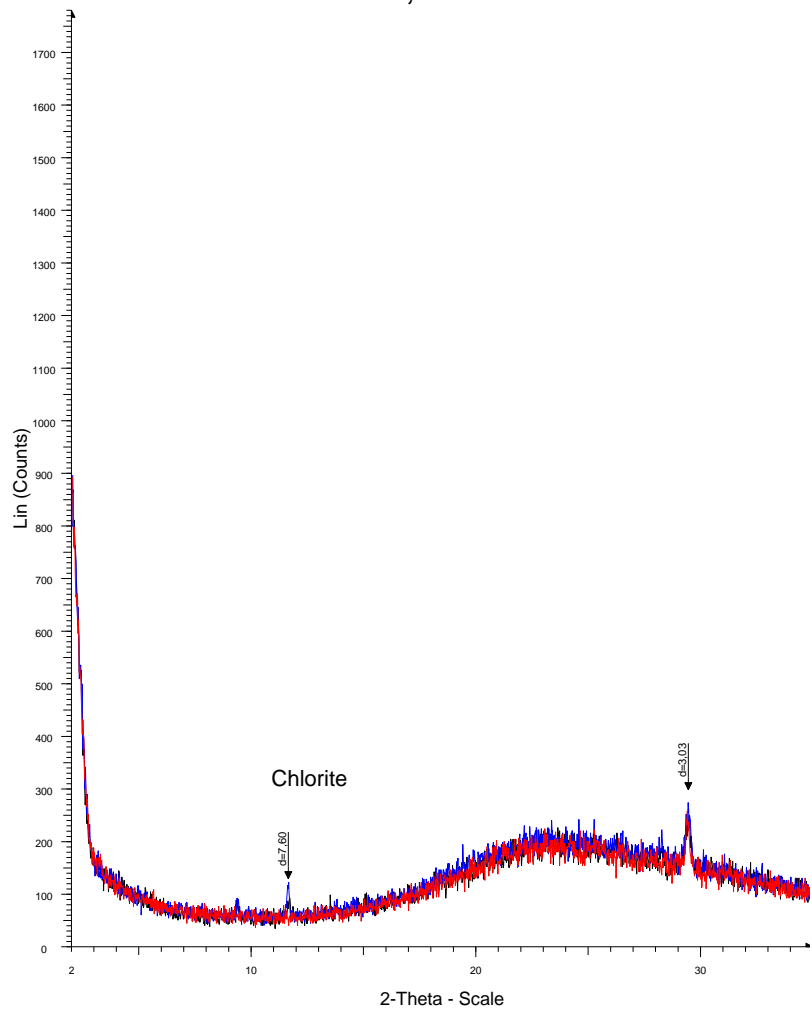
APPENDIX II: MARIDADI 1B X-RAY DIFFRACTION DATA

MBIB; 3850

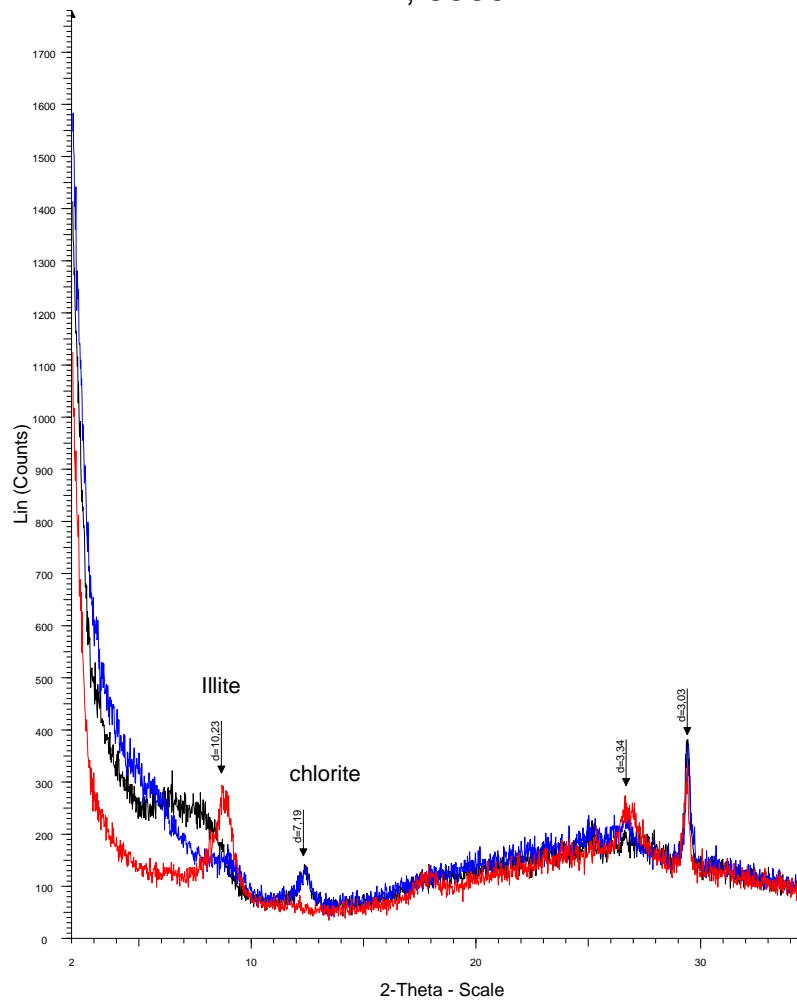
MBIB; 3110



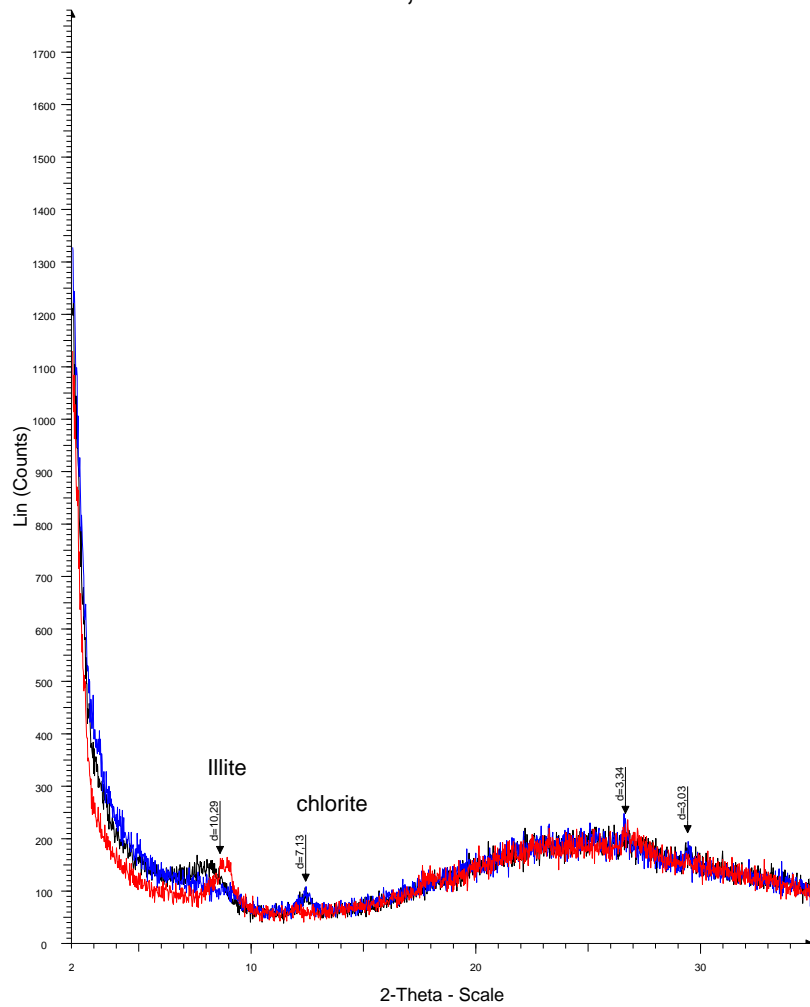
MBIB; 3550



MBIB; 3860

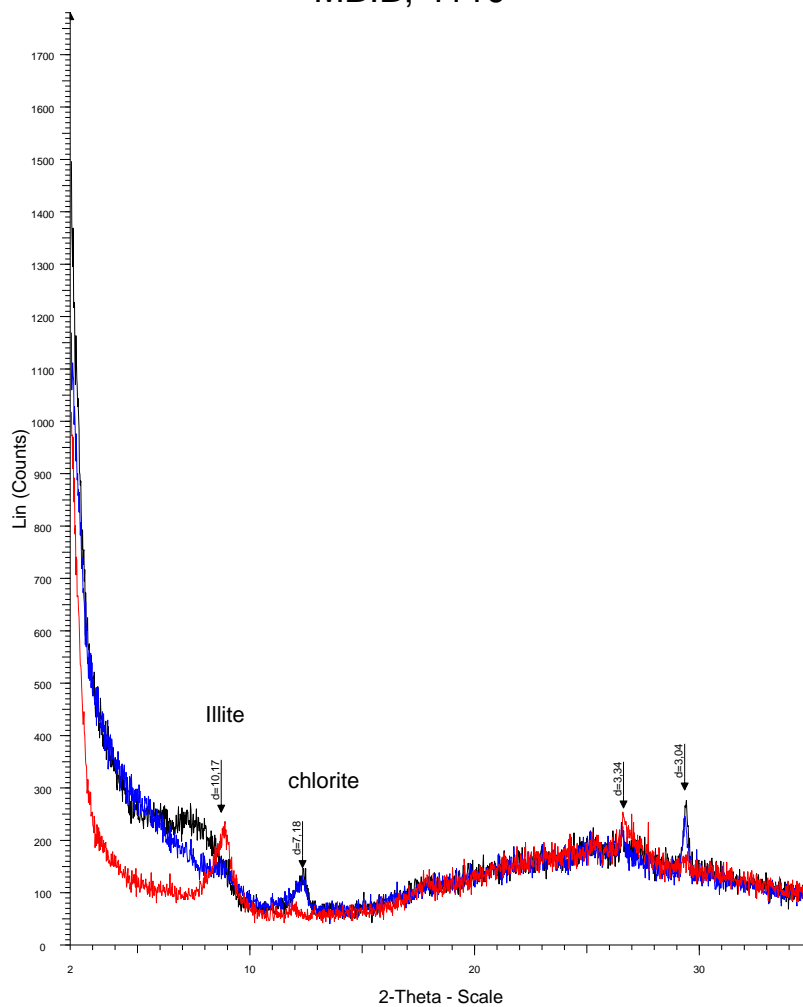


MBIB; 3930



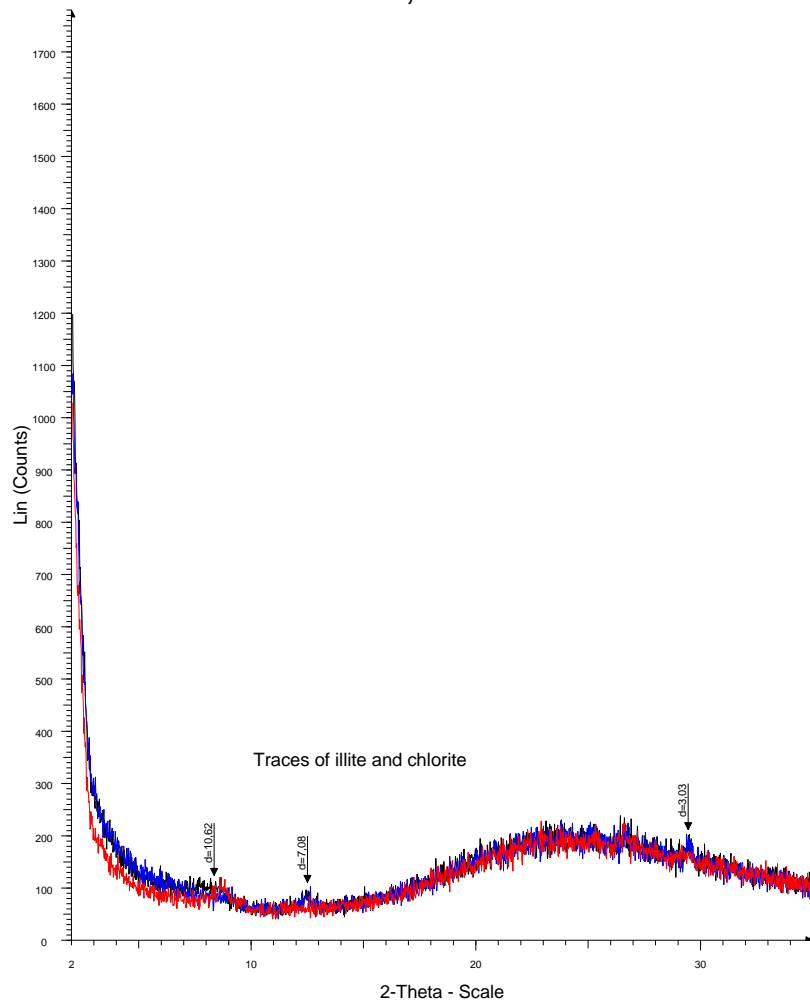
File: 3930A_1.raw - Start: 2.000 ° - End: 35.000 ° - Step: 0.020 ° - Step time: 2. s - 2-Theta: 2.000 ° - Theta: 1.000 ° - Anode: Cu - WL1: 1.54056
File: 3930G_1.raw - Start: 2.000 ° - End: 35.000 ° - Step: 0.020 ° - Step time: 2. s - 2-Theta: 2.000 ° - Theta: 1.000 ° - Anode: Cu - WL1: 1.54056
File: 3930H_1.raw - Start: 2.000 ° - End: 35.000 ° - Step: 0.020 ° - Step time: 2. s - 2-Theta: 2.000 ° - Theta: 1.000 ° - Anode: Cu - WL1: 1.54056

MBIB; 4110



File: 4110A_1.raw - Start: 2.000 ° - End: 35.000 ° - Step: 0.020 ° - Step time: 2. s - 2-Theta: 2.000 ° - Theta: 1.000 ° - Anode: Cu - WL1: 1.54056
File: 4110G_1.raw - Start: 2.000 ° - End: 35.000 ° - Step: 0.020 ° - Step time: 2. s - 2-Theta: 2.000 ° - Theta: 1.000 ° - Anode: Cu - WL1: 1.54056
File: 4110H_1.raw - Start: 2.000 ° - End: 35.000 ° - Step: 0.020 ° - Step time: 2. s - 2-Theta: 2.000 ° - Theta: 1.000 ° - Anode: Cu - WL1: 1.54056

MBIB; 4160

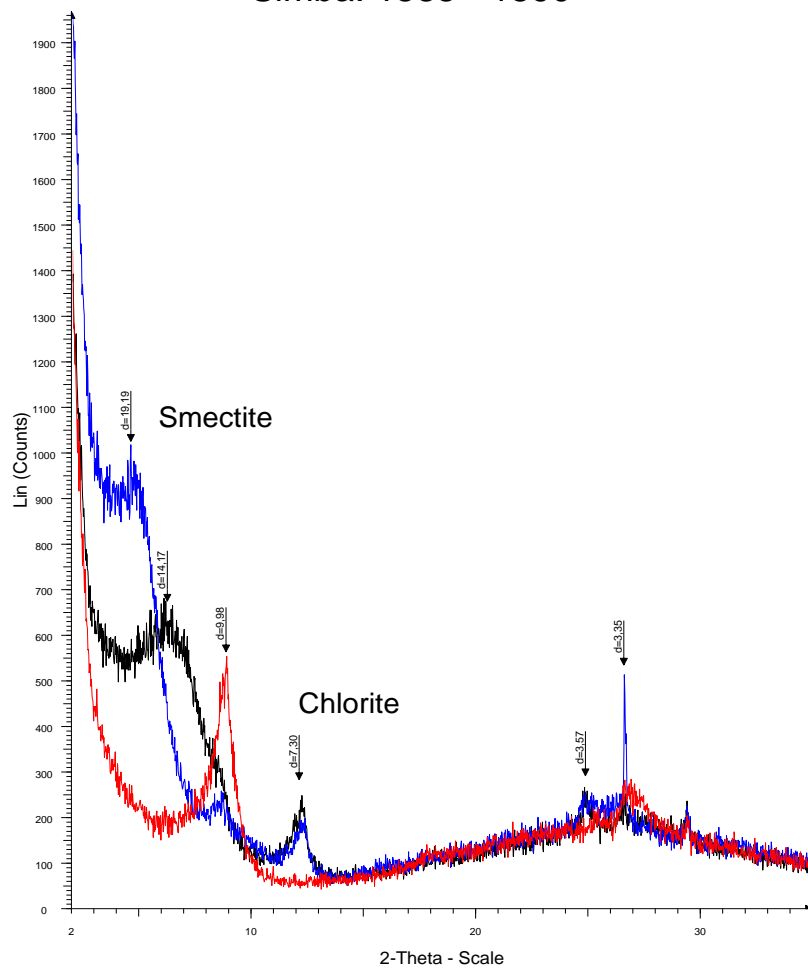


File: 4160-4190A_1.raw - Start: 2.000 ° - End: 35.000 ° - Step: 0.020 ° - Step time: 2. s - 2-Theta: 2.000 ° - Theta: 1.000 ° - Anode: Cu - WL1: 1.5
File: 4160-4190G_1.raw - Start: 2.000 ° - End: 35.000 ° - Step: 0.020 ° - Step time: 2. s - 2-Theta: 2.000 ° - Theta: 1.000 ° - Anode: Cu - WL1: 1.5
File: 4160-4190H_1.raw - Start: 2.000 ° - End: 35.000 ° - Step: 0.020 ° - Step time: 2. s - 2-Theta: 2.000 ° - Theta: 1.000 ° - Anode: Cu - WL1: 1.5

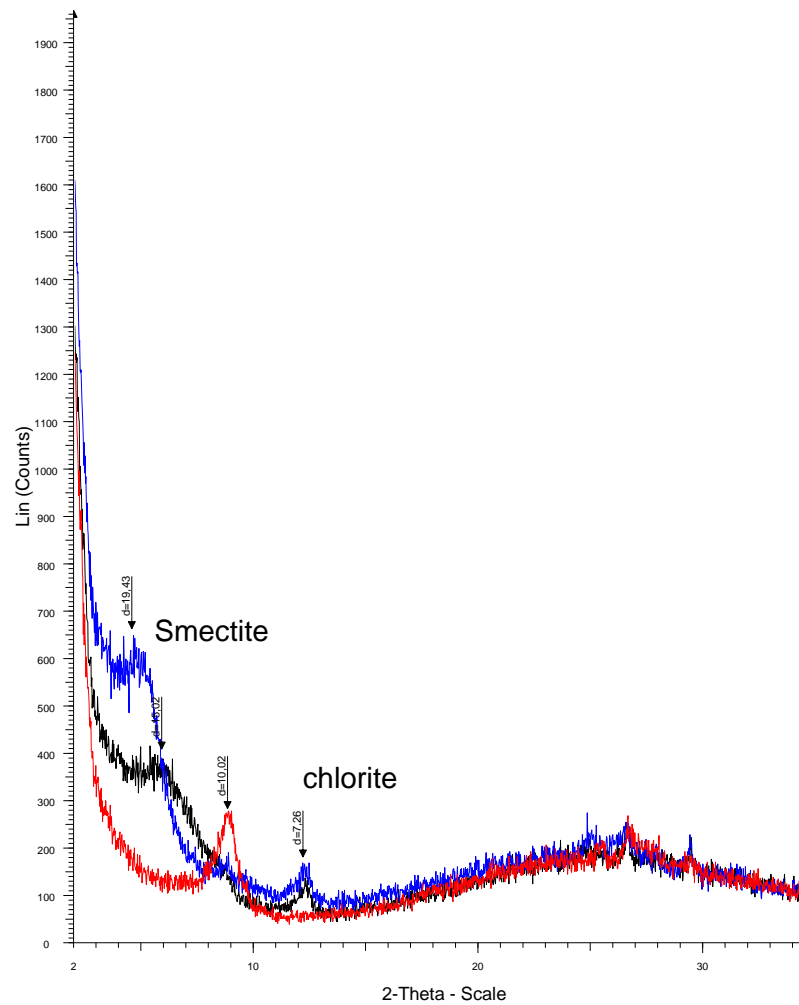
APPENDIX III: SIMBA X-RAY DIFFRACTION DATA

Simba: 1840-1845

Simba: 1585 - 1590

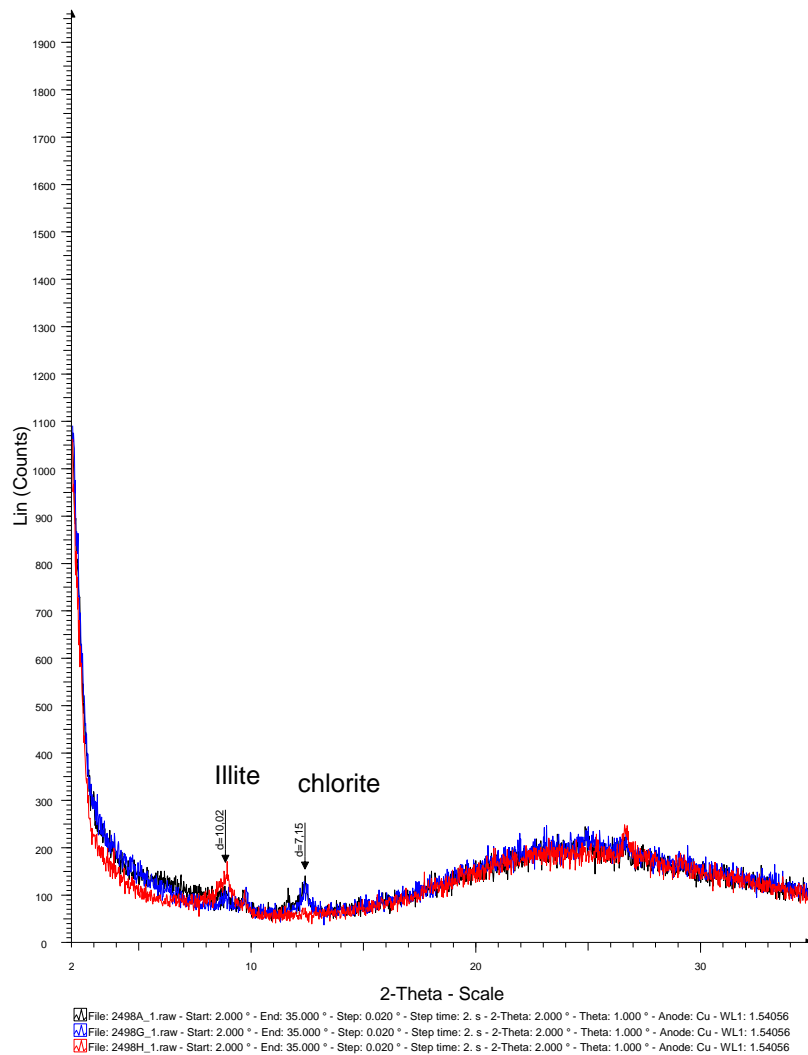


File: 1585-1590A_1.raw - Start: 2.000 ° - End: 35.000 ° - Step: 0.020 ° - Step time: 2. s - 2-Theta: 2.000 ° - Theta: 1.000 ° - Anode: Cu - WL: 1.5
 File: 1585-1590G_1.raw - Start: 2.000 ° - End: 35.000 ° - Step: 0.020 ° - Step time: 2. s - 2-Theta: 2.000 ° - Theta: 1.000 ° - Anode: Cu - WL: 1.5
 File: 1585-1590H_1.raw - Start: 2.000 ° - End: 35.000 ° - Step: 0.020 ° - Step time: 2. s - 2-Theta: 2.000 ° - Theta: 1.000 ° - Anode: Cu - WL: 1.5

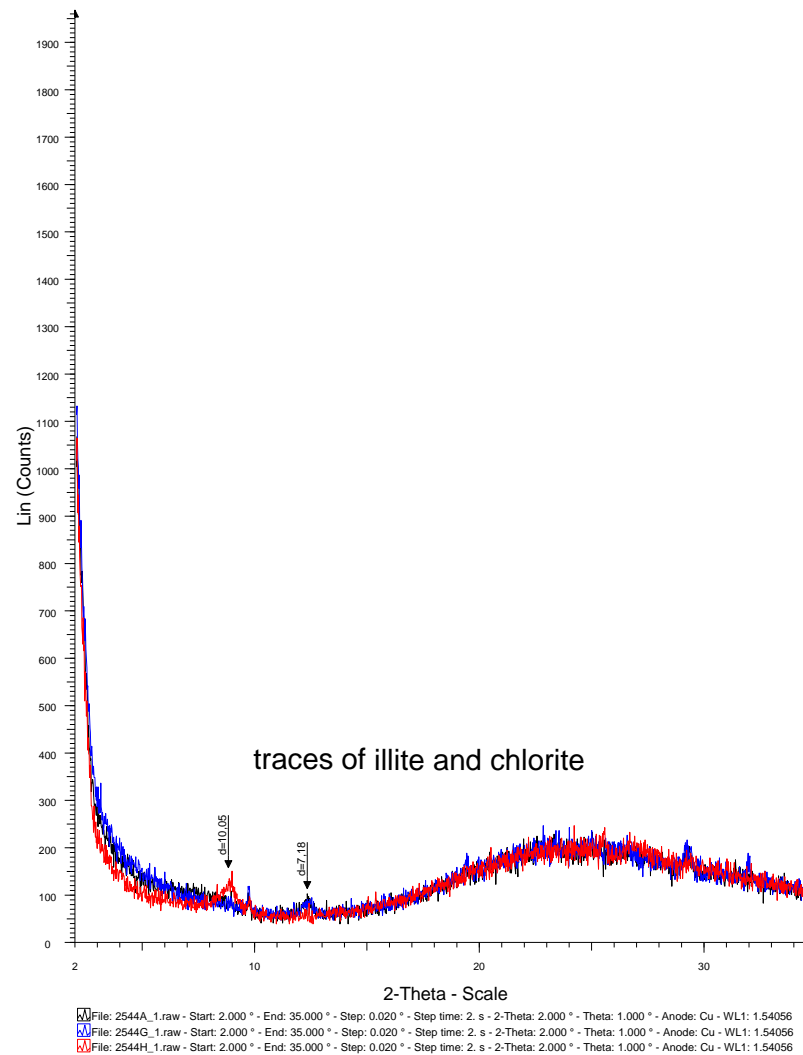


File: 1840-1845A_1.raw - Start: 2.000 ° - End: 35.000 ° - Step: 0.020 ° - Step time: 2. s - 2-Theta: 2.000 ° - Theta: 1.000 ° - Anode: Cu - WL: 1.5
 File: 1840-1845G_1.raw - Start: 2.000 ° - End: 35.000 ° - Step: 0.020 ° - Step time: 2. s - 2-Theta: 2.000 ° - Theta: 1.000 ° - Anode: Cu - WL: 1.5
 File: 1840-1845H_1.raw - Start: 2.000 ° - End: 35.000 ° - Step: 0.020 ° - Step time: 2. s - 2-Theta: 2.000 ° - Theta: 1.000 ° - Anode: Cu - WL: 1.5

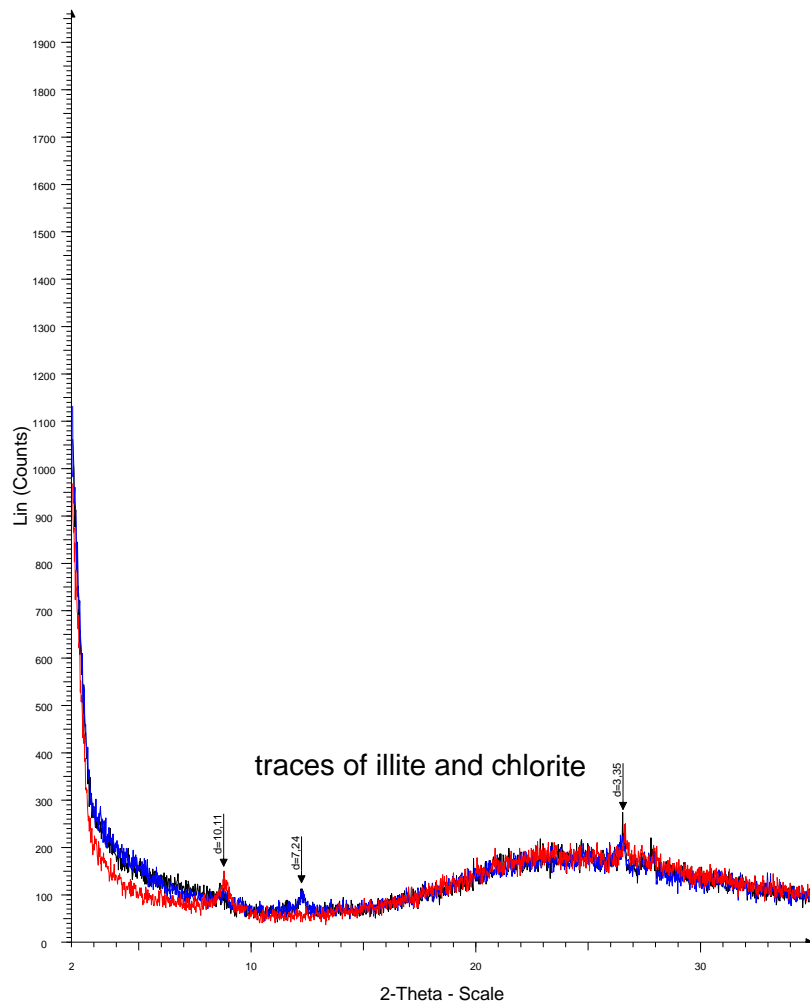
Simba: 2498



Simba: 2544

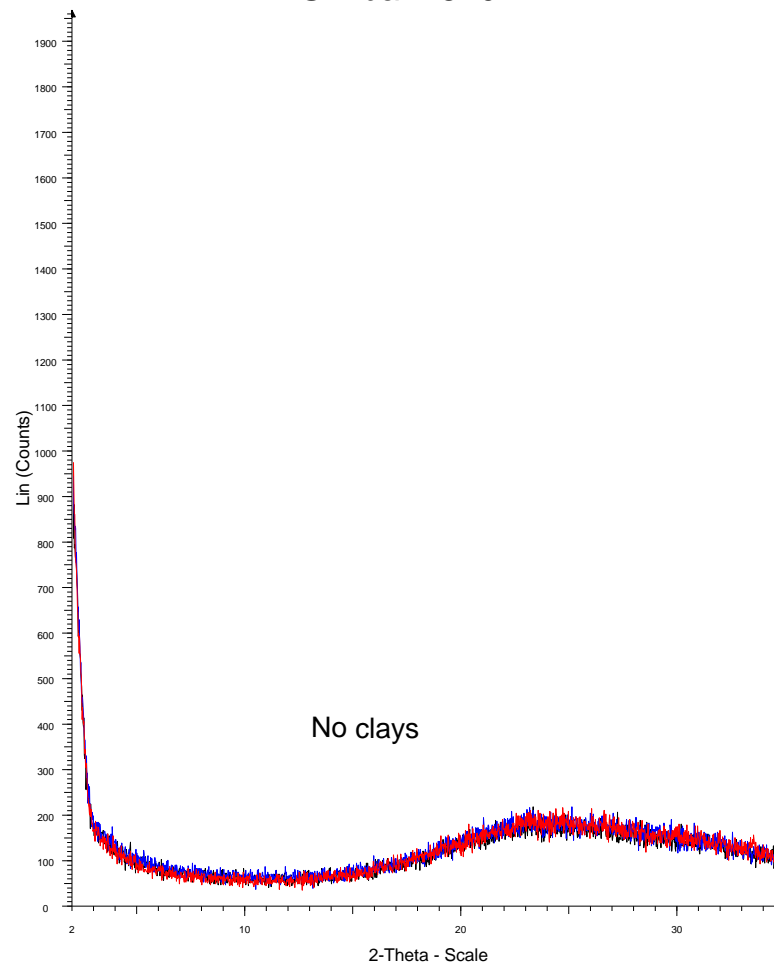


Simba: 2670



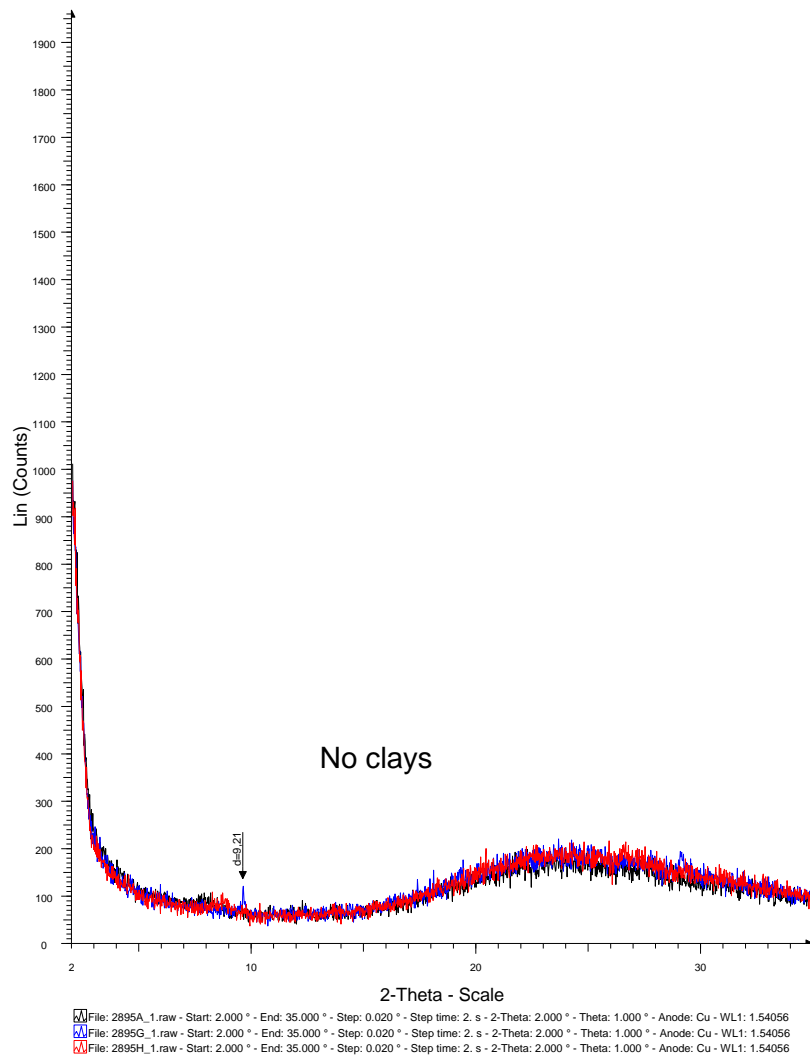
File: 2670A_1.raw - Start: 2.000 ° - End: 35.000 ° - Step: 0.020 ° - Step time: 2. s - 2-Theta: 2.000 ° - Theta: 1.000 ° - Anode: Cu - WL1: 1.54056
File: 2670G_1.raw - Start: 2.000 ° - End: 35.000 ° - Step: 0.020 ° - Step time: 2. s - 2-Theta: 2.000 ° - Theta: 1.000 ° - Anode: Cu - WL1: 1.54056
File: 2670H_1.raw - Start: 2.000 ° - End: 35.000 ° - Step: 0.020 ° - Step time: 2. s - 2-Theta: 2.000 ° - Theta: 1.000 ° - Anode: Cu - WL1: 1.54056

Simba: 2820

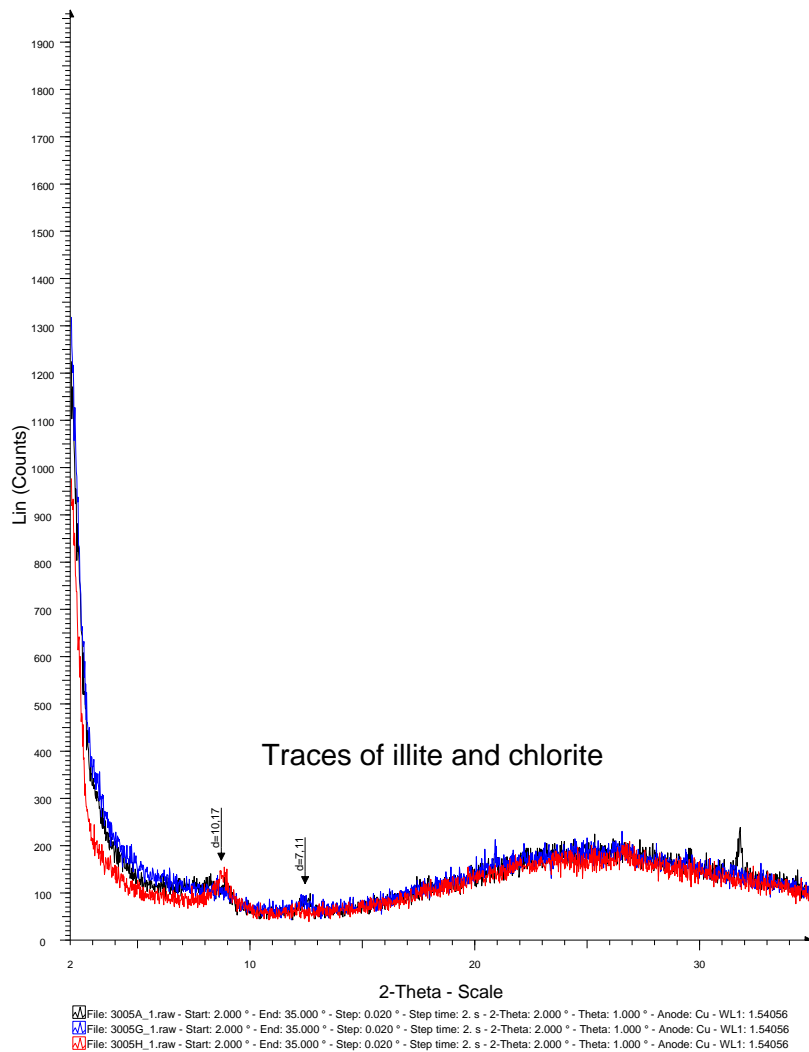


File: 2820A_1.raw - Start: 2.000 ° - End: 35.000 ° - Step: 0.020 ° - Step time: 2. s - 2-Theta: 2.000 ° - Theta: 1.000 ° - Anode: Cu - WL1: 1.54056
File: 2820G_1.raw - Start: 2.000 ° - End: 35.000 ° - Step: 0.020 ° - Step time: 2. s - 2-Theta: 2.000 ° - Theta: 1.000 ° - Anode: Cu - WL1: 1.54056
File: 2820H_1.raw - Start: 2.000 ° - End: 35.000 ° - Step: 0.020 ° - Step time: 2. s - 2-Theta: 2.000 ° - Theta: 1.000 ° - Anode: Cu - WL1: 1.54056

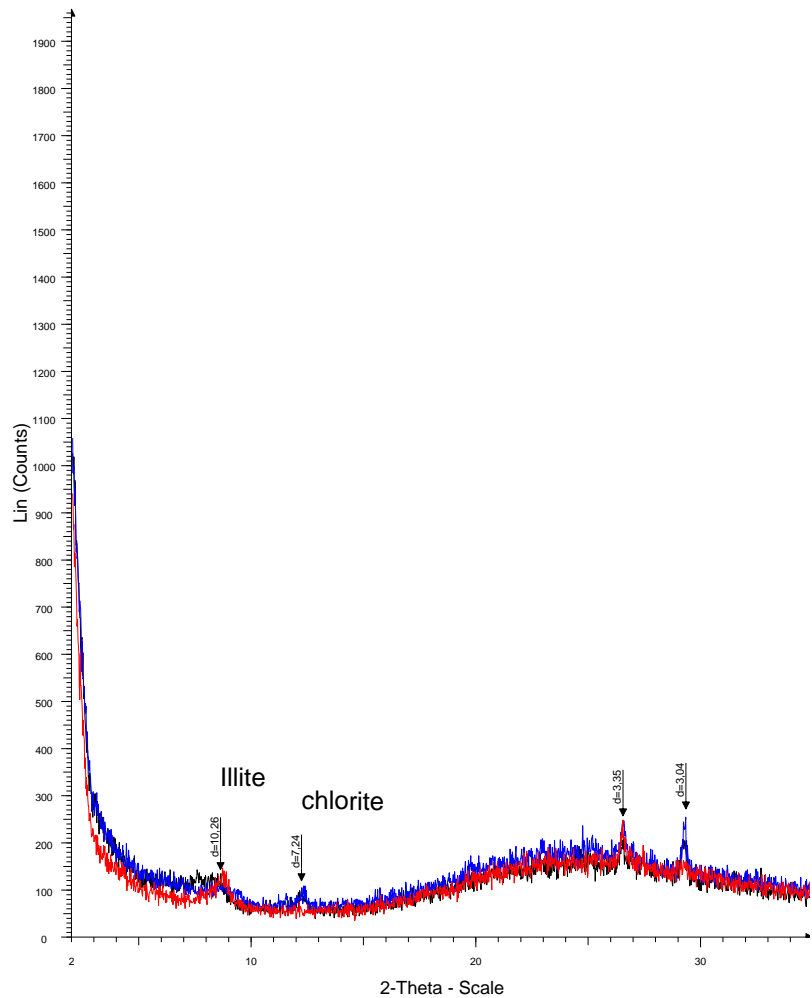
Simba: 2895



Simba: 3005

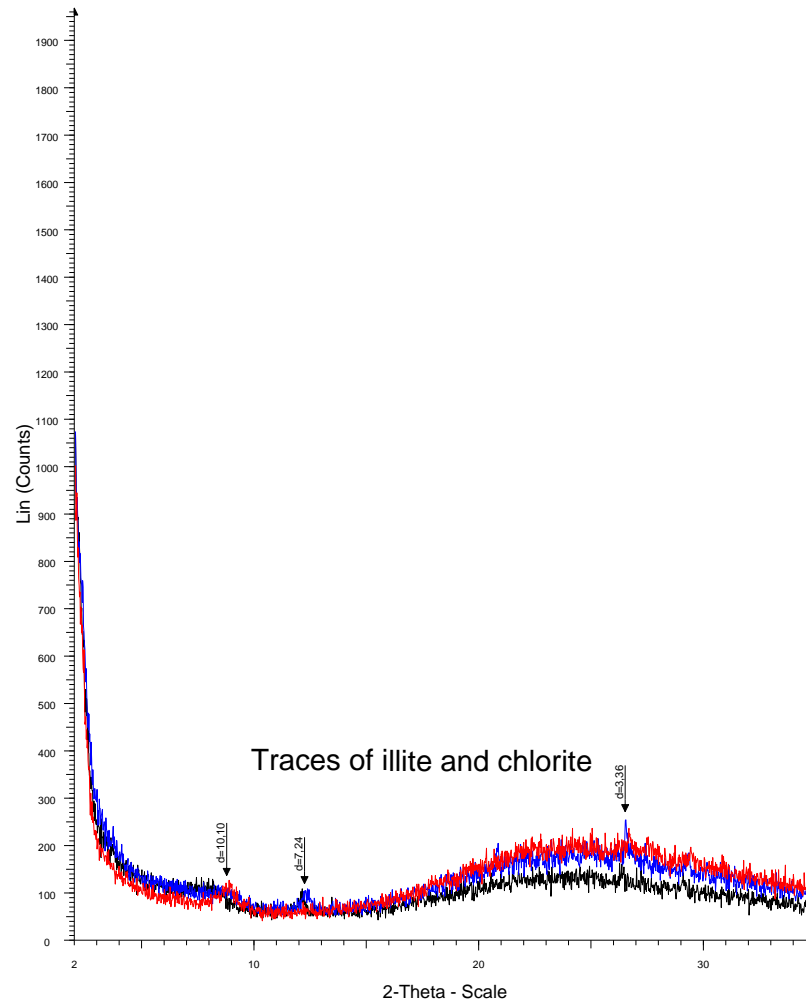


Simba: 3142



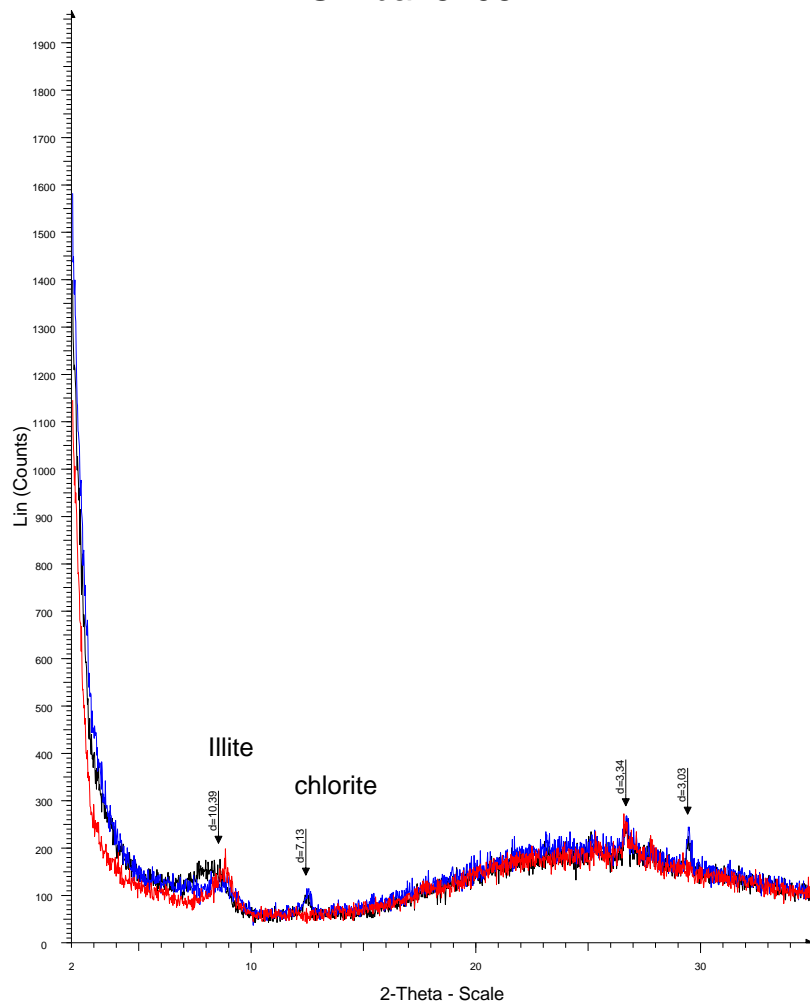
File: 3142A_1.raw - Start: 2.000 ° - End: 35.000 ° - Step: 0.020 ° - Step time: 2. s - 2-Theta: 2.000 ° - Theta: 1.000 ° - Anode: Cu - WL1: 1.54056
File: 3142G_1.raw - Start: 2.000 ° - End: 35.000 ° - Step: 0.020 ° - Step time: 2. s - 2-Theta: 2.000 ° - Theta: 1.000 ° - Anode: Cu - WL1: 1.54056
File: 3142H_1.raw - Start: 2.000 ° - End: 35.000 ° - Step: 0.020 ° - Step time: 2. s - 2-Theta: 2.000 ° - Theta: 1.000 ° - Anode: Cu - WL1: 1.54056

Simba: 3206



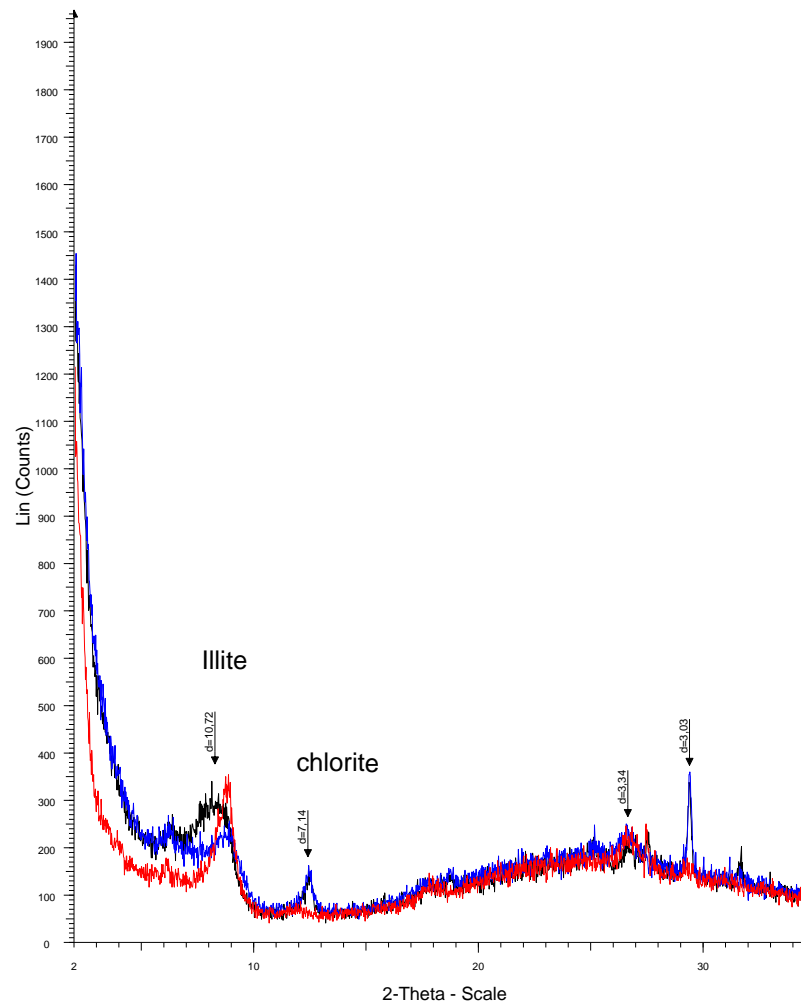
File: 3206A_1.raw - Start: 2.000 ° - End: 35.000 ° - Step: 0.020 ° - Step time: 2. s - 2-Theta: 2.000 ° - Theta: 1.000 ° - Anode: Cu - WL1: 1.54056
File: 3206G_1.raw - Start: 2.000 ° - End: 35.000 ° - Step: 0.020 ° - Step time: 2. s - 2-Theta: 2.000 ° - Theta: 1.000 ° - Anode: Cu - WL1: 1.54056
File: 3206H_1.raw - Start: 2.000 ° - End: 35.000 ° - Step: 0.020 ° - Step time: 2. s - 2-Theta: 2.000 ° - Theta: 1.000 ° - Anode: Cu - WL1: 1.54056

Simba: 3298



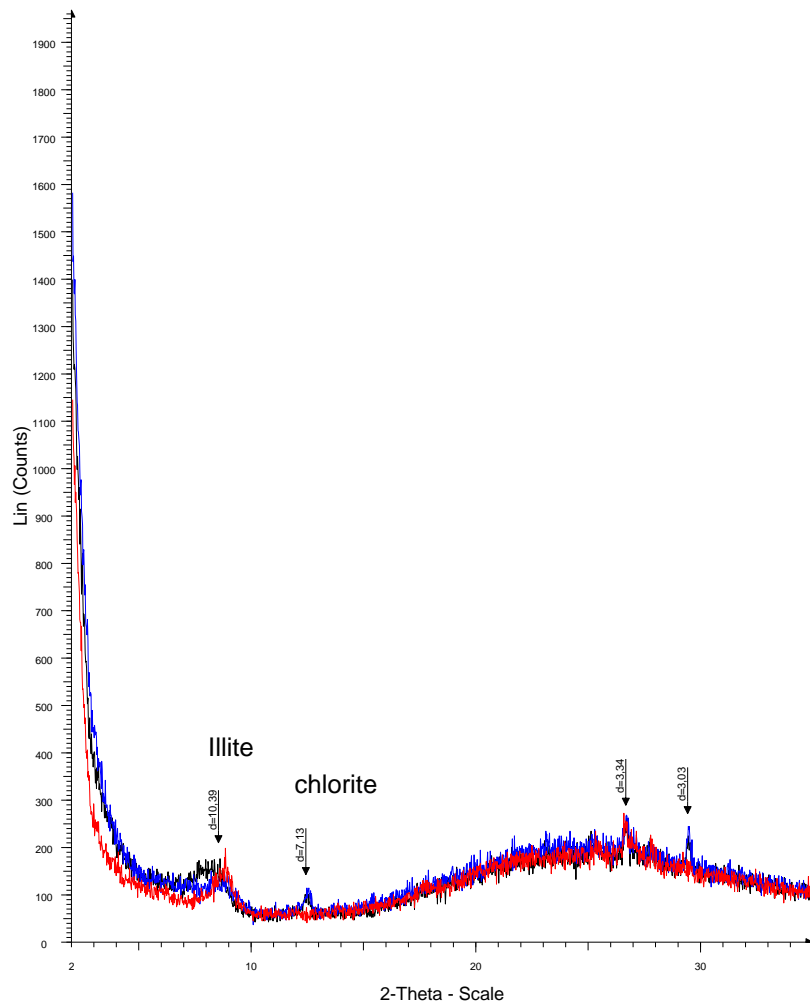
■ File: 3298A_1.raw - Start: 2.000 ° - End: 35.000 ° - Step: 0.020 ° - Step time: 2. s - 2-Theta: 2.000 ° - Theta: 1.000 ° - Anode: Cu - WL1: 1.54056
■ File: 3298G_1.raw - Start: 2.000 ° - End: 35.000 ° - Step: 0.020 ° - Step time: 2. s - 2-Theta: 2.000 ° - Theta: 1.000 ° - Anode: Cu - WL1: 1.54056
■ File: 3298H_1.raw - Start: 2.000 ° - End: 35.000 ° - Step: 0.020 ° - Step time: 2. s - 2-Theta: 2.000 ° - Theta: 1.000 ° - Anode: Cu - WL1: 1.54056

Simba: 3480



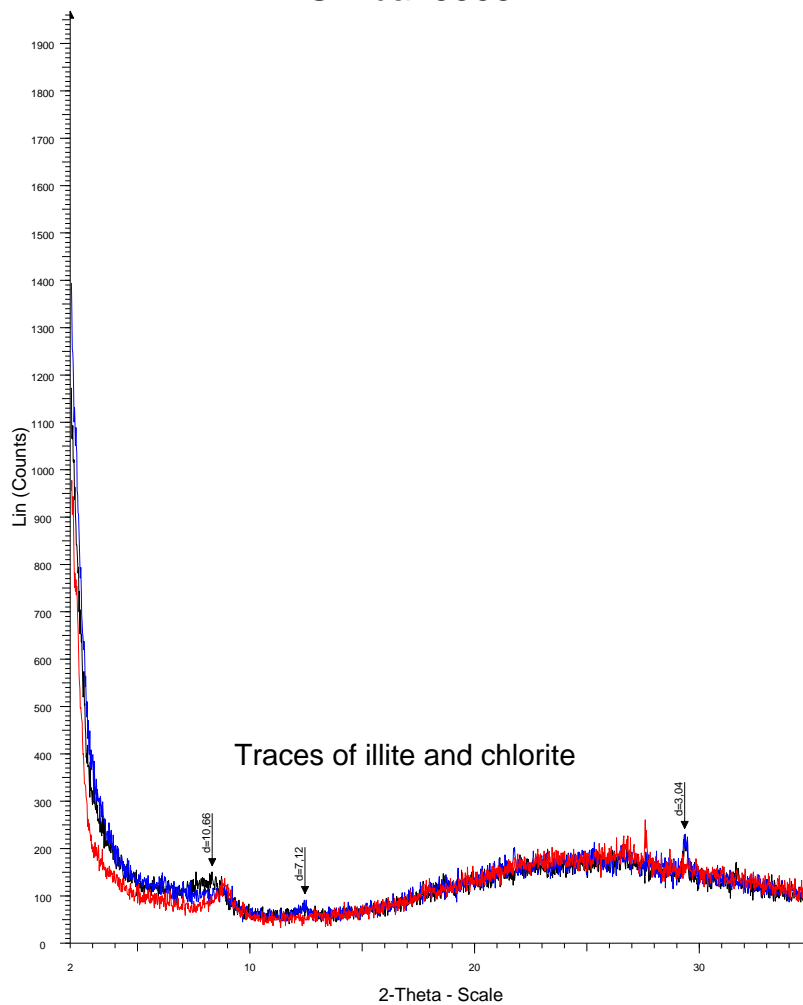
■ File: 3480A_1.raw - Start: 2.000 ° - End: 35.000 ° - Step: 0.020 ° - Step time: 2. s - 2-Theta: 2.000 ° - Theta: 1.000 ° - Anode: Cu - WL1: 1.54056
■ File: 3480G_1.raw - Start: 2.000 ° - End: 35.000 ° - Step: 0.020 ° - Step time: 2. s - 2-Theta: 2.000 ° - Theta: 1.000 ° - Anode: Cu - WL1: 1.54056
■ File: 3480H_1.raw - Start: 2.000 ° - End: 35.000 ° - Step: 0.020 ° - Step time: 2. s - 2-Theta: 2.000 ° - Theta: 1.000 ° - Anode: Cu - WL1: 1.54056

Simba: 3298



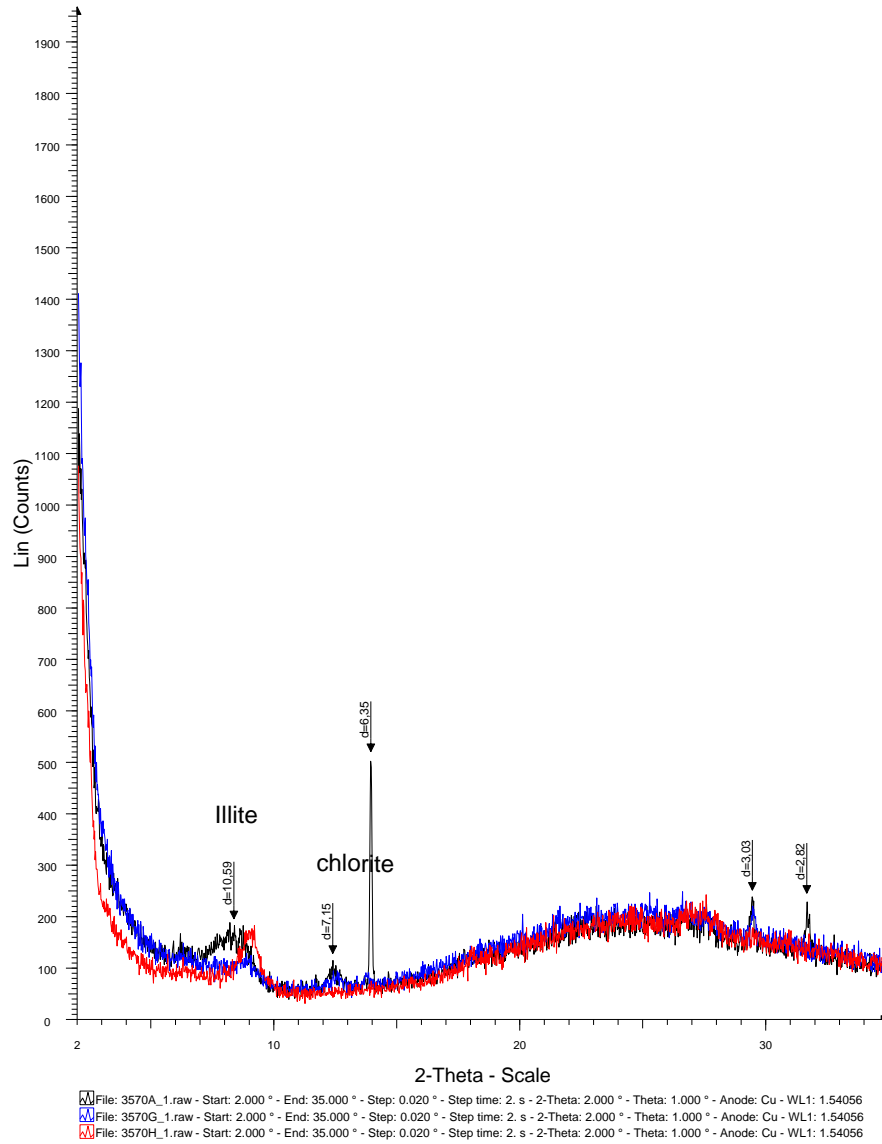
File: 3298A_1.raw - Start: 2.000 ° - End: 35.000 ° - Step: 0.020 ° - Step time: 2. s - 2-Theta: 2.000 ° - Theta: 1.000 ° - Anode: Cu - WL1: 1.54056
File: 3298G_1.raw - Start: 2.000 ° - End: 35.000 ° - Step: 0.020 ° - Step time: 2. s - 2-Theta: 2.000 ° - Theta: 1.000 ° - Anode: Cu - WL1: 1.54056
File: 3298H_1.raw - Start: 2.000 ° - End: 35.000 ° - Step: 0.020 ° - Step time: 2. s - 2-Theta: 2.000 ° - Theta: 1.000 ° - Anode: Cu - WL1: 1.54056

Simba: 3568



File: 3568A_1.raw - Start: 2.000 ° - End: 35.000 ° - Step: 0.020 ° - Step time: 2. s - 2-Theta: 2.000 ° - Theta: 1.000 ° - Anode: Cu - WL1: 1.54056
File: 3568G_1.raw - Start: 2.000 ° - End: 35.000 ° - Step: 0.020 ° - Step time: 2. s - 2-Theta: 2.000 ° - Theta: 1.000 ° - Anode: Cu - WL1: 1.54056
File: 3568H_1.raw - Start: 2.000 ° - End: 35.000 ° - Step: 0.020 ° - Step time: 2. s - 2-Theta: 2.000 ° - Theta: 1.000 ° - Anode: Cu - WL1: 1.54056

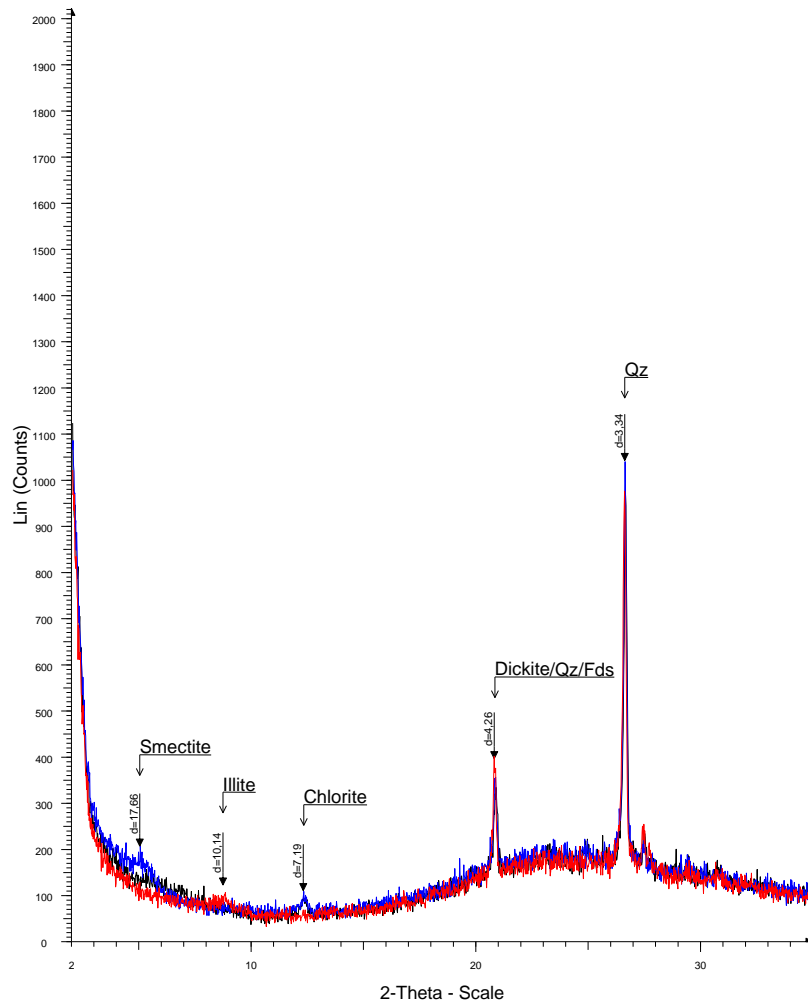
Simba: 3570



APPENDIX IV: WALU 1 X-RAY DIFFRACTION DATA

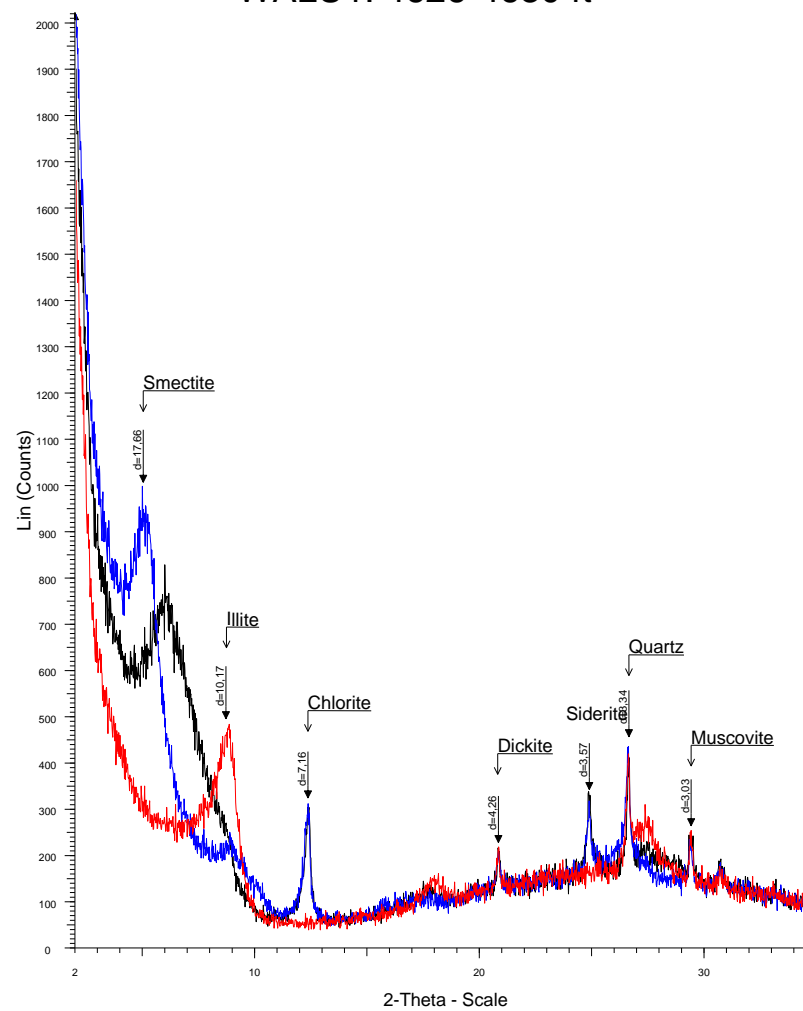
WALU1: 3604-3608 ft

WALU1: 4626-4630 ft



File: 3604-3608A_1.raw - Start: 2.000 ° - End: 35.000 ° - Step: 0.020 ° - Step time: 2. s - 2-Theta: 2.000 ° - Theta: 1.000 ° - Anode: Cu - WL1: 1.5
 File: 3604-3608G_1.raw - Start: 2.000 ° - End: 35.000 ° - Step: 0.020 ° - Step time: 2. s - 2-Theta: 2.000 ° - Theta: 1.000 ° - Anode: Cu - WL1: 1.5
 File: 3604-3608H_1.raw - Start: 2.000 ° - End: 35.000 ° - Step: 0.020 ° - Step time: 2. s - 2-Theta: 2.000 ° - Theta: 1.000 ° - Anode: Cu - WL1: 1.5

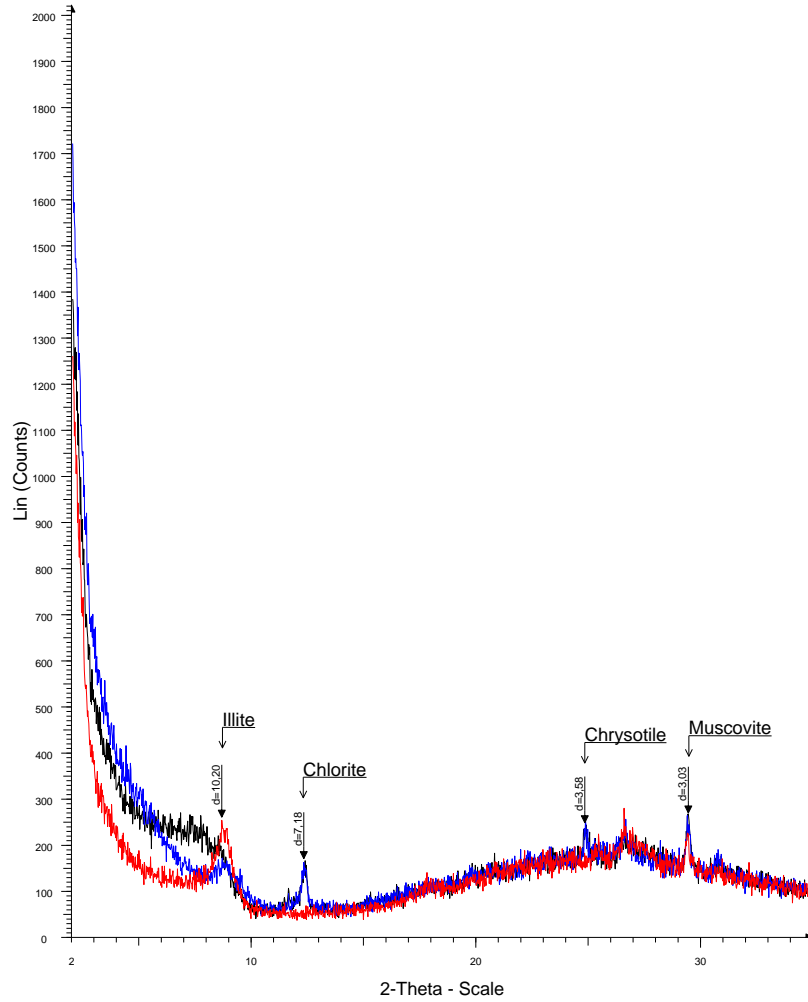
1098-1100m



File: 4626-4630A_1.raw - Start: 2.000 ° - End: 35.000 ° - Step: 0.020 ° - Step time: 2. s - 2-Theta: 2.000 ° - Theta: 1.000 ° - Anode: Cu - WL1: 1.5
 File: 4626-4630G_1.raw - Start: 2.000 ° - End: 35.000 ° - Step: 0.020 ° - Step time: 2. s - 2-Theta: 2.000 ° - Theta: 1.000 ° - Anode: Cu - WL1: 1.5
 File: 4626-4630H_1.raw - Start: 2.000 ° - End: 35.000 ° - Step: 0.020 ° - Step time: 2. s - 2-Theta: 2.000 ° - Theta: 1.000 ° - Anode: Cu - WL1: 1.5

1410-1411m

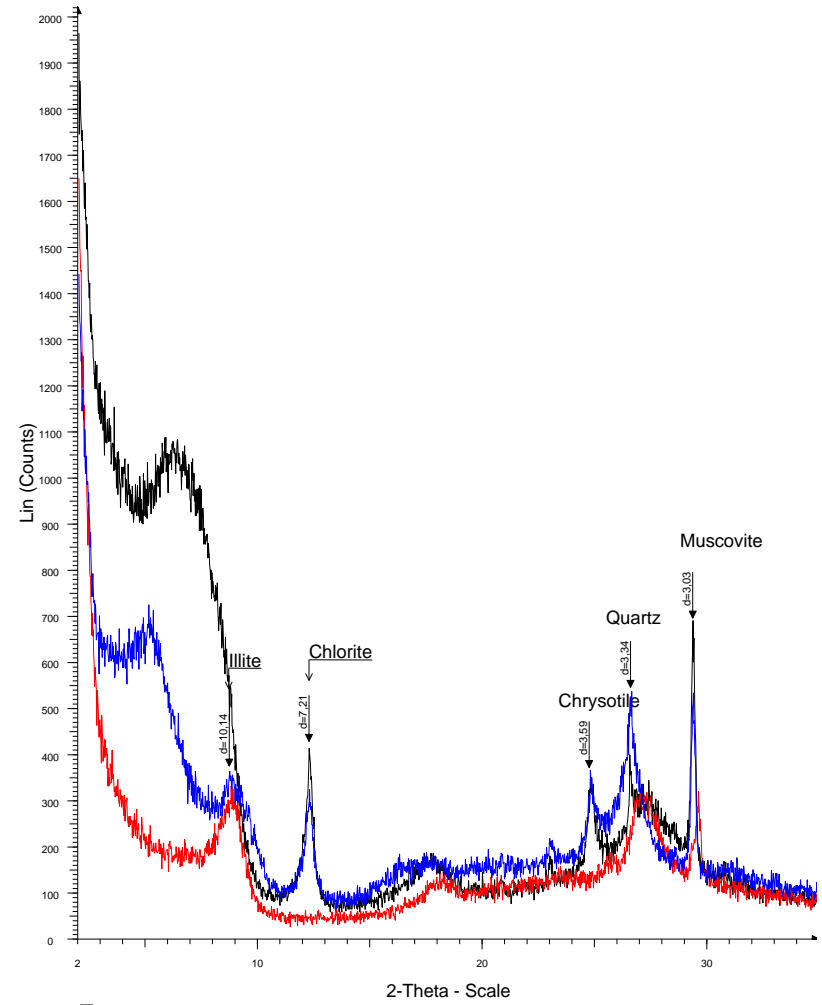
WALU1: 5264-5268 ft



File: 5264-5268A_1.raw - Start: 2.000 ° - End: 35.000 ° - Step: 0.020 ° - Step time: 2. s - 2-Theta: 2.000 ° - Theta: 1.000 ° - Anode: Cu - WL1: 1.5
 File: 5264-5268G_1.raw - Start: 2.000 ° - End: 35.000 ° - Step: 0.020 ° - Step time: 2. s - 2-Theta: 2.000 ° - Theta: 1.000 ° - Anode: Cu - WL1: 1.5
 File: 5264-5268H_1.raw - Start: 2.000 ° - End: 35.000 ° - Step: 0.020 ° - Step time: 2. s - 2-Theta: 2.000 ° - Theta: 1.000 ° - Anode: Cu - WL1: 1.5

1604-1606m

WALU1: 5683-5687 ft



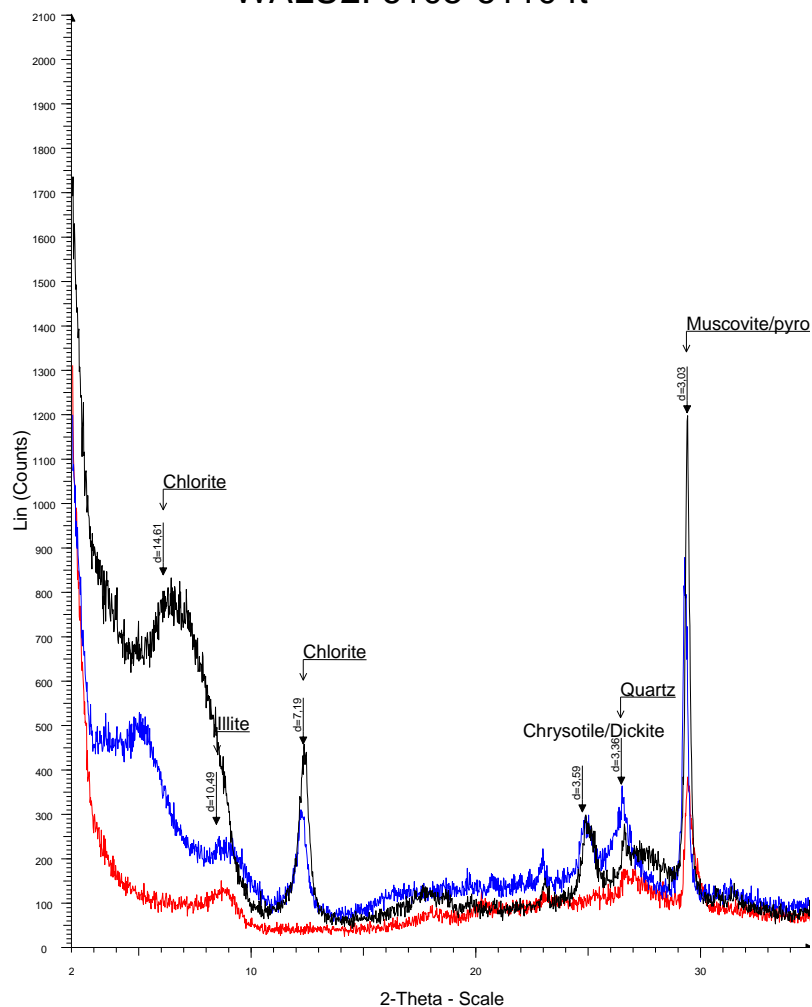
File: 5683-5687A_1.raw - Start: 2.000 ° - End: 35.000 ° - Step: 0.020 ° - Step time: 2. s - 2-Theta: 2.000 ° - Theta: 1.000 ° - Anode: Cu - WL1: 1.5
 File: 5683-5687G_1.raw - Start: 2.000 ° - End: 35.000 ° - Step: 0.020 ° - Step time: 2. s - 2-Theta: 2.000 ° - Theta: 1.000 ° - Anode: Cu - WL1: 1.5
 File: 5683-5687H_1.raw - Start: 2.000 ° - End: 35.000 ° - Step: 0.020 ° - Step time: 2. s - 2-Theta: 2.000 ° - Theta: 1.000 ° - Anode: Cu - WL1: 1.5

1732-1733m

APPENDIX V: WALU-2 X-RAY DIFFRACTION DATA

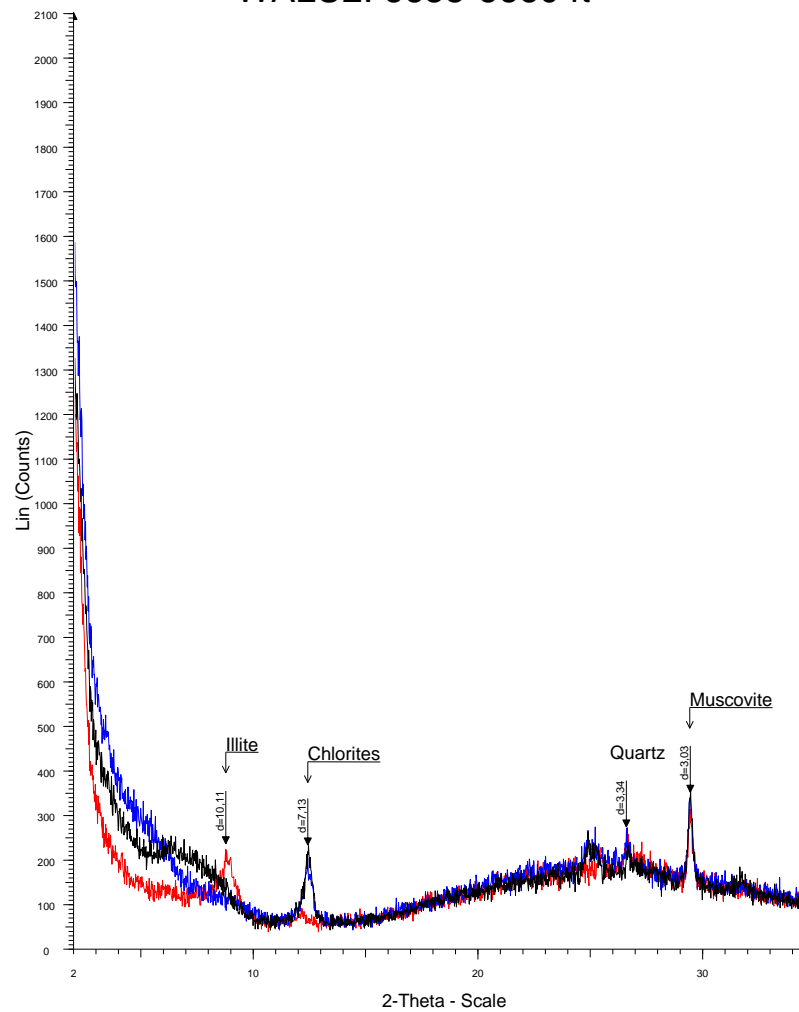
WALU2: 6105-6110 ft

WALU2: 6655-6660 ft



■ File: 6105-6110H_1.raw - Start: 2.000 ° - End: 35.000 ° - Step: 0.020 ° - Step time: 2. s - 2-Theta: 2.000 ° - Theta: 1.000 ° - Anode: Cu - WL1: 1.5
■ File: 6105-6110G_1.raw - Start: 2.000 ° - End: 35.000 ° - Step: 0.020 ° - Step time: 2. s - 2-Theta: 2.000 ° - Theta: 1.000 ° - Anode: Cu - WL1: 1.5
■ File: 6105-6110A_1.raw - Start: 2.000 ° - End: 35.000 ° - Step: 0.020 ° - Step time: 2. s - 2-Theta: 2.000 ° - Theta: 1.000 ° - Anode: Cu - WL1: 1.5

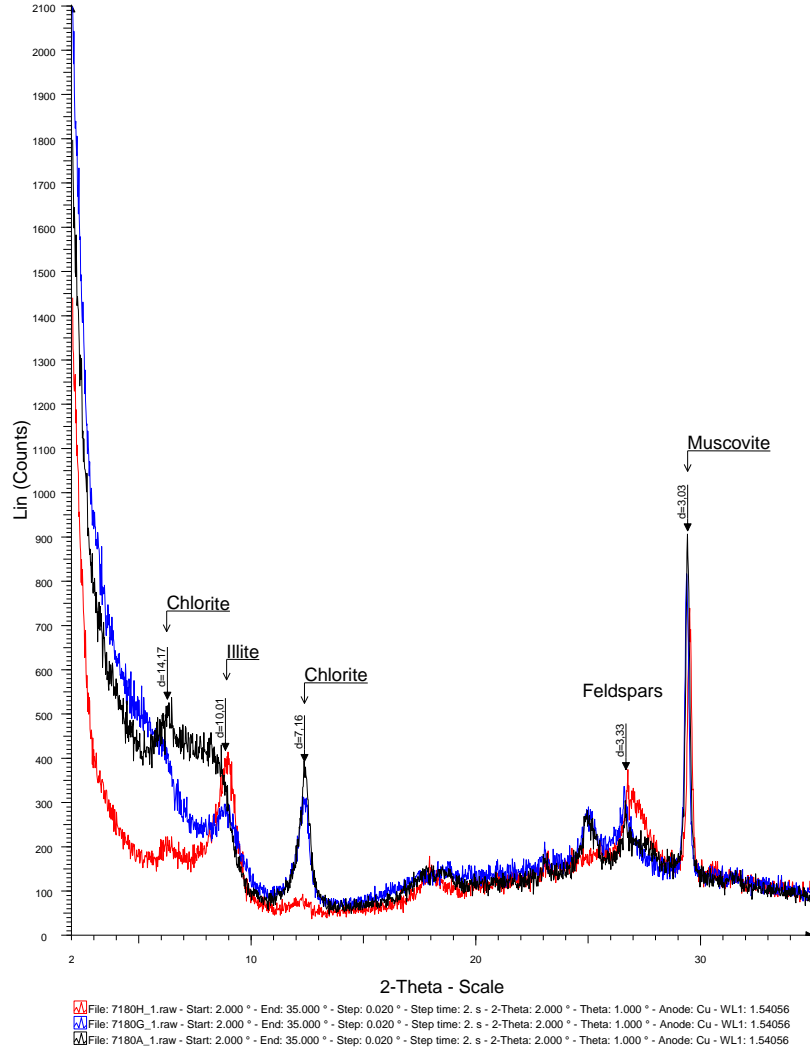
1861-1862m



■ File: 6655-6660H_1.raw - Start: 2.000 ° - End: 35.000 ° - Step: 0.020 ° - Step time: 2. s - 2-Theta: 2.000 ° - Theta: 1.000 ° - Anode: Cu - WL1: 1.5
■ File: 6655-6660G_1.raw - Start: 2.000 ° - End: 35.000 ° - Step: 0.020 ° - Step time: 2. s - 2-Theta: 2.000 ° - Theta: 1.000 ° - Anode: Cu - WL1: 1.5
■ File: 6655-6660A_1.raw - Start: 2.000 ° - End: 35.000 ° - Step: 0.020 ° - Step time: 2. s - 2-Theta: 2.000 ° - Theta: 1.000 ° - Anode: Cu - WL1: 1.5

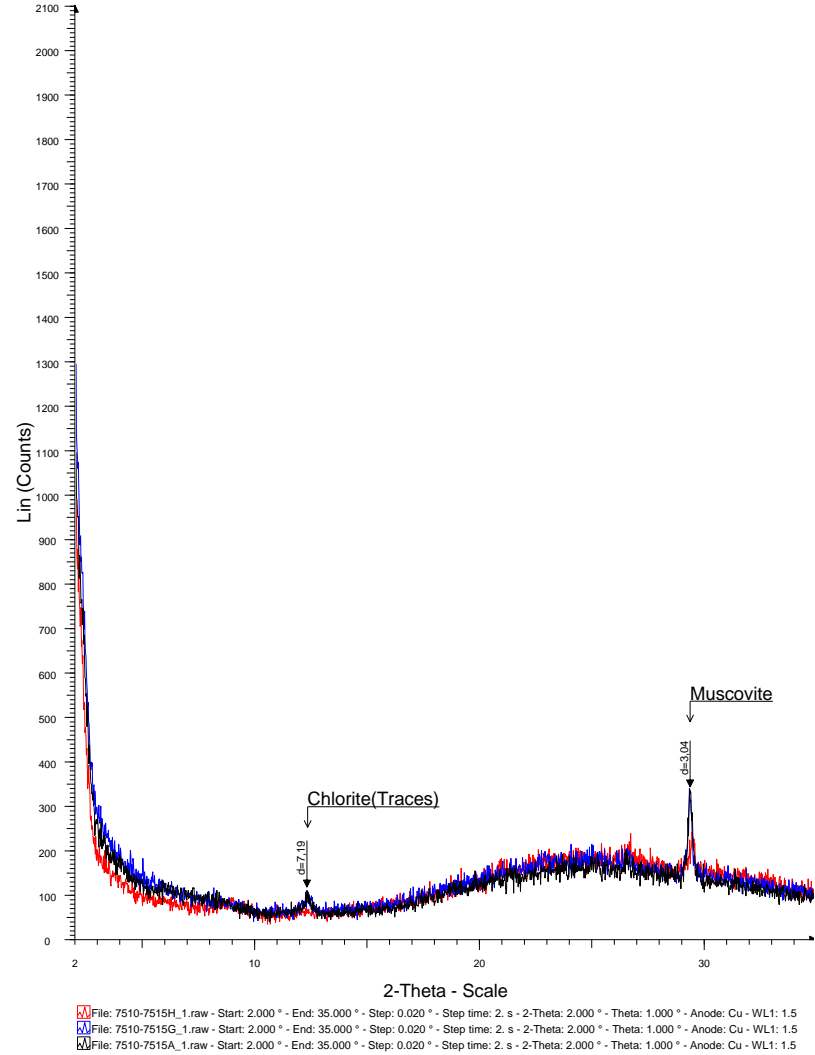
2028-2030m

WALU2: 7180ft



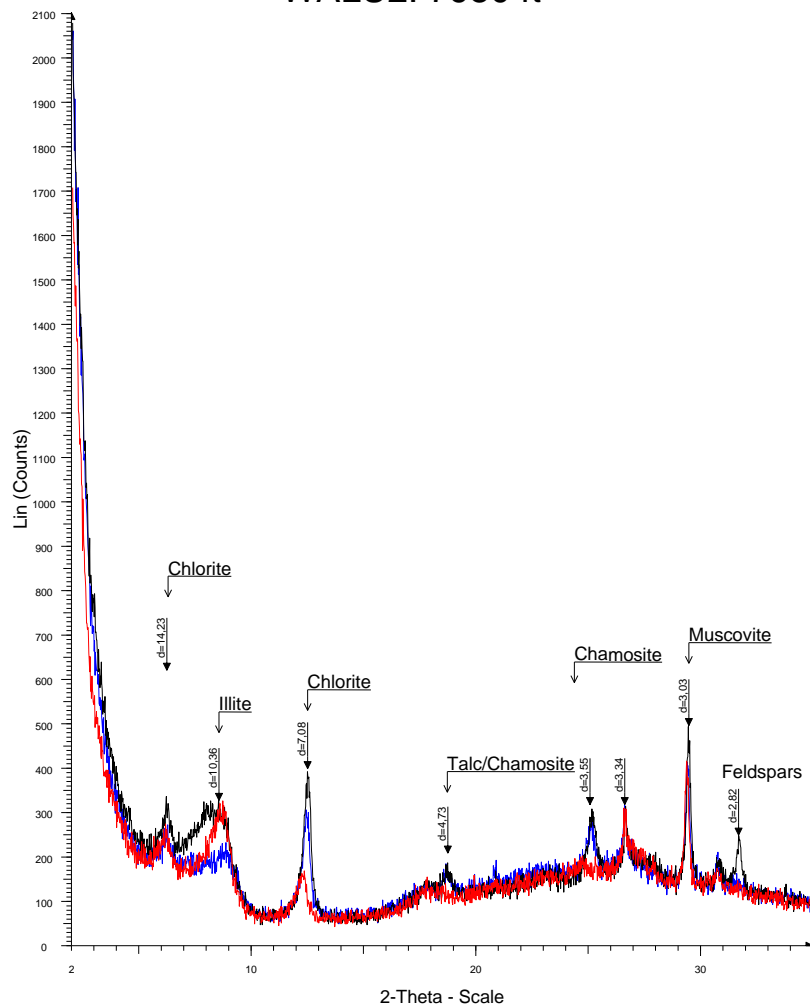
2189m

WALU2: 7510-7515ft



2289-2291m

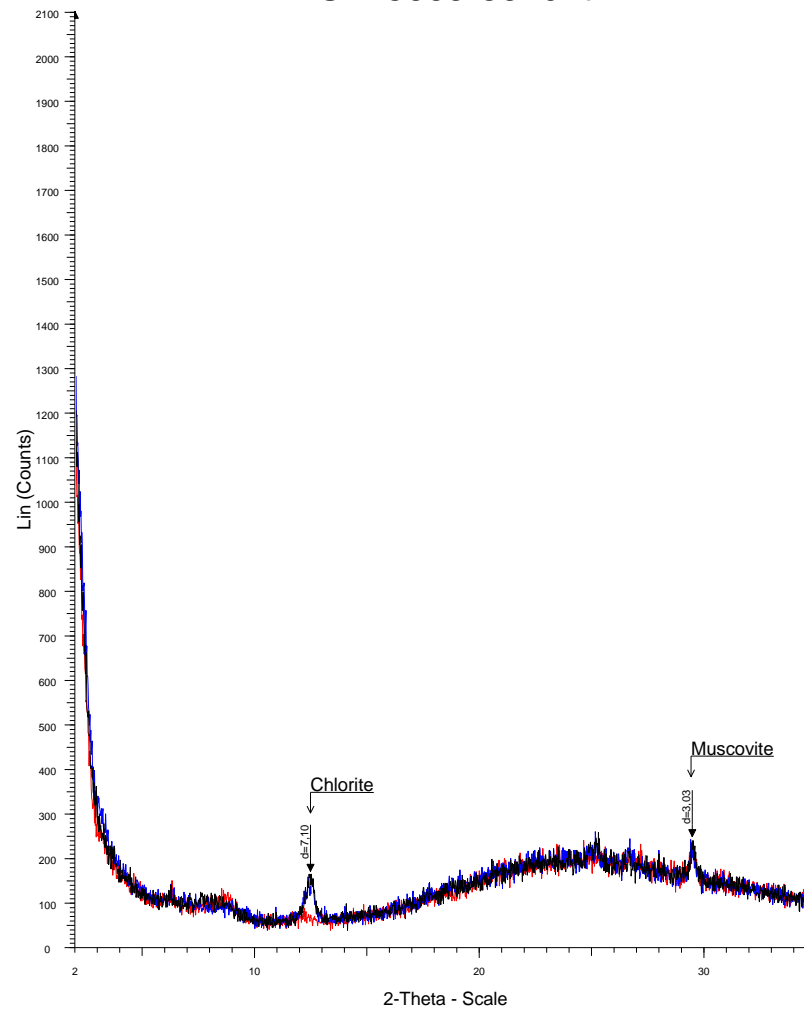
WALU2: 7950 ft



File: 7950H_1.raw - Start: 2.000 ° - End: 35.000 ° - Step: 0.020 ° - Step time: 2. s - 2-Theta: 2.000 ° - Theta: 1.000 ° - Anode: Cu - WL1: 1.54056
File: 7950G_1.raw - Start: 2.000 ° - End: 35.000 ° - Step: 0.020 ° - Step time: 2. s - 2-Theta: 2.000 ° - Theta: 1.000 ° - Anode: Cu - WL1: 1.54056
File: 7950A_1.raw - Start: 2.000 ° - End: 35.000 ° - Step: 0.020 ° - Step time: 2. s - 2-Theta: 2.000 ° - Theta: 1.000 ° - Anode: Cu - WL1: 1.54056

2423m

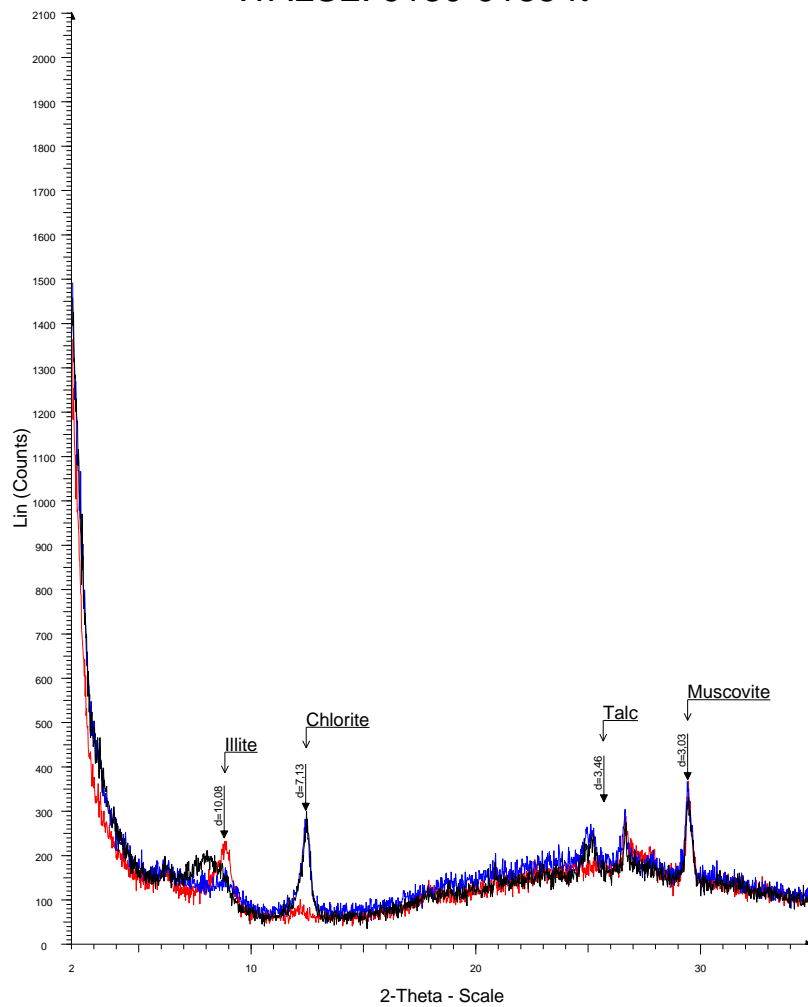
WALU2: 8665-8670 ft



File: 8665-8670H_1.raw - Start: 2.000 ° - End: 35.000 ° - Step: 0.020 ° - Step time: 2. s - 2-Theta: 2.000 ° - Theta: 1.000 ° - Anode: Cu - WL1: 1.5
File: 8665-8670G_1.raw - Start: 2.000 ° - End: 35.000 ° - Step: 0.020 ° - Step time: 2. s - 2-Theta: 2.000 ° - Theta: 1.000 ° - Anode: Cu - WL1: 1.5
File: 8665-8670A_1.raw - Start: 2.000 ° - End: 35.000 ° - Step: 0.020 ° - Step time: 2. s - 2-Theta: 2.000 ° - Theta: 1.000 ° - Anode: Cu - WL1: 1.5

2641-2642m

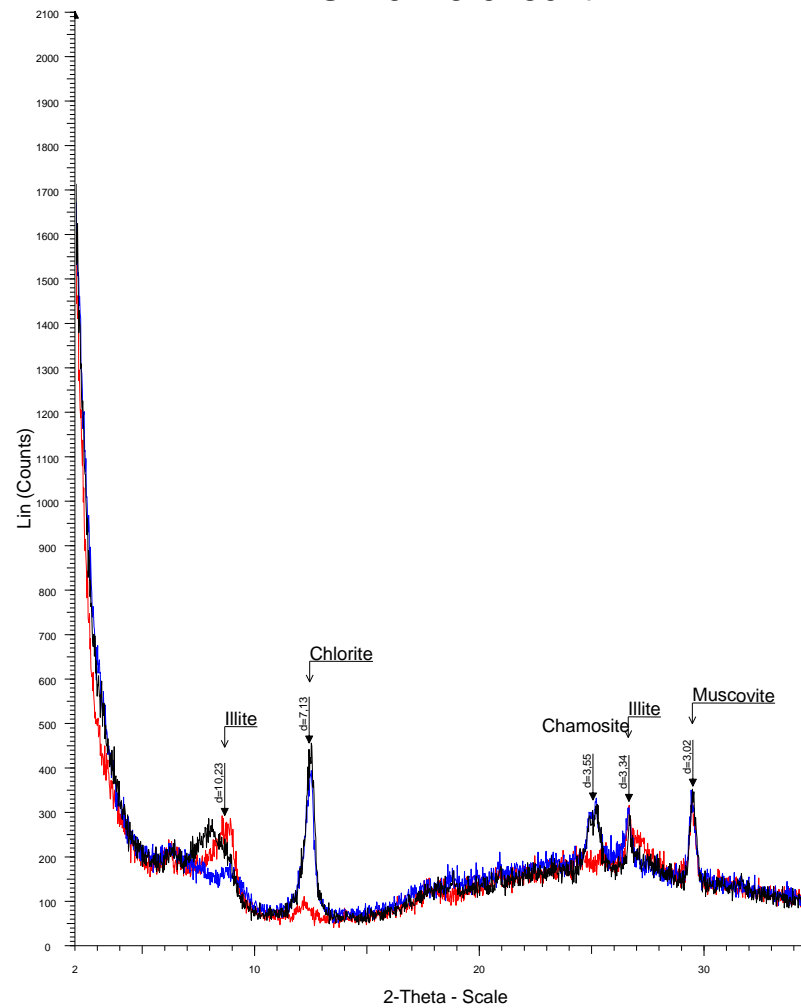
WALU2: 9130-9135 ft



File: 9130-9135H_1.raw - Start: 2.000 ° - End: 35.000 ° - Step: 0.020 ° - Step time: 2. s - 2-Theta: 2.000 ° - Theta: 1.000 ° - Anode: Cu - WL1: 1.5
 File: 9130-9135G_1.raw - Start: 2.000 ° - End: 35.000 ° - Step: 0.020 ° - Step time: 2. s - 2-Theta: 2.000 ° - Theta: 1.000 ° - Anode: Cu - WL1: 1.5
 File: 9130-9135A_1.raw - Start: 2.000 ° - End: 35.000 ° - Step: 0.020 ° - Step time: 2. s - 2-Theta: 2.000 ° - Theta: 1.000 ° - Anode: Cu - WL1: 1.5

2783-2784m

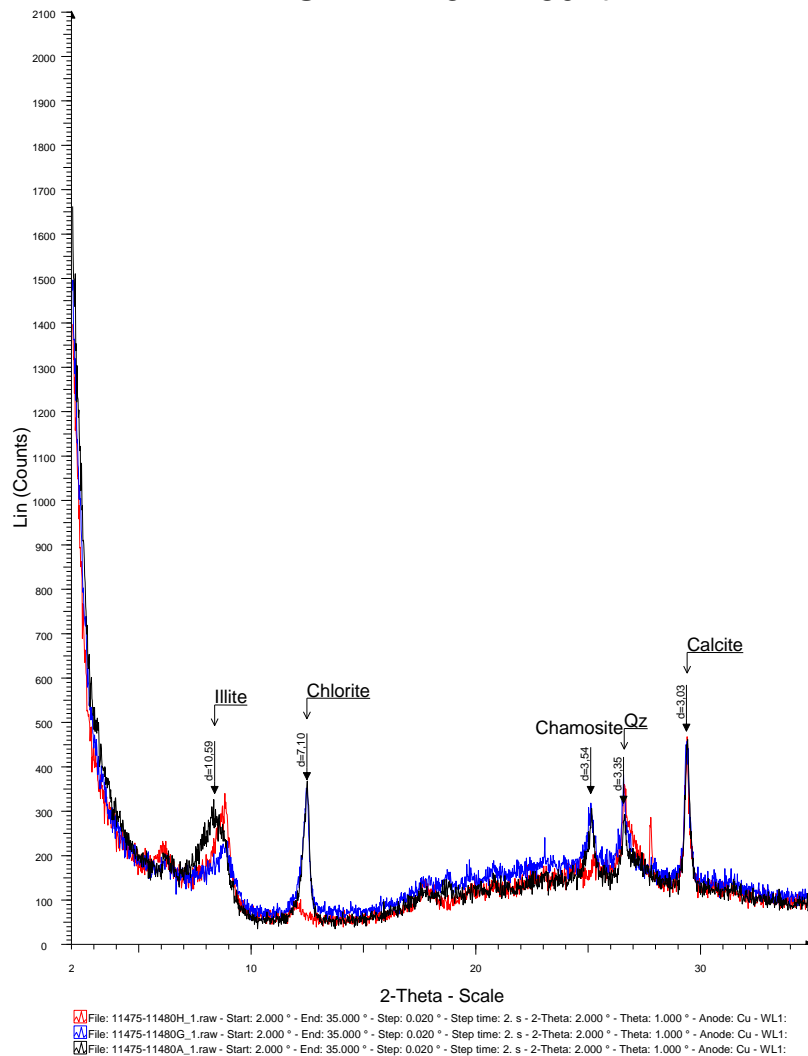
WALU2: 9425-9430 ft



File: 9425-9430H_1.raw - Start: 2.000 ° - End: 35.000 ° - Step: 0.020 ° - Step time: 2. s - 2-Theta: 2.000 ° - Theta: 1.000 ° - Anode: Cu - WL1: 1.5
 File: 9425-9430G_1.raw - Start: 2.000 ° - End: 35.000 ° - Step: 0.020 ° - Step time: 2. s - 2-Theta: 2.000 ° - Theta: 1.000 ° - Anode: Cu - WL1: 1.5
 File: 9425-9430A_1.raw - Start: 2.000 ° - End: 35.000 ° - Step: 0.020 ° - Step time: 2. s - 2-Theta: 2.000 ° - Theta: 1.000 ° - Anode: Cu - WL1: 1.5

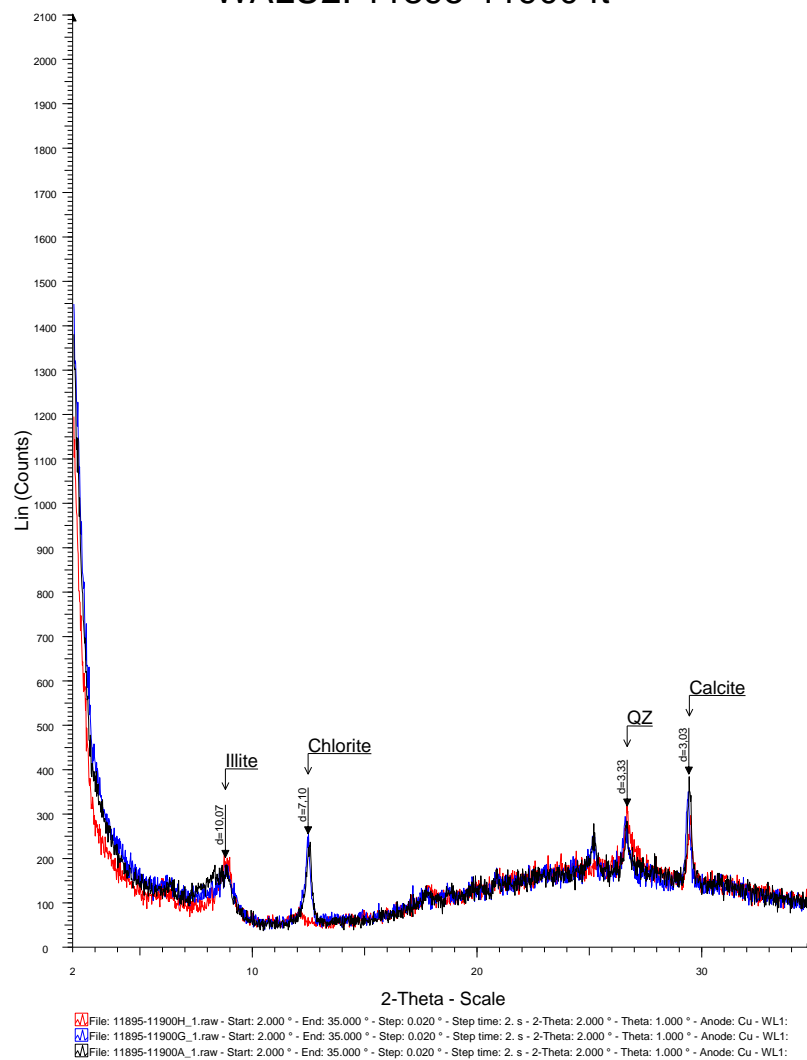
2873-2874m

WALU2: 11475-11480 ft



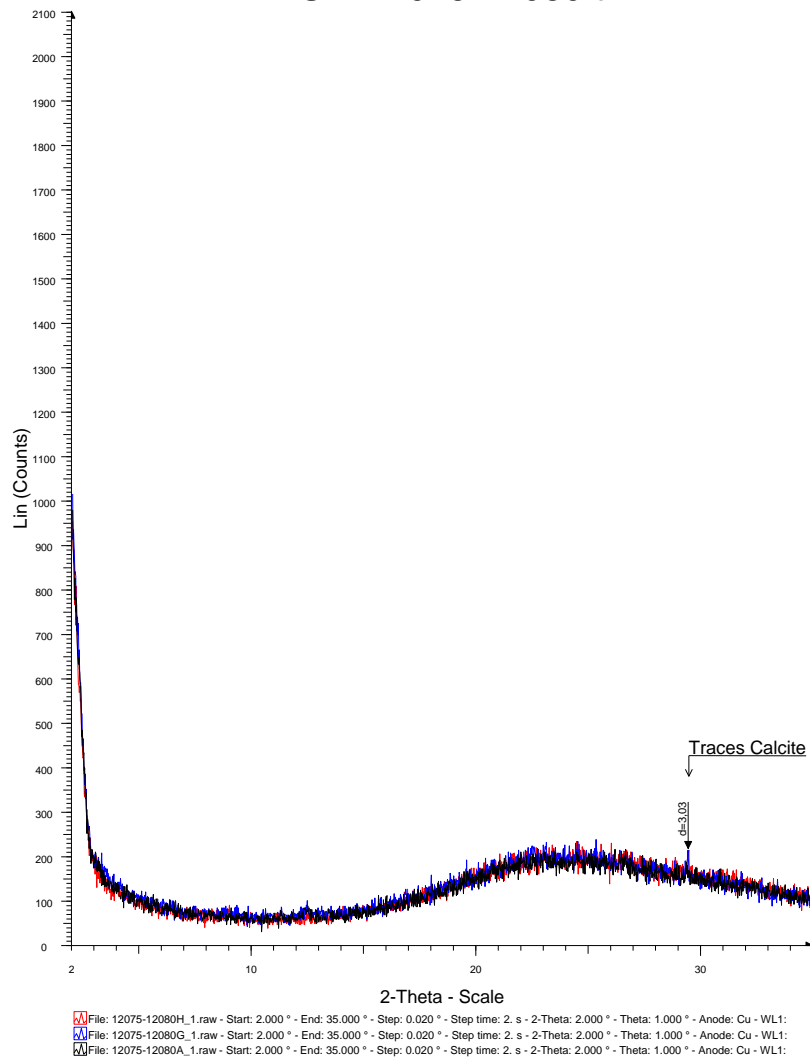
3498-3499m

WALU2: 11895-11900 ft



3626-3627m

WALU2: 12075-12080ft



3681-3682m

APPENDIX VI

Vitrinite reflectance data obtained from National Oil Corporation of Kenya (NOCK) is as below.

Well	Depth (meters)	Vitrinite Reflectance (R _o) in %	Well	Depth (m)	Vitrinite Reflectance (R _o) in %	Well	Depth (m)	Vitrinite Reflectance (R _o) in %
Simba-1	1593	0.28	Kipini-1	982	0.31	Walu-1	1093	0.21
	1840	0.3		1867	0.44		1459	0.33
	2354	0.43		1912	0.44		1610	0.4
	2545	0.41		2004	0.49		1733	0.43
	2668	0.46		2148	0.51		1862	0.56
	2820	0.51		2263	0.54		2035	0.64
	2894	0.52		2491	0.57		2190	0.79
	3004	0.54		2583	0.62		2291	0.79
	3143	0.59		2799	0.66		2425	0.8
	3207	0.57		3032	0.75		2640	0.86
	3297	0.65		3147	0.74		2785	0.85
	3479	0.78		3398	0.71		2873	0.95
	3569	0.86		3454	0.76		3066	0.97
				3651	0.76		3222	0.96
							3222	0.97
							3499	1.13
							3626	1.21
							3673	1.22
Well	Depth (m)	Vitrinite Reflectance (R _o) in %						
Maridadi-1	3116	0.53						
	3855	0.64						
	3925	0.72						
	4105	0.74						
	4175	0.77						